CHALMERS

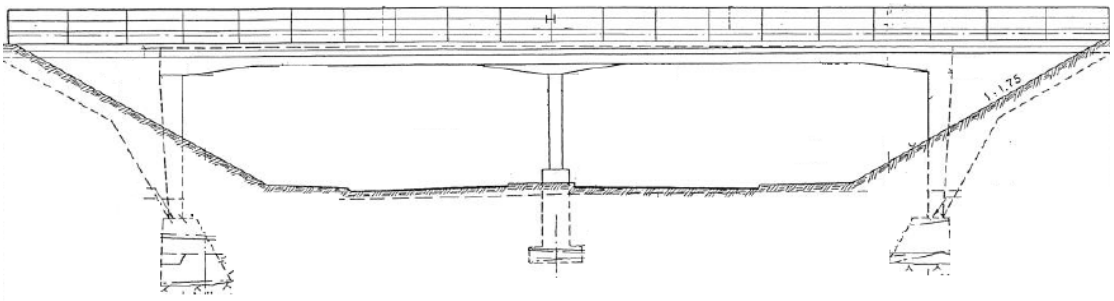

Strengthening of Concrete Slab Bridges with Regard to Shear Capacity

Master of Science Thesis in the Master's Programme Structural Engineering and Building Performance Design

ANDERS BOHLIN
KARIN OLOFSSON

Department of Civil and Environmental Engineering
Division of Structural Engineering
Concrete Structures
CHALMERS UNIVERSITY OF TECHNOLOGY
Göteborg, Sweden 2010

Master's Thesis 2010:44

MASTER'S THESIS 2010:44

Strengthening of Concrete Slab Bridges with Regard to Shear Capacity

Master of Science Thesis in the Master's Programme Structural Engineering and Building Performance Design

ANDERS BOHLIN

KARIN OLOFSSON

Department of Civil and Environmental Engineering
Division of Structural Engineering
Concrete Structures
CHALMERS UNIVERSITY OF TECHNOLOGY
Göteborg, Sweden 2010

Strengthening of Concrete Slab Bridges with Regard to Shear Capacity

Master of Science Thesis in the Master's Programme Structural Engineering and Building Performance Design

ANDERS BOHLIN
KARIN OLOFSSON

Examensarbete / Institutionen för bygg- och miljöteknik,
Chalmers tekniska högskola 2010:44

Department of Civil and Environmental Engineering
Division of Structural Engineering
Concrete Structures
Chalmers University of Technology
SE-412 96 Göteborg
Sweden
Telephone: + 46 (0)31-772 1000

Cover:
Elevation of bridge extracted from drawing in Appendix C

Name of the printers / Department of Civil and Environmental Engineering Göteborg, Sweden 2010

Strengthening of Concrete Slab Bridges with Regard to Shear Capacity

Master of Science Thesis in the Master's Programme Structural Engineering and Building Performance Design

ANDERS BOHLIN
KARIN OLOFSSON
Department of Civil and Environmental Engineering
Division of Structural Engineering
Concrete Structures
Chalmers University of Technology

ABSTRACT

Many old concrete slab bridges have problems reaching sufficient shear capacity when their load bearing capacity is investigated with regard to the present code for design. The subject of shear strengthening of reinforced concrete slabs is in small extent handled in literature. Due to this, there is a strong need for further knowledge in this specific area and the purpose of this project is to examine various methods for strengthening of slab bridges with regard to shear capacity.

In order to summarise information and gather inspiration, this report contains an overview of strengthening methods found in literature. The overview is limited to strengthening with regard to shear and the methods included here are applicable on reinforced concrete slabs or beams. This overview acts as a foundation for the subsequent chapter where a set of suitable methods are chosen and adapted to suit bridge slabs. Here, the methodology of conceptual design is used and requirements are stated which the methods should fulfil. The chosen suitable methods are: 1) Near surface mounted longitudinal post-tensioned carbon fibre reinforced polymer (FRP), 2) Vertical post-tensioned steel wires with external anchors, 3) Vertical post-tensioned steel bars with internal anchor, 4) Vertical FRP bars with anchorage by bond and 5) Closed carbon FRP links.

Furthermore, a case is studied on which the strengthening methods are theoretically applied as a part of the evaluation. When calculations are performed it is noticed that the calculation model for Method 4 does not seem to be applicable on slabs, hence it is excluded from the further evaluation. In order to arrive at the most suitable method for the studied case a set of evaluation parameters are chosen. These parameters are weighted according to their importance and grades are put on the methods with regard to the parameters. Due to the large costs related to traffic disturbance, this is the most heavily weighted parameter. This is the main reason for why Method 3 proved to be most suitable for this case. This method is the only one which does not require removing of the road topping during the strengthening procedure.

All methods are considered to have potential for shear strengthening; however, some methods are in need of further development.

Key words: Reinforced concrete, bridge slab, shear strengthening, retrofitting, conceptual design

Förstärkning av betongplattbroar med avseende på tvärkraftskapacitet

Examensarbete inom Structural Engineering and Building Performance Design

ANDERS BOHLIN
KARIN OLOFSSON
Institutionen för bygg- och miljöteknik
Avdelningen för konstruktionsteknik
Betongbyggnad
Chalmers tekniska högskola

SAMMANFATTNING

Många gamla betongplattbroar har problem med att uppnå tillräcklig tvärkraftskapacitet vid bärighetsutredningar enligt dagens beräkningsnormer. Tvärkraftsförstärkning av plattor i armerad betong är i liten utsträckning behandlat i litteratur. Med anledning av detta finns det ett stort behov av vidare kunskap inom det aktuella området och syftet med detta projekt är undersöka olika metoder för förstärkning av plattbroar med avseende på tvärkraft.

För att sammanfatta information och samla inspiration innehåller denna rapport en inventering av förstärkningsmetoder hittade i litteraturen. Inventeringen är avgränsad till att omfatta förstärkning med avseende på tvärkraft och metoderna som behandlas här är applicerbara på armerade betongplattor eller balkar. Denna inventering utgör en grund för det efterföljande kapitlet där ett antal lämpliga metoder är utvalda och anpassade till broplattor. Här är metodiken ”conceptual design” tillämpad och krav som metoderna ska uppfylla är fastställda. De utvalda lämpliga metoderna är: 1) Ytligt monterad längsgående efterspänd kolfiberarmering, 2) Vertikala efterspända spänntrådar med externa förankringar, 3) Vertikala efterspända stålstänger med intern förankring, 4) Vertikala kolfiberstavar förankrade med vidhäftning och 5) Omslutande kolfiberlänkar.

Vidare är förstärkningsmetoderna teoretiskt applicerade på ett fall som en del av utvärderingen. När beräkningar utförs noteras att beräkningsmodellen för Metod 4 inte verkar vara tillämpbar på plattor, varför den utesluts från vidare utvärdering. För att komma fram till den bäst lämpade metoden för det aktuella fallet är ett antal utvärderingsparametrar utvalda. Dessa parametrar är viktade efter betydelse och betyg är satta på metoderna med avseende på parametrarna. På grund av den höga kostnaden för trafikstörningar är denna parameter viktad tyngst. Detta är huvudorsaken till att Metod 3 visade sig vara bäst lämpad för det aktuella fallet, då det är den enda av metoderna som inte erfordrar upprivning av beläggningen under förstärkningsarbetet.

Alla metoderna bedöms ha potential för tvärkraftsförstärkning, men vissa av dem är i behov av vidare utveckling

Nyckelord: Armerad betong, plattbro, platta, förstärkning, tvärkraft, conceptual design

Contents

Preface

The aim of this study was to investigate suitable methods for shear strengthening of slab bridges. This master's project was carried out in Göteborg in the spring of 2010 at the Department of Civil and Environmental Engineering at Chalmers University of Technology, Sweden. The project was initiated by Sweco Infrastructure AB where also the project was performed.

We could not have done this without all help and we would therefore like to thank everyone who has been involved. Firstly, thanks goes to Sweco Infrastructure AB for letting us perform our project there and for providing us with free coffee and "fredagsbulle". There we got a lot of help from our supervisors; the Structural Engineers Jonas Westerdahl and Helmer Palmgren who shared their bridge experience from practice with us.

Special appreciation is directed to our supervisor and examiner Professor Björn Engström at the Department of Civil and Environmental Engineering at Chalmers, for his never ceasing engagement in advising us.

Furthermore, we would like to thank Stig Öberg at Firma Spännbalkkonsult for letting us discuss his Ph.D. thesis with him. At last we would also like to thank our opponents Nikolaus Ljungström and Olof Karlberg for inspiring discussions in "Byssjan".

Göteborg, May 2010

Anders Bohlin and Karin Olofsson

Notations

Roman upper case letters

A_c	Cross-sectional area of concrete
A_{FRP}	Cross-sectional area of FRP
$A_{FRP,tot}$	Total cross-sectional area of FRP strips through one hole
A_{plate}	Area of anchor plate
A_s	Steel area
A_{sl}	Cross-sectional area of fully anchored tensile reinforcement
A_{sv}	Cross-sectional area of shear reinforcement
A_{sw}	Cross-sectional area of shear reinforcement
A_{swi}	Cross-sectional area of one shear reinforcement unit
A_{washer}	Area of washer
$C_{Rd,c}$	National parameter
E_{FRP}	Modulus of elasticity of FRP
F_{sy}	Tensile force in longitudinal reinforcement at yielding
F_{td}	Tensile force in longitudinal reinforcement
L_i	Effective length of an FRP bar crossed by a shear crack
$\overline{L}_i$	Effective length of an FRP bar corresponding to strain of 4‰
L_{tot}	The sum of all effective lengths of the bars crossed by a shear crack
M_0	Decompression moment
M_d	Bending moment caused by applied load
M_{Ed}	Design value of load effect from bending moment
$M_{Ed,max}$	Design value of load effect from maximum bending moment
N_{Ed}	Design value of axial force
$N_{Rd,c}$	Design value of resistance to concrete cone failure
$N_{Rd,p}$	Design value of pull-out resistance of anchor
$N^0_{Rd,p}$	Empirical value of design pull-out resistance of anchor
$N_{Rd,s}$	Design value of steel resistance of anchor
$N_{Rd,sp}$	Design value of concrete splitting resistance
$N_{Rk,c}$	Characteristic value of resistance to concrete cone failure
$N_{Rk,p}$	Characteristic value of pull-out resistance of anchor
$N_{Rk,s}$	Characteristic value of steel resistance of anchor
$N_{Rk,sp}$	Characteristic value of concrete splitting resistance
P_{max}	Maximum force in wire
P_{FRP}	Tendon force in FRP bar
S	First moment of area
V	Shear force
V_{1F}	Shear resistance of FRP bars with regard to bond failure
V_{2F}	Shear resistance of FRP bars with regard to tensile failure
V_c	Shear resistance of concrete
V_{Ed}	Design value of load effect from shear force
V_{FRP}	Contribution to shear resistance from FRP
V_p	Contribution to shear resistance from an axial compressive force
$V_{Rd,c}$	Shear resistance of concrete without shear reinforcement
$V_{Rd,cw}$	Resistance with regard to web shear tension failure

$V_{Rd,FRP}$ Shear resistance of section with FRP reinforcement
$V_{Rd,max}$ Resistance with regard to web shear compression failure
$V_{Rd,s}$ Shear resistance of shear reinforcement for variable inclination model
V_s Contribution to shear resistance from shear reinforcement
V_{sd} Design value of load effect from shear force
V_u Ultimate shear capacity
V_{uc} Calculated shear capacity
V_{ue} Measured shear capacity
I Second moment of area

Roman lower case letters

b Width of cross-section
b_{plate} Width of anchor plate
b_{slab} Width of bridge slab
b_w Width of web
d Effective height of cross-section
d_{net} Reduced length of FRP bars
d_r Length of FRP bars
$f_{0.2}$ 0.2% proof-stress
f_b Bond strength
f_B Factor regarding the influence of concrete strength on pull-out resistance
f'_c Concrete compressive strength (ACI)
f_{cc} Concrete compressive strength
f_{cd} Design value of concrete compressive strength
f_{ck} Characteristic value of concrete compressive strength
$f_{ck,cube}$ Characteristic value of concrete compressive strength based on cube tests
f_{ctd} Design value of concrete tensile strength
$f_{FRP,tu}$ Ultimate tensile strength of FRP
f_{sv} Yield strength of shear reinforcement
f_{uk} Characteristic value of ultimate strength
f_y Yield strength
f_{yk} Characteristic value of yield strength
f_{ywd} Design value of yield strength of shear reinforcement
h_0 Height of slab at thickest part
h_{ef} Effective height of anchor
k Factor regarding effective height of cross-section
k_1 National parameter
l_x Distance from the considered section to the starting point of the transmission length
l_{pt2} Upper bound value of the transmission length
m_v Mean ratio between measured and calculated shear capacity
n_{trans} Number of bars in the transversal direction
n_{lay} Number of FRP strip layers
n_{units} Total number of reinforcement units

s	Spacing between shear reinforcement units
s_{long}	Longitudinal spacing between shear reinforcement units
s_{trans}	Transversal spacing between shear reinforcement units
z	Internal lever arm

Greek upper case letters

ΔF_{td}	Additional force in tensile reinforcement
Δl	Assumed length of strengthened region
$\Delta\sigma_{sv}$	Additional steel stress at shear failure of a member

Greek lower case letters

α_{cw}	Factor regarding the prestressing effect on web shear compression failure
α_l	Factor regarding the influence of the transmission length
β	Inclination of shear reinforcement
γ_c	Partial coefficient regarding uncertainties in concrete material parameters
γ_{Mc}	Partial coefficient regarding uncertainties in concrete material parameters
γ_{Mp}	Partial coefficient regarding uncertainties in pull-out capacity
γ_{Ms}	Partial coefficient regarding uncertainties in steel material parameters
γ_{Msp}	Partial coefficient regarding uncertainties in splitting capacity
γ_n	Partial coefficient regarding safety class
ε	Strain
ε_{eff}	Maximum allowed strain in FRP
ε_u	Ultimate strain
ε_y	Yield strain
θ	Strut inclination
v	National parameter
v_{min}	National parameter
ρ_l	Reinforcement ratio
σ	Stress
σ_1	Principal stress in direction 1
σ_2	Principal stress in direction 2
σ_c	Concrete stress
σ_{cp}	Axial compressive stress in concrete
$\sigma_{cp,r}$	Resultant from axial and vertical compressive stress in concrete
$\sigma_{cp,v}$	Vertical compressive stress in concrete
σ_{FRP}	FRP stress
σ_{pw}	Stress in reinforcement wires
$\sigma_{sv,o}$	Effective prestress in steel
$\sigma_{sv,max}$	Steel stress at shear failure of a member
σ_x	Stress in *x*-direction
σ_z	Stress in *z*-direction
τ	Shear stress
φ	Angle of principal stress direction to the longitudinal axis of a member

ϕ	Diameter of reinforcement bars
ω_v	Mechanical shear reinforcement ratio

1 Introduction

1.1 Background

During the past decades the code for design with regard to shear resistance in slab bridges has been debated and sharpened. This has resulted in that many bridges constructed earlier have insufficient shear capacity according to the present code. In order to fulfil the demands stated in the code today the alternatives for these bridges are either demolition followed by reconstruction, or strengthening of the existing structures. It is preferable in many aspects, such as environmental and economical, to choose strengthening rather than demolition. Today there are great uncertainties in the industry about which strengthening methods that are preferable and when to use them. Beam bridges are much more accessible for shear strengthening, since they can be strengthened externally on each side of the beam web. Slabs on the other hand do not have that accessibility.

1.2 Purpose

The purpose of this master's project was to examine various methods for strengthening slab bridges with regard to shear capacity. The examination should result in recommendations of suitable solutions with regard to strengthening efficiency and production procedure. Ideally, the pre-study should result in a set of methods which can directly be applied in the industry.

1.3 Method

Initially, a literature study was performed in order to gather information about present available strengthening methods concerning both national and international publications. Various kinds of strengthening of different types of concrete members were considered in order to provide a solid foundation for the subsequent stage where methods suitable for slabs were developed. This overview is also performed in order to identify advantages and disadvantages with different methods. Henceforth, the strengthening methods were, when considered necessary, adjusted to fit the actual problem, namely shear strengthening of slab bridges.

In order to arrive at suitable solutions the methodology of conceptual design is applied. In this process requirements and other demands were identified and different possible methods were evaluated and compared more deeply to each other. Also own invented solutions were included in this evaluation.

Finally, a case study was performed where promising solutions were theoretically applied on a reference object. The reference object was chosen among slab bridges with insufficient shear capacity. In this way the solutions' applicability in practice was tested and evaluated.

1.4 Limitations

In the investigation flexural strengthening will not be considered unless it also affects the shear capacity.

The work in this project will be focused on the ultimate limit state.

1.5 Outline

Chapter 2 presents the shear behaviour of beams and slabs. The response of uncracked members is described followed by the response during cracking and also how this ends up in different types of shear failures.

Chapter 3 presents an overview of various strengthening methods with regard to shear capacity. This overview regards both solutions for slabs and beams.

Chapter 4 presents the most promising of the strengthening methods described in Chapter 3 adapted for strengthening of bridge slabs. In this chapter, implementation in practice and mechanical behaviour of these further developed methods are described. Also what requirements the methods need to fulfil are presented in this chapter.

Chapter 5 contains a case study where a real life case has been chosen in order to exemplify the different strengthening methods presented in Chapter 4. Here, the case is described and results from calculations are presented. This chapter also contains an evaluation, where the adapted methods are compared to each other with regard to predefined evaluation parameters based on own estimations. The evaluation is performed according to a methodology suitable for conceptual design.

2 Shear behaviour

In this chapter, the shear behaviour of beams and slabs is presented. The response of uncracked members is described followed by the response during cracking and also how this ends up in different types of shear failures.

2.1 Shear response before cracking

For a structural member to be able to fulfil equilibrium, while subjected to a transverse load, the load must somehow be transferred to its supports. This action is described by the shear force, which represents the actual part of the applied transversal load that is transferred through a certain section towards a support.

The shear force in a cross-section of the member gives rise to shear stresses which, for a rectangular cross-section, are distributed with a parabolic shape, see Figure 2.1. The magnitude of the shear stress is zero at the top and bottom edges of the section and reaches its maximum in the gravity centre. The shear stress at a coordinate *z* from the sectional centroid can be calculated according to equation (2-1).

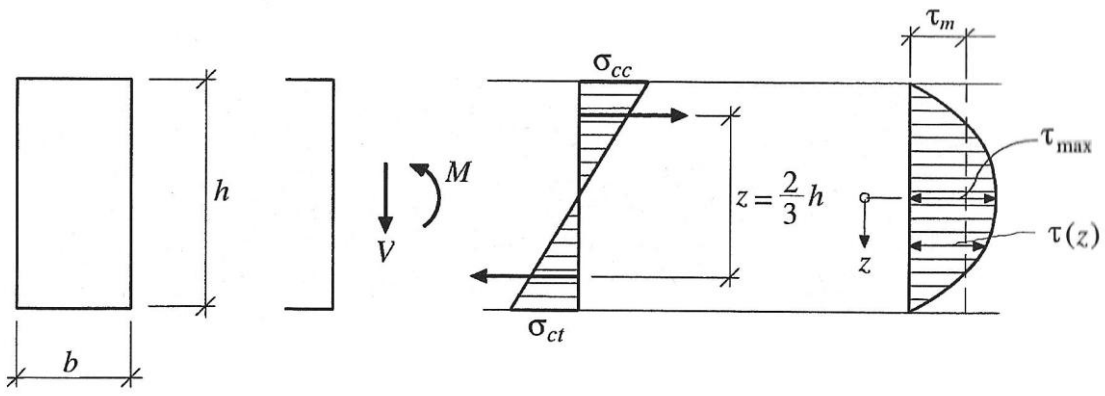

Figure 2.1 Normal stress and shear stress distributions over homogenous rectangular cross-section.

$$\tau(z) = \frac{S(z) \cdot V}{I \cdot b(z)} \tag{2-1}$$

where

$S(z)$ is the first moment of area of the part of the cross-section beyond the coordinate *z* about the sectional centroid.

V is the shear force in the section.

I is the second moment of area of the cross-section about the sectional centroid.

b(z) is the width of the cross-section at the considered coordinate z.

The state of stresses at a point of a member can be represented by the principal stresses. If a regarded infinitesimal element loaded in pure shear is rotated according to Figure 2.2, it can be seen that the principal stress directions are 45° relative to the longitudinal axis.

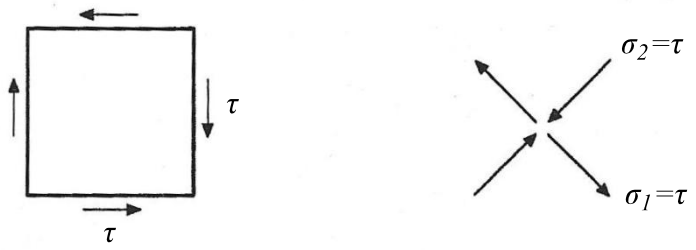

a) b)

Figure 2.2 State of stresses in the sectional centroid, a) Shear stress (τ), b) tensile principal stress (σ_1) and compressive principal stress (σ_2) on infinitesimal element.

In sections which are subjected to pure bending the principal stress is equal to the bending normal stress and its direction is in the longitudinal direction of the member.

In most of the beam sections both shear and bending are acting simultaneously, which results in a variation of the magnitude of the principal stress and its direction depending on both the longitudinal position of the section and the transverse coordinate z within the section itself. The variation in the longitudinal direction depends on the actual bending moment and shear force distributions. (Engström, 2007)

2.2 Shear response during cracking

Cracks will form in a concrete member, if the tensile principal stress reaches the tensile strength of the concrete. These cracks will be oriented perpendicular to the principal tensile stress, thus the cracks will form a pattern throughout the member where the directions of the cracks will vary depending on their location.

Furthermore, the way the cracks are formed will depend highly on the stress state. In a section where bending moment is at its maximum, as in section C in Figure 2.3, flexural cracks will form starting at the tensile edge of the member. Since the principal stress direction over such a section is constant, the crack will propagate perpendicular to the longitudinal axis. Where both shear force and bending moment are of considerable magnitude, on the other hand, the process will be different, see Section B in Figure 2.3. The crack will start as a flexural crack, but will then propagate with a changing direction up through the depth of the member. This type of crack is named flexural shear crack. A third way for a crack to develop is when high shear force and low bending moment are combined, as in section A in Figure 2.3. Here, the principal tensile stress in the web will initiate the crack, which will have a

45° angle in relation to the longitudinal axis. The three crack types are shown in Figure 2.4.

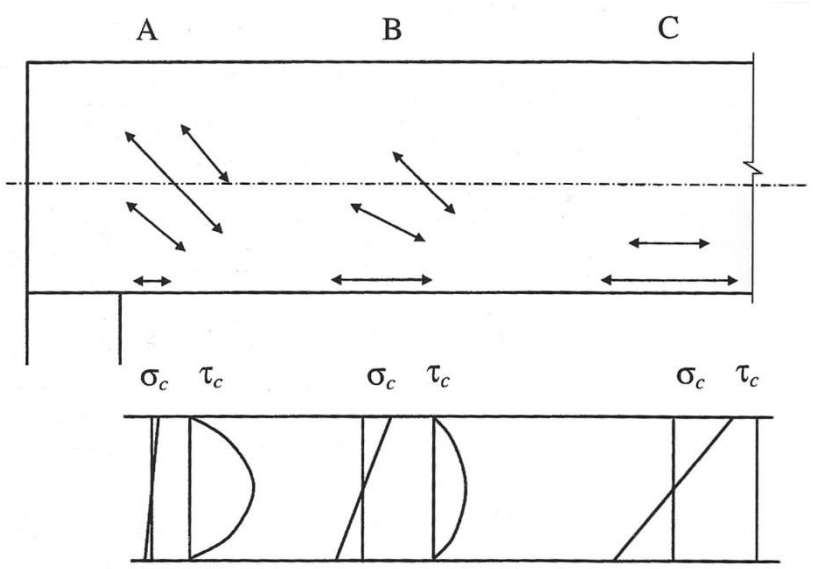

Figure 2.3 Tensile principal stresses in different sections of a beam subjected to shear force and bending moment together with corresponding stress distributions.

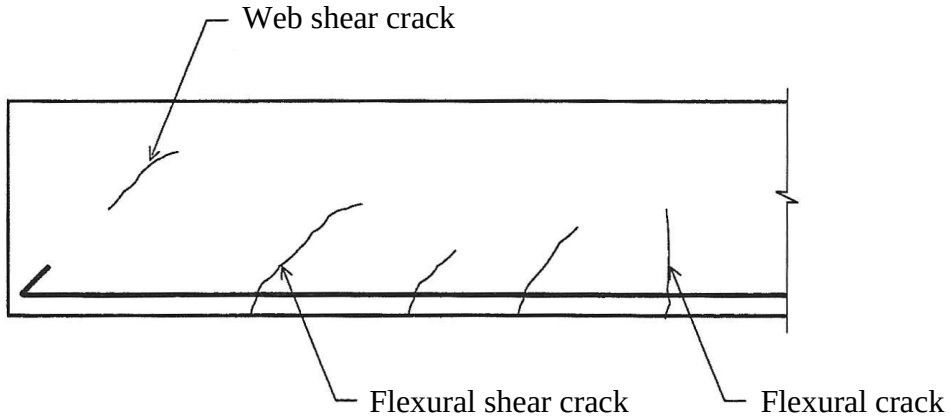

Figure 2.4 Cracks formed in three different ways.

When inclined cracks have formed the principal tensile stresses can no longer be resisted by the concrete and a new stress state is obtained for which equilibrium must be fulfilled. At this point, the vertical component of the principal compressive stresses must alone carry the shear force, thus the principal compressive stress will be twice as large as just before cracking. If inclined cracks have propagated throughout the whole cross-section, there must be some additional effect which equilibrates the horizontal component of the diagonal compressive stresses. In this case longitudinal reinforcement is needed to balance the horizontal component and vertical or inclined reinforcement must be inserted in order to balance the vertical component of the

diagonal compression, see Figure 2.5. It is possible to transfer shear forces to some extent also without shear reinforcement if the cracks only have opened slightly, although, the bending reinforcement in the tensile zone is necessary in order to keep the shear cracks in the concrete together. In this case the transfer of shear occurs mainly due to friction and interlocking effects along the cracks and some contribution is also possible due to the shear resistance of the uncracked compressive zone and dowel action of the bending reinforcement. However, the shear resistance of a concrete section without shear reinforcement is difficult to explain and predict. Tests have been performed in order to estimate this capacity.

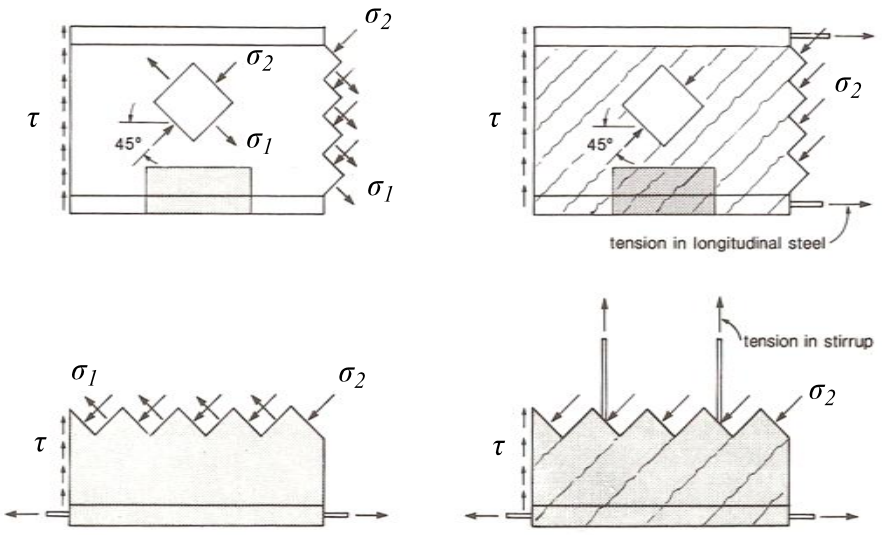

a) Before cracking
$\sigma_1=\sigma_2=\tau$

b) After cracking
$\sigma_1=0,\ \sigma_2=2\tau$

Figure 2.5 Shear resistance of a reinforced concrete beam a) before and b) after cracking. σ_1 denotes tensile principal stress, σ_2 denotes compressive principal stress and τ denotes shear stress. (Collins & Mitchell, 1991)

This way of obtaining equilibrium can be represented by a truss model, schematically shown in Figure 2.6. Here, the concrete in between the diagonal cracks and in the compression zone in the top of the member forms struts and the vertical as well as the longitudinal reinforcement form ties in the imagined truss.

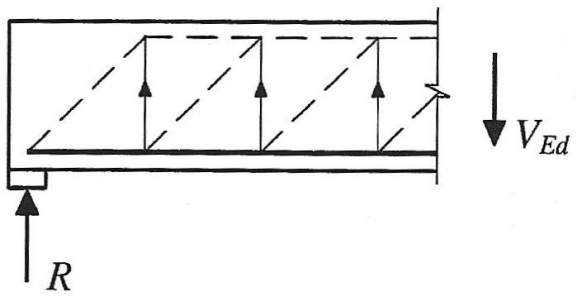

Figure 2.6 Truss model where dashed lines symbolise compression struts and solid lines ties.

In the truss model described above the whole shear force is resisted by the system of struts and ties. However, there is a contribution to the shear capacity from the crack interfaces, which is omitted in this model. The magnitude of this contribution depends on the strut inclination; for a small angle the concrete contribution is small and for a large angle the contribution is large. Hence, for a case with a steep strut inclination the shear capacity will be underestimated with the truss model. (Engström, 2007; Broo, 2006)

2.3 Failure modes

The shear failure of a reinforced concrete member can be categorised into the modes presented in this section. Depending on the sectional geometry, the concrete strength and the reinforcement arrangement, one of the modes will be critical for the shear resistance of the member.

2.3.1 Shear sliding failure

When a shear crack has formed in a concrete member which contains bending reinforcement only, the remaining shear capacity is normally rather low. Shear sliding failure occurs when the maximum resistance is reached and the failure mode is characterised by large shear displacement along a shear crack, see Figure 2.7. The crack must not necessarily have propagated throughout the whole height before failure occurs.

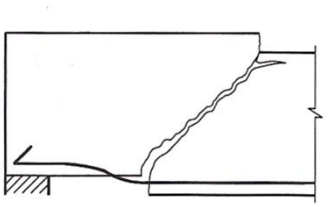

Figure 2.7 After shear sliding failure in a reinforced concrete beam.

For a member with shear reinforcement the failure mode is rather similar but with the difference that the ultimate load is not reached until yielding occurs in the shear reinforcement, see Figure 2.8. To be more specific, this failure mode can be referred to as shear sliding failure with yielding shear reinforcement.

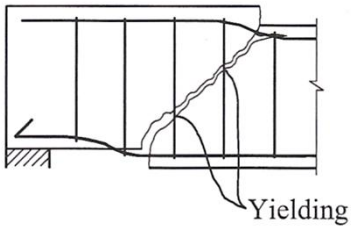

Figure 2.8 After shear sliding failure with yielding shear reinforcement in a reinforced concrete beam.

If the failure mode described above is initiated by a bending crack it is sometimes referred to as a flexural-shear failure. However, there is no difference in the behaviour with regard to the response in shear.

2.3.2 Web shear compression failure

If the compressive principal stresses in the inclined struts between the shear cracks reach the compressive strength of the concrete, web shear compression failure occurs, see Figure 2.9. This mode represents an upper boundary of the shear capacity of a reinforced concrete member. This mode might be critical if the member either contains a large amount of shear reinforcement or has a thin web.

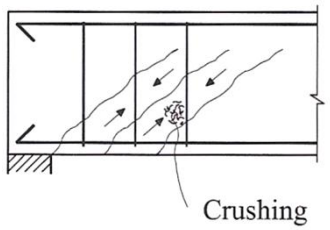

Figure 2.9 Web shear compression failure in a reinforced concrete beam.

2.3.3 Punching shear failure

A special type of local shear failure which can occur in slabs is punching shear failure. This can occur in a thin slab over supports as in Figure 2.10 or if a concentrated load is applied on a small area as in Figure 2.11. Initially bending cracks occur which develop into inclined shear cracks along a critical perimeter in the vicinity of the applied load or support and form a cone which slides relative to the surrounding structure. This failure appears similarly to shear sliding failure; however, a three dimensional stress state is necessary to regard which makes the analysis more complex.

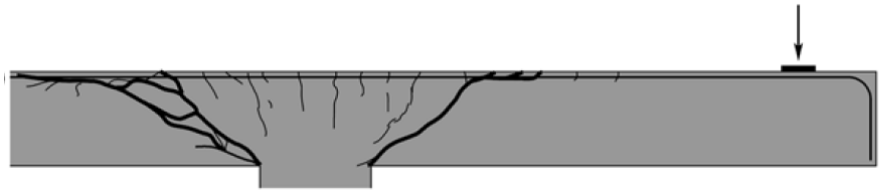

Figure 2.10 Cracking pattern of slab at punching shear failure at a slab-column support. (Muttoni, 2008)

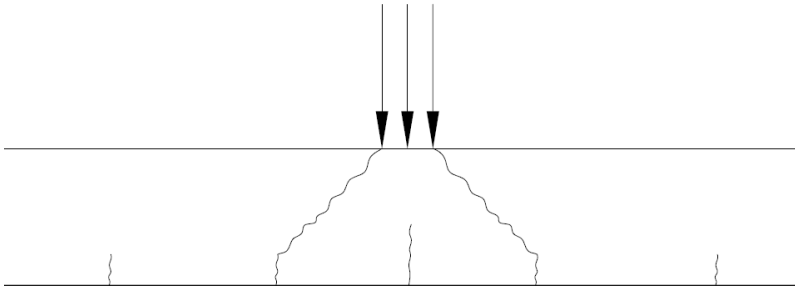

Figure 2.11 Cracking pattern of slab at punching shear failure under concentrated load.

2.4 Effect of prestressing

2.4.1 Cracking process

Prestressing has a positive influence on the cracking behaviour of concrete members. Not only does it delay the flexural cracking, but also the shear cracking due to the arch effect. As seen in Figure 2.12, an axial compressive stress, σ_{cp}, on an infinitesimal element at the sectional centroid similar to the one in Figure 2.2, will decrease the tensile principal stress, σ_1, and increase the compressive principal stress, σ_2. Since one of the major disadvantages of concrete is its limited tensile strength, this decrease is favourable. The decreased tensile principal stress due to prestressing increases the critical load for web shear cracking since it takes a larger shear force before the tensile strength of the concrete is reached. Moreover, the principal stress direction will change such that the shear cracks form with an angle less than 45° due to the axial force. (Collins & Mitchell, 1991)

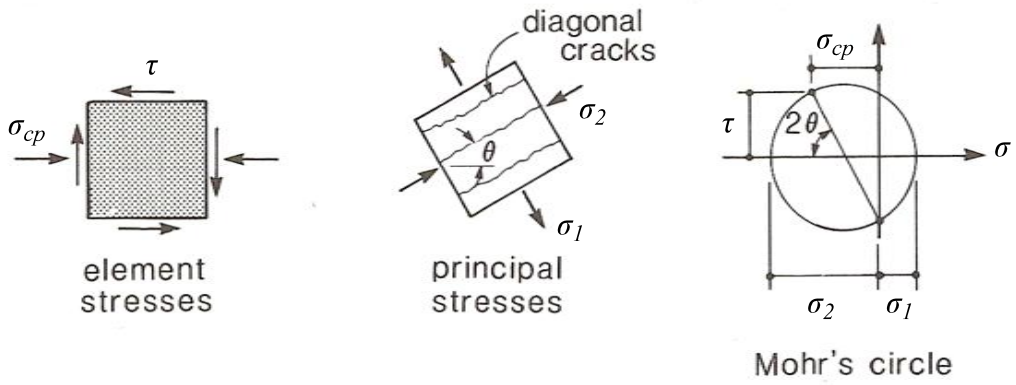

Figure 2.12 Stress state in element of prestressed beam. σ_{cp} is the axial compressive stress, σ_1 is the tensile principal stress, σ_2 is the compressive principal stress and τ is the shear stress. (Collins & Mitchell, 1991)

2.4.2 Failure modes

Shear sliding failure

This failure can occur in prestressed concrete as well. Since the cracking is delayed due to the arch effect the capacity with regard to this failure will be higher.

Web shear compression failure

With regard to web shear compression failure very high prestress has an unfavourable effect, since the principal compressive stress will increase significantly, although, a

moderate prestress will have a favourable effect due to the biaxial compression which occurs in the compressive struts. This behaviour is illustrated in Figure 2.14 in Section 2.6.2 regarding Eurocode 2, (CEN/TC250/SC2, 2004).

Web shear tension failure

When it comes to prestressed members, there exists another failure mode in addition to the ones mentioned previously for reinforced concrete members.

In the regions near the supports, in case of simply supported beams, there will be compressive stresses over the whole cross-section in the ultimate state; hence no flexural cracks can appear. Consequently, no flexural shear cracks can appear in the actual region. For members without shear reinforcement the higher critical load for web shear cracking leads to drastic crack propagation in prestressed concrete members. The explanation for this is that there is no possibility to obtain a new equilibrium when a shear crack occurs, since interlocking effects and friction are insufficient to transfer the higher shear force. A brittle 'web shear tension failure' is the result. However, if sufficient shear reinforcement is provided, a new equilibrium can be reached when web shear cracks appear. The governing failure mode is then shear sliding failure, which is more ductile.

In regions where flexural shear cracks appear there is no risk for web shear tension failure, even if no shear reinforcement is provided. The behaviour will be rather similar to that of regular reinforced concrete members, but with the difference that a higher load is required in order to initiate cracks. (Engström, 2009)

2.5 Design according to BBK 04

The code for structural design in Sweden, BBK 04 (Boverket, 2004), which is now being phased out states two different methods for design with regard to shear. The first one is based on a truss model with 45° strut inclination combined with a concrete contribution term which takes the effect of interlocking etc. into account. If the regarded member has no shear reinforcement the following design criterion is stated in BBK 04, Section 3.7.3.1:

$$V_{sd} \leq V_c \tag{2-2}$$

where

V_{sd} is the design value of the load effect from the shear force

V_c is the shear resistance of the concrete

The concrete contribution, V_c, is calculated according to an empirical expression and depends on cross-sectional geometry, amount of longitudinal reinforcement in the tensile zone and the concrete tensile strength.

If shear reinforcement exists in the member the following design criterion is instead stated in BBK 04, Section 3.7.4.1:

$$V_{sd} \leq V_c + V_s \tag{2-3}$$

where

V_{sd} is the design value of the load effect from the shear force

V_c is the 'concrete contribution' to the shear resistance

V_s is the shear reinforcement contribution in a truss model with 45° strut inclination

The shear reinforcement contribution, V_s, is obtained from the truss model in Figure 2.13.

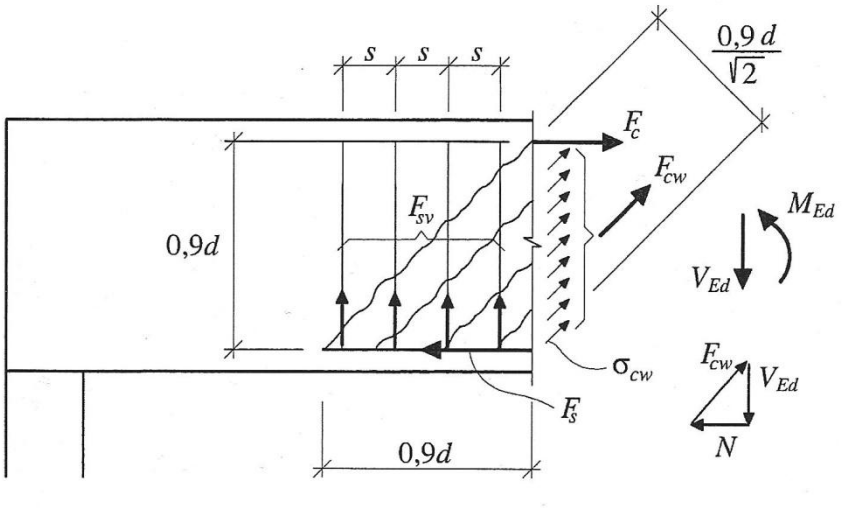

Figure 2.13 Truss model for beam with 45° crack angle.(Engström, 2007)

The effect on the shear resistance from a prestressing force can be regarded by adding a term, V_p, to the concrete term. The V_p term is calculated according to Equation (2-4).

$$V_p = \frac{V_{sd}}{1.2\gamma_n}\left(\frac{M_0}{M_d}\right)_{min} \tag{2-4}$$

where

M_0 is the decompression moment

M_d is the bending moment caused by the applied load

min indicates the minimum value of the ratio in the considered part

The increase of the force in the tensile reinforcement due to shear cracking is regarded in Section 3.9.2 in BBK 04 by dislocation of the tension force curve with a distance a_l which depends on the shear reinforcement amount. In this procedure a variable strut inclination is used instead of the 45° inclination which was used when the shear reinforcement amount was determined.

Also an alternative method for shear reinforcement design is presented in BBK 04. This method corresponds to the one in Eurocode 2, which is described more in detail in the next section. This method was not given in the previous version of the code, BBK 94, second edition (Boverket, 1998).

When it comes to evaluation of the load carrying capacity of existing bridges, the rules in the publication Vägverket (2009) should be applied in case of road bridges. Here, one of the two methods described above should be adopted.

For evaluation of existing railway bridges, the rules in the publication Banverket (2005) should instead be followed. This publication refers to the same methods as Vägverket (2009) above.

2.6 Design according to Eurocode 2

In Eurocode 2 (CEN/TC250/SC2, 2004), the shear resistance of reinforced and prestressed concrete members with shear reinforcement is determined by means of a truss model with variable strut inclination. This method takes account of plastic stress redistribution in the ultimate state, which can be controlled by the reinforcement arrangement. The choice of strut inclination is limited to the interval between 21.8° and 45°.

Furthermore it is not permitted to take advantage of the concrete contribution term, V_c, for members with shear reinforcement. It was considered that a pure truss model would be more transparent than a truss model combined with an entirely empirical concrete term, as in the first method in BBK 04. In addition, the laboratory tests, which the concrete contribution term is based on, do not entirely represent practice. Test specimens are usually small beams with rectangular cross-section but in real situations it is more common with thin-webbed members such as I-beams or box beams, for which the variable strut inclination model well describes the behaviour.

The contribution to the force in the tensile reinforcement due to shear force is handled in EC2 with a term ΔF_{td} which is added to the force caused by bending moment. This additional term depends on the strut inclination and it can easily be derived from the truss model used to design the shear reinforcement.

Structural improvements of bridges conducted by the Swedish Road Administration or Railway Administration should be performed according to Banverket & Vägverket (2009). The design method adopted in this publication is the one in EC2.

2.6.1 Shear sliding failure

In order to determine whether the shear capacity without shear reinforcement is sufficient, the criterion below is stated in EC2 with regard to shear sliding failure. This is an empirical expression for the concrete contribution including the effect of prestressing or other axial force.

$$V_{Ed} \leq V_{Rd,c} \tag{2-5}$$

where

$$V_{Rd,c} = \left[C_{Rd,c} k \left(100 \rho_1 f_{ck}\right)^{1/3} + k_1 \sigma_{cp} \right] b_w d \tag{2-6}$$

with a minimum of

$$V_{Rd,c} = \left(v_{min} + k_1 \sigma_{cp}\right) b_w d \tag{2-7}$$

$C_{Rd,c} = \dfrac{0.18}{\gamma_c}$ (national parameter)

$k = 1 + \sqrt{\dfrac{200}{d}} \leq 2.0$ with d in [mm]

$\rho_1 = \dfrac{A_{sl}}{b_w d} \leq 0.02$

A_{sl} area of fully anchored tensile reinforcement

f_{ck} characteristic value of the concrete's compressive strength [MPa]

$k_1 = 0.15$ (national parameter)

$\sigma_{cp} = \dfrac{N_{Ed}}{A_c} < 0.2 f_{cd}$

N_{Ed} design value of axial force, positive for compression

A_c cross-sectional area

b_w smallest width of the cross-section in the tensile area

$v_{min} = 0.035k^{3/2}f_{ck}^{1/2}$ (national parameter)

If this shear resistance is not sufficient, shear reinforcement is needed for the full shear force and the condition below should be fulfilled. This expression is based on a truss model with variable strut inclination

$$V_{Ed} \leq V_{Rd,s} \tag{2-8}$$

where

$$V_{Rd,s} = \frac{A_{sw}}{s} z f_{ywd} \cot\theta \tag{2-9}$$

A_{sw} cross-sectional area of shear reinforcement

s spacing of shear reinforcement

z internal lever arm ($\approx 0.9d$ for reinforced concrete without axial force)

f_{ywd} design yield strength of shear reinforcement

θ strut inclination ($21.8° \leq \theta \leq 45°$)

2.6.2 Web shear compression failure

It is also necessary to check the capacity with regard to web shear compression failure, for which the condition is:

$$V_{Ed} \leq V_{Rd,max} \tag{2-10}$$

where without shear reinforcement

$$V_{Rd,max} = 0.5 b_w d v f_{cd} \tag{2-11}$$

and with shear reinforcement

$$V_{Rd,max} = \alpha_{cw} b_w z v f_{cd} \frac{1}{\cot\theta + \tan\theta} \qquad (2\text{-}12)$$

$$v = 0.6\left(1 - \frac{f_{ck}}{250}\right) \qquad f_{ck} \text{ in [MPa]}$$

α_{cw} =1.0 for non-prestressed members (national parameter)

$= 1 + \sigma_{cp}/f_{cd}$ for $0 < \sigma_{cp} \le 0.25 f_{cd}$

$= 1.25$ for $0.25 f_{cd} < \sigma_{cp} \le 0.5 f_{cd}$

$= 2.5(1 - \sigma_{cp}/f_{cd})$ for $0.5 f_{cd} < \sigma_{cp} \le 1.0 f_{cd}$

b_w the minimum width between tension and compression chords

The influence of prestressing on the web shear compression failure is regarded by the factor α_{cw}, which is shown in Figure 2.14.

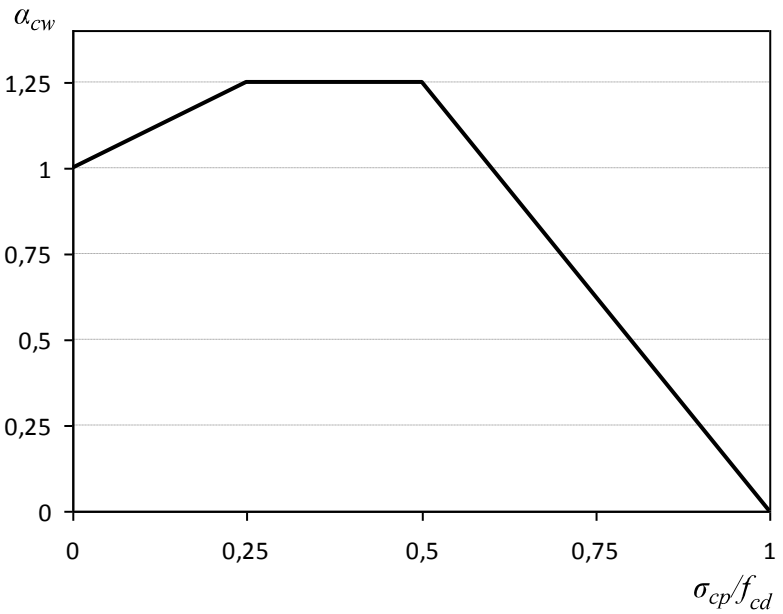

Figure 2.14 The factor α_{cw} as a function of the relation between the average concrete compressive stress and the concrete strength (CEN/TC250/SC2, 2004).

2.6.3 Web shear tension failure

In regions without flexural cracks in simply supported prestressed members without shear reinforcement the capacity with regard to web shear tension failure can be utilised according to EC2. Under these conditions the only shear crack which can occur is if the principal tensile stress in the web becomes larger than the tensile strength of the concrete. If this crack forms there is no possibility to obtain a new equilibrium, hence failure occurs. In order to check the capacity with regard to this failure mode the following condition should be fulfilled:

$$V_{Ed} \leq V_{Rd,cw} \tag{2-13}$$

where

$$V_{Rd,cw} = \frac{I \cdot b_w}{S} \sqrt{\left(f_{ctd}\right)^2 + \alpha_l \sigma_{cp} f_{ctd}} \tag{2-14}$$

I second moment of area

b_w width of the section at the centroidal axis

S first moment of area above and about the centroidal axis

f_{ctd} design value of the concrete tensile strength

$\alpha_l = \frac{l_x}{l_{pt2}} \leq 1$ (for pretensioned tendons)

$\alpha_l = 1.0$ (for other types of prestressing)

2.7 Comparison between calculation methods

The main differences between the methods for shear reinforcement design in BBK 04 and EC2 are that BBK 04 utilises a truss model with a fixed strut inclination combined with a concrete contribution term, while EC2 utilises a variable inclination truss model without a concrete contribution term. However, BBK 04 is not consistent in the use of this method. When it comes to the additional force in the tensile reinforcement due to the shear force BBK 04 recommends the use of a variable inclination and the concrete contribution cannot be utilised in this case. In EC2 on the other hand it is more consistent and due to the use of a pure truss the relation between shear reinforcement design and design of anchorage of the tensile reinforcement can easily be understood.

The procedure for calculating the capacity without shear reinforcement is also somewhat different in the two methods.

3 Overview of present strengthening methods

This chapter presents various strengthening methods with regard to shear capacity. This overview regards both solutions for slabs and beams.

3.1 Strengthening with fibre reinforced polymer

A widely spread material for strengthening concrete members is fibre reinforced polymer (FRP) which is composite materials made of a polymer matrix reinforced with fibres. The fibres are usually glass, carbon or aramid, while the polymer is usually an epoxy, vinylester or polyester thermosetting plastic.

For strengthening the material is available in the form of rods similar to the elaboration of reinforcement steel, strips which are unidirectional with thickness in the order of 1 mm, sheets or fabrics that are flexible and have fibres in either one or at least two different directions. These are being bonded either externally or internally to the concrete member.

These composites have many advantages in comparison to for example steel, e.g. the composites cannot corrode, the weight is about one fourth of steel and it has higher tensile strength. However, the behaviour of the composites is linear elastic up to failure and no yielding occurs; hence the failure is brittle, as seen in Figure 3.1. The material is sensitive to fire since its binder, resin, is organic (fib , 2001).

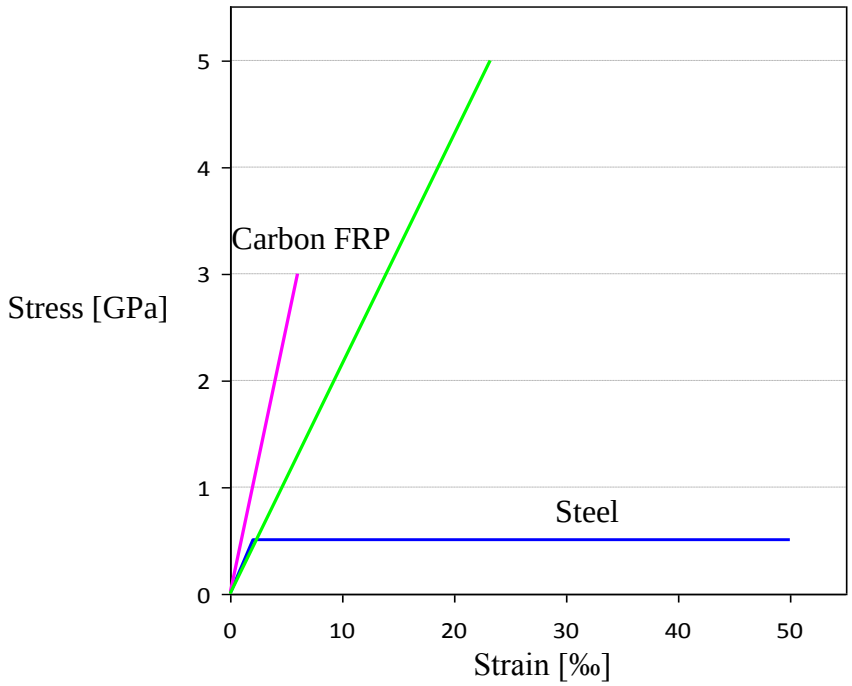

Figure 3.1 Stress-strain diagrams for CFRP (carbon FRP) and steel. (fib , 2001)

3.1.1 Externally mounted

Shear strengthening of concrete members can be done by bonding FRP strips, sheets or fabrics externally to the concrete surface. To maximize the efficiency of the strengthening the FRP should be mounted with the fibre direction as parallel as practically possible to the maximum principal tensile stresses. In shear critical zones the stress trajectories form an angle that is roughly equal to 45˚ to the member axis. However, for practical reasons the FRP strips are normally attached with the fibre direction perpendicular to the member axis. Figure 3.2 shows two examples of configurations along a beam. Figure 3.3 shows examples of arrangements in the cross-section. Depending on practical conditions, such as accessibility and strengthening requirements, the member can be strengthened either by side bonding, U-jacketing or wrapping, as is shown in Figure 3.3. (Triantafillou, 2006)

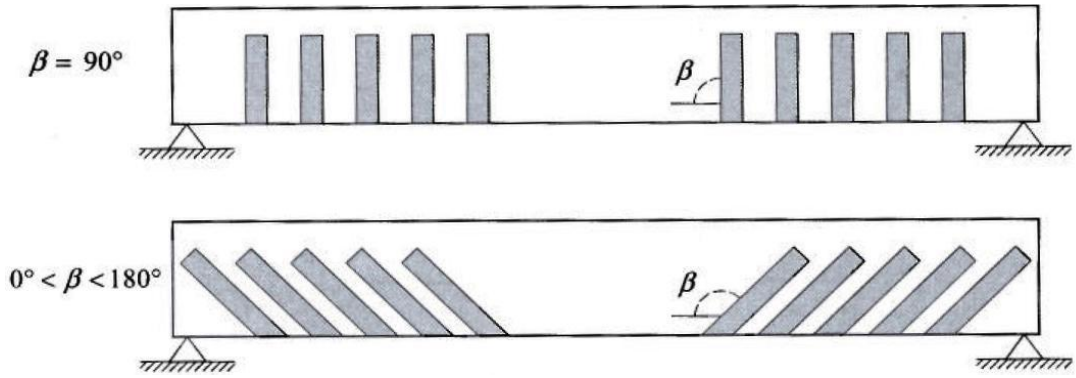

Figure 3.2 Alternative configurations of FRP strips for shear strengthening along a beam.(Monti, 2006)

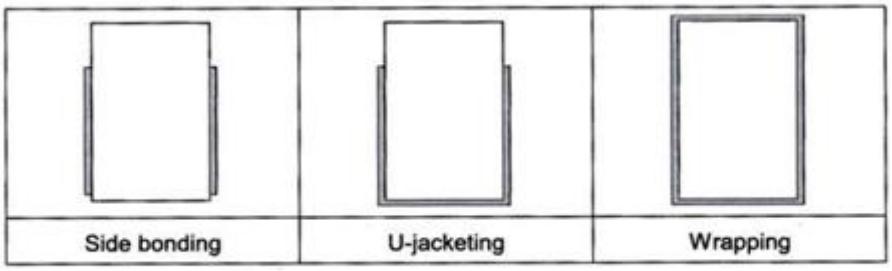

Figure 3.3 Alternative arrangements of FRP strips/sheets or fabric for shear strengthening in the cross-section (Monti, 2006).

To strengthen slabs by means of this method would be difficult since the slab is much wider than a beam. Therefore the distance between the vertical FRP units would be too large to affect the inner part of the slab.

Another strengthening approach using FRP strips is to bond them onto the tensioned face of a member. This method has been studied by Esfahani et al. (2009), where the punching shear failure of slabs was in focus. A load concentrated on a small area, representing a column support, was applied in the centre of a slab. Carbon FRP strips were bonded onto the tension face in order to act as additional tensile reinforcement,

see Figure 3.4. As mentioned in Section 2.6.1 the reinforcement ratio ρ influences the capacity with regard to shear sliding failure. ρ considers the tying effect and also in some cases the dowel effect. The tying effect prevents flexural shear cracks from opening and friction between the crack interfaces can be utilised. According to the paper a significant increase of the punching shear capacity was found. Furthermore, rather good correspondence with the British code BS 8110 was achieved by adopting an equivalent reinforcement ratio, where both the internal steel and the external carbon FRP were regarded.

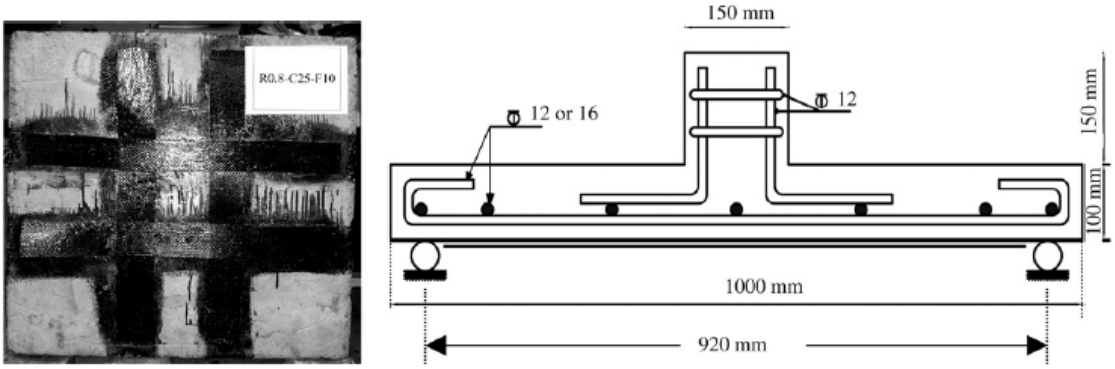

Figure 3.4 Details of specimen and position of carbon FRP on slabs.(Esfahani et al., 2009)

To strengthen slabs with this method would mean that the carbon FRP strips would have to be mounted on the upper surface of the slab over interior and frame supports, consequently the road topping would have to be removed. An exception is the case of a simply supported slab where the whole bottom side of the slab is tensioned. Also a continuous slab would have a tensioned bottom side near the end supports.

It is also possible to bond the FRP onto the concrete surface in a pre-tensioned state. According to Section 2.4 longitudinal prestressing can give a favourable contribution to the shear capacity. By pre-tensioning strips and bonding them longitudinally to the concrete member, see Figure 3.5, beneficial effects will be obtained and the shear capacity will be enhanced. The concrete at the ends of the strips will be subjected to large stresses. It is therefore important to anchor the strips properly with suitable anchorage devices. (Triantafillou, 2006)

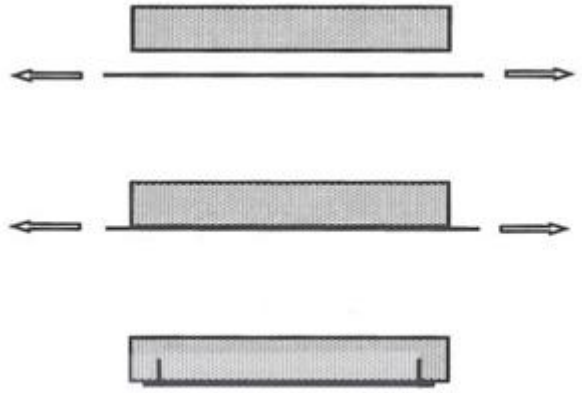

Figure 3.5 Strengthening with pre-tensioned FRP strips: a) pre-tensioning b) bonding c) end anchorage and release of prestressing force upon hardening of the adhesive (Triantafillou, 2006).

Various tests with external pre-tensioned fibre composites have been made. Mukherjee & Rai (2008) loaded an under-reinforced concrete beam and repaired it by using pre-tensioned FRP. When the beam was loaded, bending cracks developed and at higher load levels shear and flexural shear cracks near the ends appeared. Failure in the beam occurred due to yielding of the reinforcing steel. To enhance the shear capacity carbon FRP wrapping was applied in the shear critical zone, see Figure 3.6 b). The wrapping also provides anchorage for the longitudinal pre-tensioned carbon FRP sheet, called laminate in Figure 3.6 a). The carbon FRP sheet was pre-tensioned with a specially designed pre-tensioning machine that works according to Figure 3.6 a). The bottom face of the beam was cleaned with air blower and acetone for better adhesion. An adhesive was uniformly spread over the top face of the sheet and it was pressed against the beam. The set up was left for curing of the adhesive and the prestressing force was released on the sixth day.

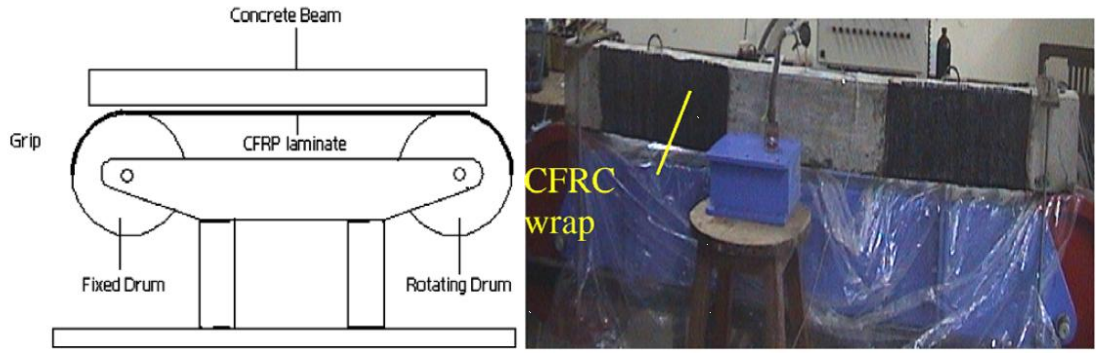

Figure 3.6 Strengthening with pre-tensioned FRP sheets. a) Schematic figure of pre-tensioning machine. b) Pre-tensioning in progress. (Mukherjee & Rai, 2008)

The method cannot directly be applied on slabs, because it is not possible to use wrapping as anchorage in the same way. It would be difficult to apply the method on a

bridge slab because of the pre-tensioning machine's inability to access the slab ends. The pre-tensioning machine's mobility is also a critical question.

Another way to prestress concrete bridges is to apply externally post-tensioned carbon FRP tendons as presented by Matta et al., (2007). The idea is to apply the tendons to the bottom side of a concrete slab. The system consists of un-bonded carbon FRP bars with a live and a dead end stainless steel anchor and a deviator see Figure 3.7. By means of operating a turnbuckle at the live end the tendon is post-tensioned. The purpose with the deviator is mainly to reduce the deflection, since it will give an additional negative bending moment but it has no influence on the shear capacity. The prestressing force can also be increased by extending the deviator. Since procedures such as bonding of FRP sheets, as Mukherjee & Rai (2008) did, and use of hydraulic jack is avoided, the system is less time consuming.

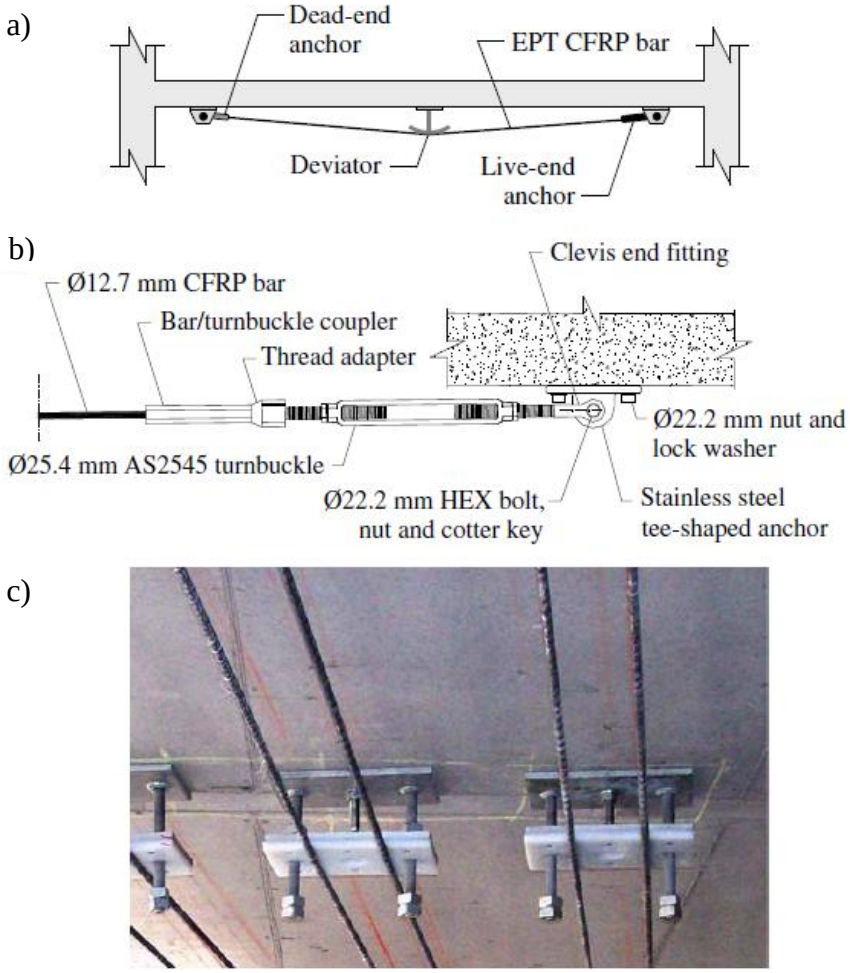

Figure 3.7 Strengthening system with externally post-tensioned carbon FRP bars: a) Configuration, b) Live-end anchor, c) Deviator at bottom side of concrete slab. (Matta et al., 2007)

3.1.2 Internally mounted

By drilling holes in the concrete member it is also possible to mount the reinforcement internally. It is preferable to use high strength reinforcement to minimize the amount; hence fewer holes will be drilled.

Bayrak & Binici (2006) suggest to drill holes through the depth of the slab in order to let carbon FRP strips pass through, see Figure 3.8. The carbon FRP strips are arranged to form closed links around the height of the section and consequently no transmission length is needed for anchorage of the FRP strip. This will efficiently enhance the shear capacity. The holes are later filled with epoxy and left for curing.

By using a rather similar method, Sissakis & Sheikh (2007) managed in their experimental study to increase the punching shear capacity with up to 82 %. Also here carbon FRP strips were arranged as closed links.

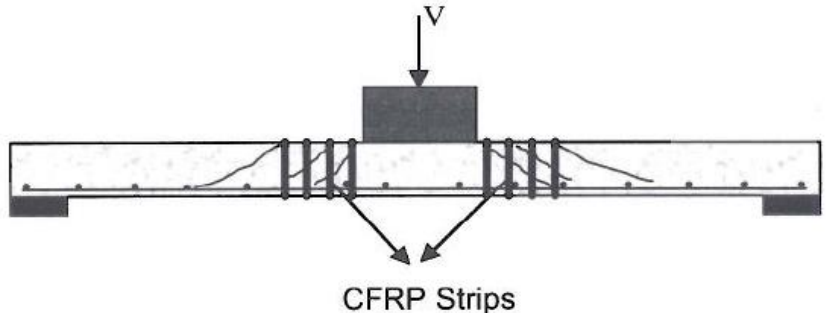

a)

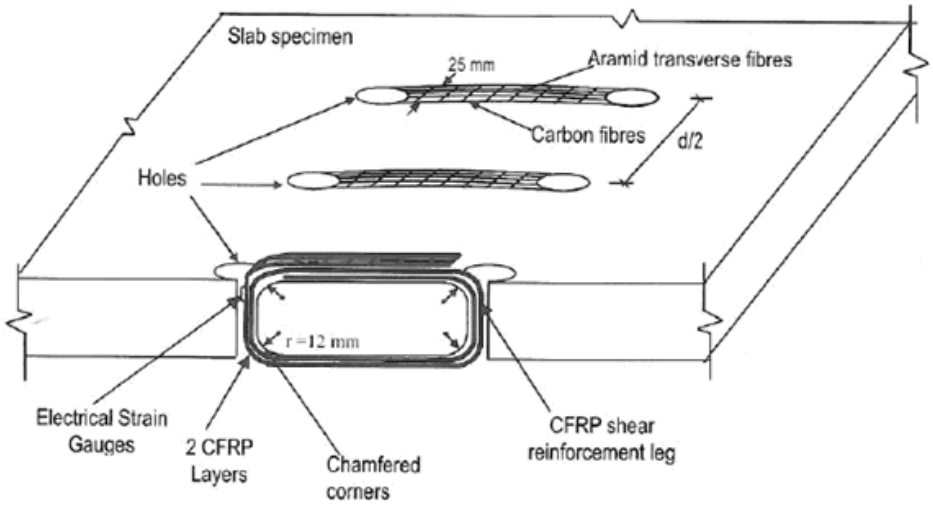

b)

Figure 3.8 Installation of internal closed links of carbon FRP strips: a) elevation view b) 3D view. (Bayrak & Binici, 2006)

Installing such closed links in a bridge slab would result in having to remove large parts of the road topping.

3.1.3 Near surface mounted

When applying near surface mounted reinforcement, slots are cut by sawing in the concrete face wherein reinforcement bars are placed and bonded, as seen in Figure 3.9, using either epoxy or cement mortar. The slots are sawn shallowly which means that the reinforcement will be exposed to the external environment; hence carbon FRP bars are preferred instead of steel bars for this application. In addition, the carbon FRP bars are much more lightweight than steel and can easily be tailor made for a specific application. (Täljsten, 2002)

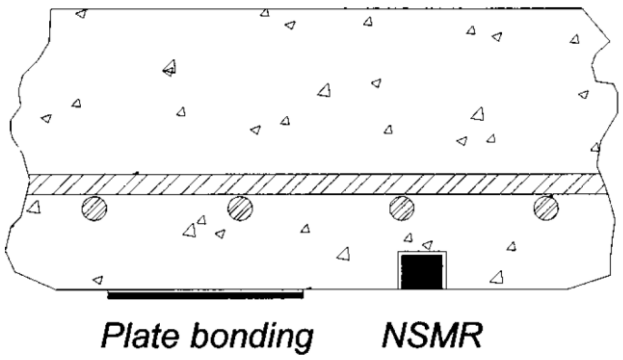

Figure 3.9 Location of an externally mounted plate and near surface mounted reinforcement. (Nordin & Täljsten, 2006)

There are many advantages with near surface mounted reinforcement compared to e.g. plates mounted externally, as shown in Figure 3.9. Near surface mounted reinforcement exhibits better bond properties, better fire resistance and less aesthetic disturbance.

An application of near surface mounted carbon FRP rods is presented by De Lorenzis & Nanni (2001). Here, eight reinforced concrete T-beams were tested. Six of them were strengthened with FRP rods mounted vertically or in 45° angle to the longitudinal axis of the beam and the remaining two were left as reference beams. The slots where the rods were placed were cut in the webs of the beams according to Figure 3.10. In two of the beams, holes were also drilled in the flanges so that the rods could continue through the whole height of the beam. In order to bond the rods to the concrete, epoxy was applied in the slots.

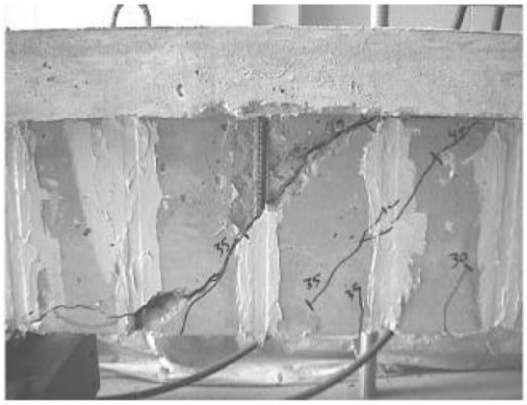

Figure 3.10 Beam with vertical near surface mounted carbon FRP rods after shear failure. (De Lorenzis & Nanni, 2001)

Figure 3.11 Beam with inclined near surface mounted carbon FRP rods after shear failure. (De Lorenzis & Nanni, 2001)

In general, this strengthening method showed good ability to increase the shear capacity. In most of the beams where the FRP rods were inserted in the web only, failure occurred by splitting of the epoxy cover as seen in Figure 3.10 and Figure 3.11. The procedure of anchoring the rods also in the flange proved to be an effective way of preventing failure of the bond between the rods and the epoxy. In this case the failure mode instead became de-bonding of the concrete cover of the longitudinal reinforcement due to, as they described it, dowel action forces. The beam with this set up achieved an increase in capacity of 106 % compared to the reference beam. This was the highest strengthening effect among the tested beams.

De Lorenzis & Nanni (2001) also present a simple calculation model which can be used in order to obtain the shear resistance of a beam strengthened with near surface mounted carbon FRP rods.

This method could be suitable for slabs if the rods instead are mounted internally in drilled holes. In this way a failure mode concerning de-bonding of the epoxy cover will be prevented. In order to avoid interference with the road topping it is preferable to drill the holes from below the slab.

Wang et al., (2009) performed strengthening with pre-tensioned carbon FRP bars on the Erhutou Bridge in China. It is a single span beam bridge with 8 main T-shaped reinforced concrete beams constructed in 1986. Because of various damages on the bridge strengthening was required. The strengthening procedure started by cutting grooves in the bottom face of the beam and cleaning them, see Figure 3.12 a). Then the beam was compressed with external steel tendons by using a hydraulic jack, see Figure 3.12 b). In the next step the carbon FRP bars were embedded in the grooves and grouted with epoxy adhesive, see Figure 3.12 c). Finally, the grooves were closed and the external steel tendons were released. The carbon FRP bars were in this way tensioned and a corresponding prestressing force acted on the concrete member which enhances the shear capacity

a) b) c)

Figure 3.12 Steps during strengthening: a) Cutting the groove, b) compressing the beam, c) Grouting and embedding of FRP rods. (Wang et al., 2009)

3.2 Strengthening with steel

Even though FRP has many advantages, as discussed in Section 3.1, steel is also used in some strengthening methods. In Öberg's (1990) Ph. D thesis a method for shear strengthening by means of post-tensioned steel wires is tested. The tests were mainly applied on beams. Also five slab specimens with the width 0.9 m were tested. The specimens were provided with $\phi = 6$ mm steel wires, either with the strength of $f_{0.2} = 325$ MPa or 1618 MPa $< f_{0.2} <$ 1630 MPa. The wires were either mounted with a 45˚ or a 90˚ angle towards the longitudinal axis. The specimens had either one or two rows of wires, Figure 3.13.

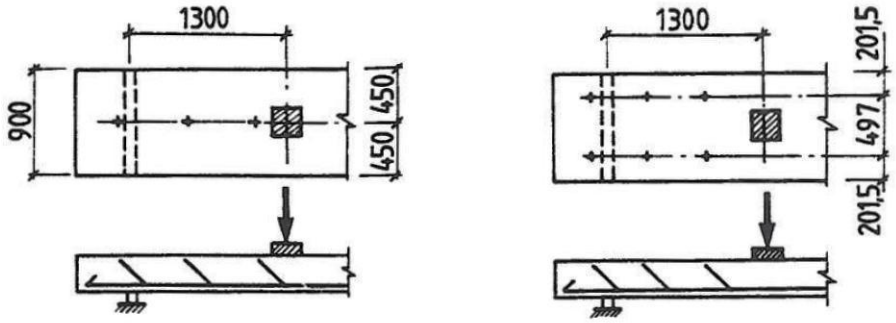

Figure 3.13 Location of post-installed shear reinforcement. (Öberg, 1990)

At casting of the specimens, recesses were made in forms of circular holes. After curing of the concrete the wires were mounted in the holes, post-tensioned and then the holes were filled with mortar, see Figure 3.14.

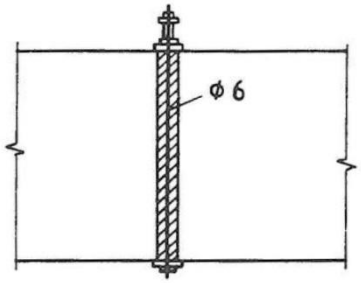

Figure 3.14 Recess with prestressing wires and filled with mortar. (Öberg, 1990)

The prestressing force was achieved through a system of a linkage member, nut, bolt and lock washer, which enables post-tensioning without twisting of the wire. Figure 3.15 shows the active anchor of an inclined wire, but the system is similar for a vertical unit.

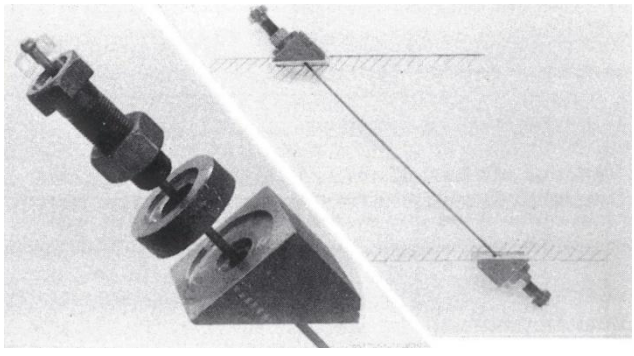

Figure 3.15 Prestressing system for an inclined reinforcement unit. (Öberg, 1990)

The calculated contribution to the shear resistance of inclined or vertical post-tensioned wires is illustrated in Figure 3.16 and Figure 3.17. The mechanical shear reinforcement ratio, ω_v, is defined as:

$$\omega_v = \frac{f_{sv}\, A_{sv}}{f_{cc} \cdot b \cdot s \cdot \sin\beta} \tag{3-1}$$

For non-tensioned wires the inclined wire arrangement acquires higher shear capacity than the vertical wire arrangement for $\omega_v > 0.05$ as shown in Figure 3.16. Though for post-tensioned wires, shown in Figure 3.17, the vertical arrangement gives higher shear capacity for $\omega_v > 0.18$.

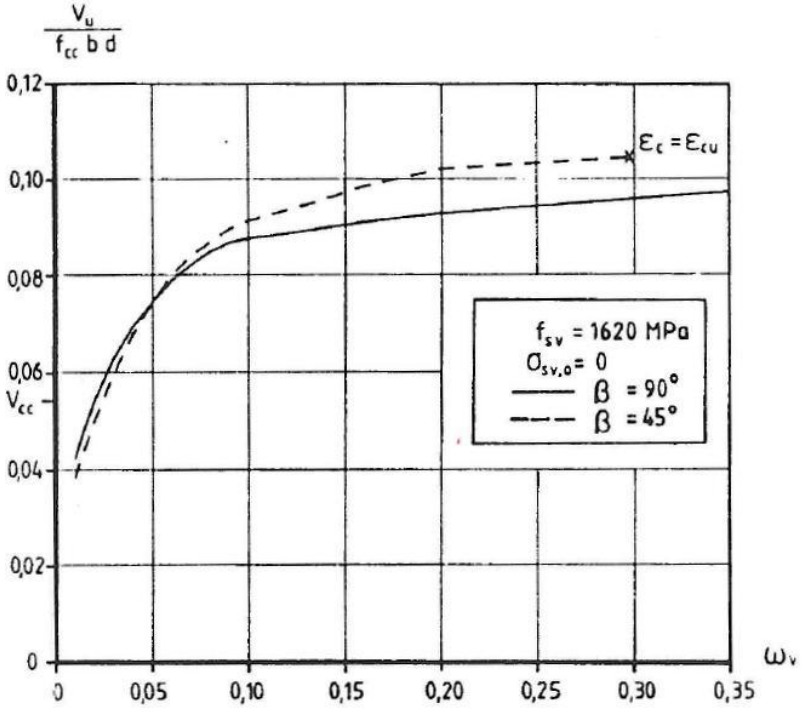

Figure 3.16 The influence of the inclination β of post-installed wires on the shear capacity V_u of various mechanical shear reinforcement ratios ω_v. Steel quality f_{sv}=1620 MPa, prestressing $\sigma_{sv,o}$= 0. (Öberg, 1990)

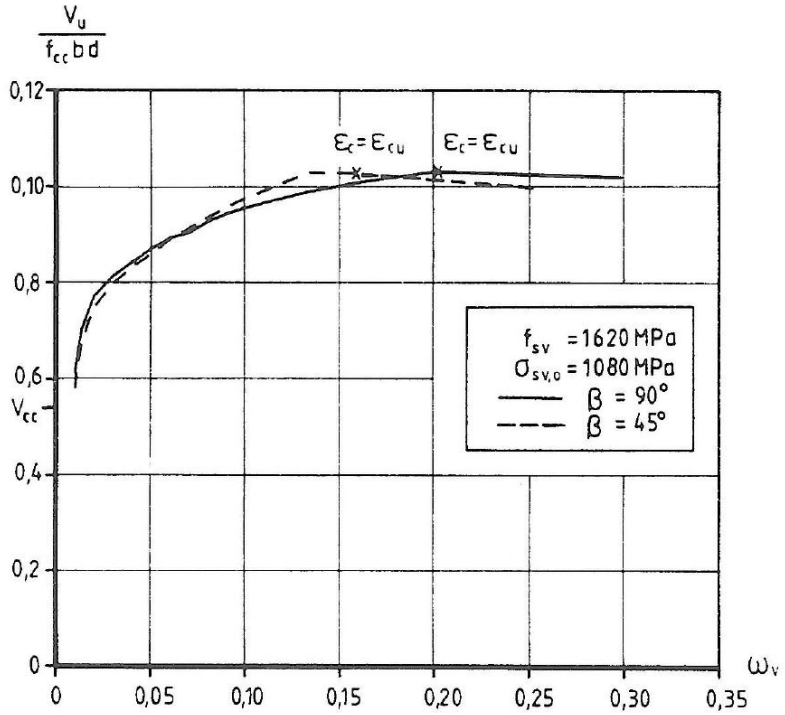

Figure 3.17 The influence of the inclination β of post-installed wires on the shear capacity V_u at various mechanical shear reinforcement ratios ω_v. Steel quality f_{sv}=1620 MPa, prestressing $\sigma_{sv,o}$=1080 MPa. (Öberg, 1990)

The calculated shear capacity corresponded well to the measured. Figure 3.18 illustrates the measured, V_{ue}, and the calculated, V_{uc}, shear capacity and the mean ratio between them is m_v= 1.001.

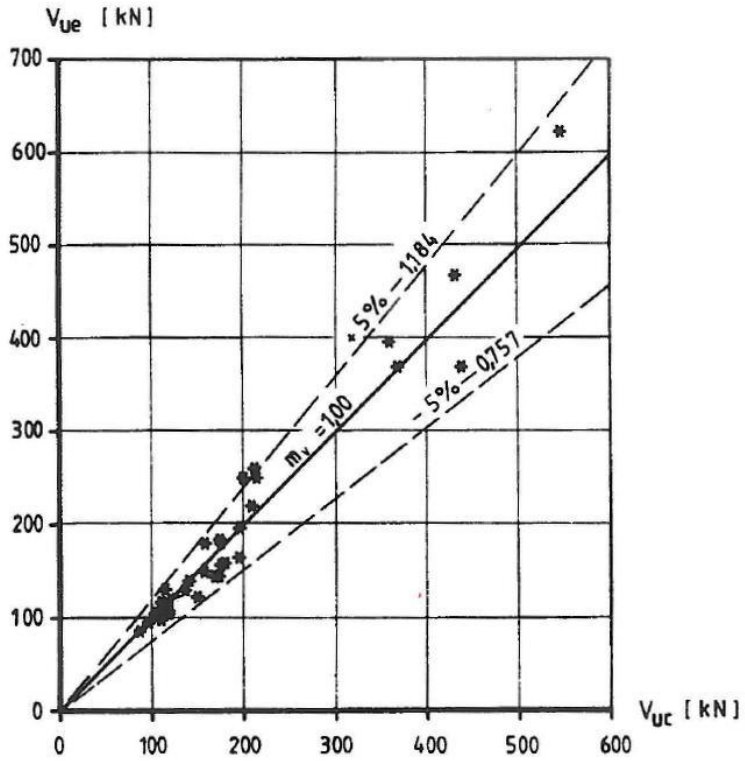

Figure 3.18 Measured, V_{ue} and calculated, V_{uc} shear capacity for specimens. (Öberg, 1990)

As presented in Figure 3.17 in the case of post-tensioned wires, there is no great advantage to install inclined wires in comparison to vertical wires in ultimate limit state. Also with this method, parts of the road topping needs to be removed in order to install the upper anchor in the prestressing system. To avoid this, some kind of internal anchor is preferable.

3.3 Strengthening with fibre reinforced mortars

Fibre reinforced mortars (FRM) is a composite consisting of continuous fibre-based textiles and mortars. It has the same favourable properties possessed by FRP except for that in FRM the binder is inorganic cement-based mortars and has good resistance to fire.

Triantafillou & Papanicolaou, (2006) present a shear strengthening method with textile reinforced mortars. By wrapping the beam with layers of textile reinforced mortars at the ends to form so called jackets, the shear resistance is increased. The application of the textile reinforced mortars is shown in Figure 3.19. Applying textile reinforced mortar jackets on a beam bridge would be difficult since the slab would hinder the jackets to enclose the beam. To apply textile reinforced mortar jackets around a slab would be useless because it would not give the desired effect distributed across the width of the slab section.

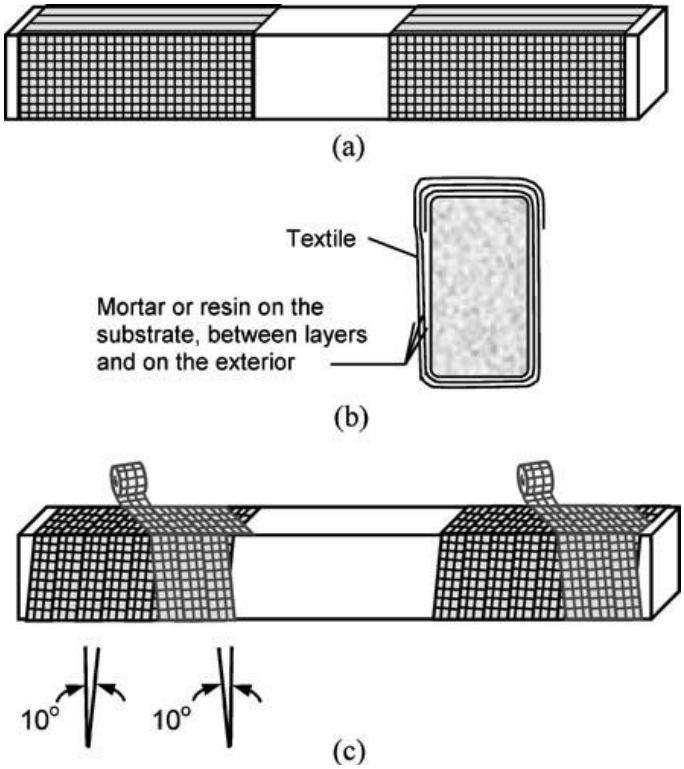

Figure 3.19 Application of the textile-reinforced mortar jackets in the shear spans a) conventional jacket, b) layers of textile and mortar or resins, c) spirally applied strips (Triantafillou & Papanicolaou, 2006).

4 Possible strengthening methods for bridge slabs

This chapter presents the most promising strengthening methods described in Chapter 3 adapted for strengthening of bridge slabs. In this chapter, implementation in practice and mechanical behaviour of these further developed methods are described. Also what requirements the methods need to fulfil are presented in this chapter.

4.1 Requirements

In order to adapt the strengthening methods to make them suitable for bridge slabs they need to fulfil special requirements. The foremost requirement is to sufficiently enhance the shear capacity of concrete bridge slabs. To verify that the strengthening methods enhance the shear capacity sufficiently, calculations should be performed according to EC2, as described in Section 2.6, or according to other similar well motivated calculation procedures.

For a strengthening method to work appropriately on a concrete slab it needs to be applied along the whole width of the slab. Namely, to apply strengthening only on the outer vertical faces of the slab will not enhance the shear capacity in the whole slab section.

The strengthening methods must also meet the specific requirements for each case. As an example, if the bridge in question has a requirement on the vertical clearance, it is not possible to choose a strengthening method which involves mounting of parts on the bottom side of the structure that violate this requirement.

In the design of a shear strengthening method it is important to consider the capacity of the existing tensile reinforcement. The actual capacity must be considered in the choice of the strut inclination in the truss model used to calculate the shear capacity. For example, to choose a flat strut inclination would result in a larger tensile force in the longitudinal reinforcement than what a steep strut inclination would, see Figure 4.1.

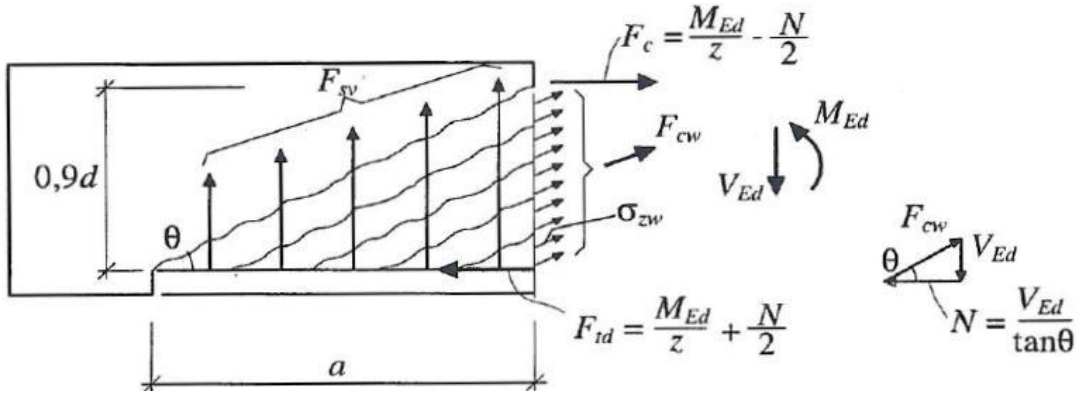

Figure 4.1 Truss model for calculation of the actual tensile force in a part of a slab with inclined shear cracks.

According to Figure 4.1 the actual tensile force can be calculated as:

$$F_{td}(x) = \frac{M_{Ed}(x)}{0.9d} + \frac{V_{Ed}(x)}{2\tan\theta} \leq \frac{M_{Ed,max}}{0.9d} \tag{4-1}$$

Capacity in tensile reinforcement:

$$F_{td}(x) \leq F_{sy}(x) \tag{4-2}$$

where

x is any section along the slab length

To assure that the chosen strut inclination does not contribute to a tensile force greater than the capacity of the tensile reinforcement it is required to perform the check in Equation (4-2). In order to find an appropriate strut inclination iteration is necessary. In addition, the bars must be fully anchored in the section where the check is performed.

If the applied strengthening method involves insertion of components which will be included in the truss model, it is necessary to observe the requirements for appropriate behaviour of the truss model. For example if vertical components acting as shear reinforcement are inserted, they need to be fully anchored in the tension and compression zones.

It is important to regard the compatibility between existing and added materials when a structure is retrofitted. It is common in the case of reinforced concrete slabs with a need for shear strengthening that no shear reinforcement exists before strengthening. In this case it is sufficient to regard the compatibility between the existing concrete and the added material.

If shear reinforcement is present in the existing structure on the other hand, some additional issues must be regarded. When new components are inserted in an existing structure they will have no strain at the same point as the existing reinforcement has an initial strain, see Figure 4.2. Due to this it is not certain that the ultimate capacities of the different components can be added. Instead, it is necessary to know the magnitude of the strain in the existing reinforcement when the new components are inserted. With this information known the strain caused by further loading of the structure can be added to the initial strain of the existing reinforcement and to the zero strain of the inserted component if they both have the same strain localisation. In order to attain full utilisation of the inserted material there must be sufficient capacity of plastic redistribution in the existing reinforcement, so that this does not reach its ultimate strain prior to the inserted material.

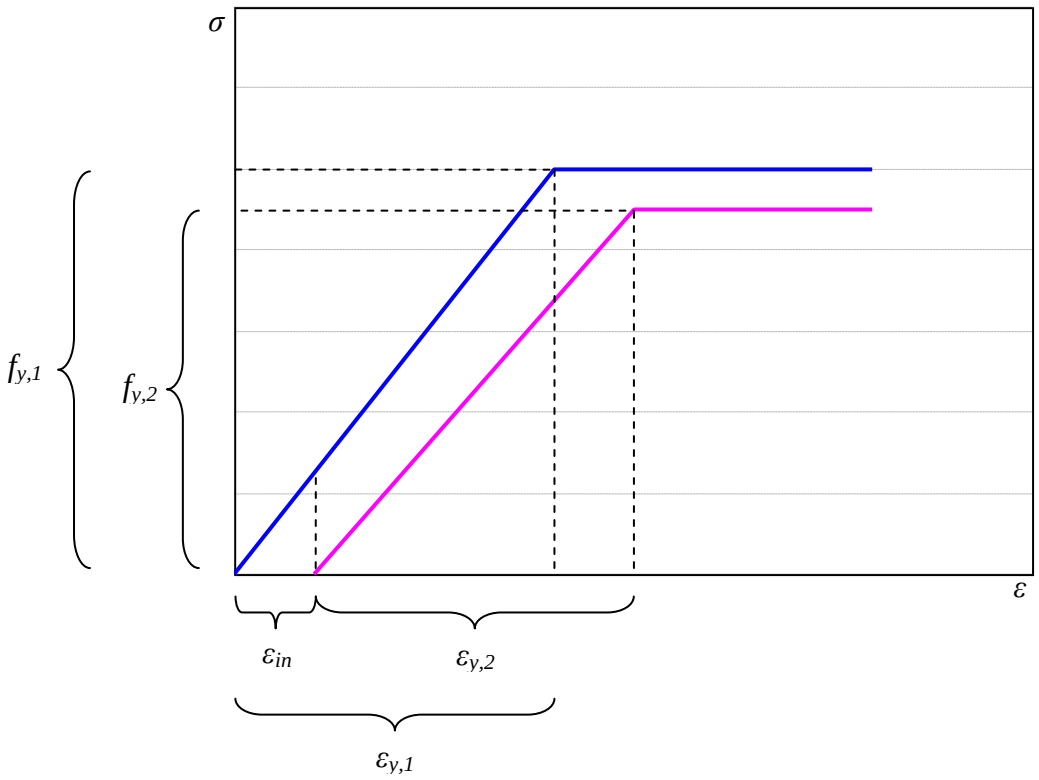

Figure 4.2 Example of stress-strain relation for existing (blue) and inserted (pink) material. The existing material has an initial strain ε_{in} when the new material is inserted. $f_{y,1}$ and $f_{y,2}$ are the yield strengths of the existing and added material, respectively. $\varepsilon_{y,1}$ and $\varepsilon_{y,2}$ are the yield strains of the existing and added material, respectively.

If there is a large difference in stiffness between the added and the existing material the contribution from the less stiff one to the total stiffness will be small or even negligible. Thus it is preferable if the added material is equally or more stiff than the existing in order to efficiently increase the capacity of the structure in question.

Furthermore, in order to distinguish which method is most suitable for a certain situation desirable properties must also be identified. This is treated in Section 5.2 for the actual case.

4.2 Method 1 – Near surface mounted longitudinal post-tensioned carbon FRP

The first method which has been chosen is strengthening with near surface mounted carbon FRP bars mounted longitudinally on the bottom side of the slab. In order to increase the shear capacity the bars will be post-tensioned and anchored at the ends of the slab. The procedure is inspired by Wang et al. (2009) whose method was described in Section 3.1.3. However, modifications based on own ideas have been made and the method described here has many differences from the original one described in Section 3.1.3. This method can beneficially be applied to slabs and the

effect on the shear resistance from an axial prestressing force can easily be handled theoretically.

4.2.1 Implementation in practice

Grooves are sawn in the concrete surface along the bottom side of the slab with an appropriate spacing in the transversal direction. At the frame corner holes are drilled from the outside with a slight inclination such that they meet the grooves according to Figure 4.3. It should be possible to insert a carbon FRP bar through the groove from one end of the slab to the other. The inclination of the drilled hole is performed in order to reduce eccentricity of the tendon force when post-tensioning is applied. The bend which is obtained where a hole meets a groove is chamfered in order to minimise stress concentrations in the bar. Furthermore, a protective tube is inserted in the region of the bend in order to reduce friction. The bars are inserted and anchored in one end and in the other a post-tensioning force is applied after which this end is anchored as well. Finally the remaining voids of the grooves are grouted.

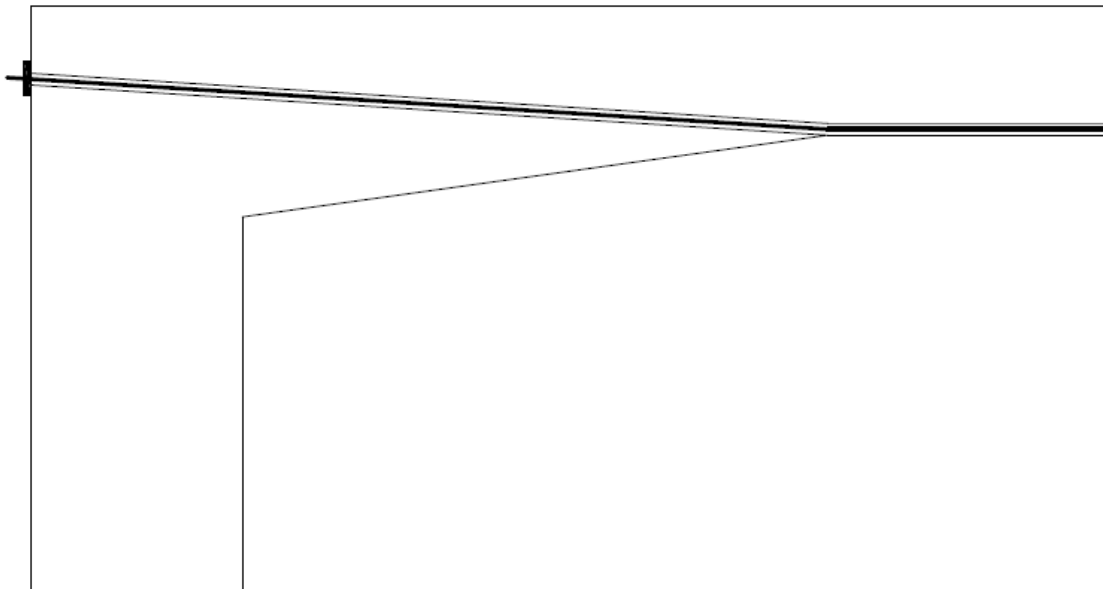

Figure 4.3 Tendon configuration at support.

The method in question is best suitable for structures in one span since it would be difficult to accomplish a continuation of the FRP bar through a middle support in the case of a continuous slab. Furthermore, the method should be applied to frame bridges since in the case of a simply supported slab it might be difficult to access the ends of the slab due to the location of the supports, as seen in Figure 4.4.

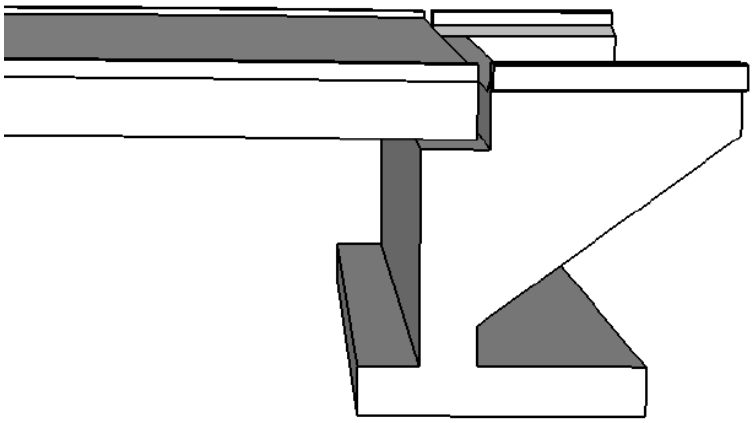

Figure 4.4 Common arrangement of support of a simply supported slab.

4.2.2 Mechanical behaviour

The behaviour of a member strengthened with this method should be similar to an ordinary post-tensioned member; hence the capacity increase can be considered according to EC2. A prestressing force applied in the longitudinal direction of a slab without shear reinforcement can increase the capacity with regard to shear sliding failure by delaying flexural shear cracks due to the arch effect. The effect on the capacity with regard to shear sliding failure is handled in EC2 with an additional term including the average longitudinal compressive stress σ_{cp} as seen in Equation (4-3).

$$V_{Rd,c} = \left[C_{Rd,c} k \left(100 \rho_l f_{ck}\right)^{1/3} + k_1 \sigma_{cp} \right] b_w d \tag{4-3}$$

In a case where shear reinforcement exists the capacity is determined by yielding of the reinforcement according to Equation (4-4) and the post-tensioning has no influence on this. However, if the concrete's capacity $V_{Rd,c}$ can be increased above this value due to post-tensioning it would be possible to take account of the prestressing effect.

$$V_{Rd,s} = \frac{z \cot \theta}{s} f_{ywd} A_{sw} \tag{4-4}$$

In addition, if flexural cracks can be prevented in region near the supports of prestressed single span members, it is according to EC2 possible to utilise the capacity with regard to web shear tension failure calculated according to Equation (4-5). However, an existing structure could be cracked in flexure prior to applying post-tensioning and it might not be safe to assume that this concrete behaves similarly to uncracked concrete even if calculations show that the cracks will be held together by

the post-tensioning. Consequently it is recommended that the state of the concrete is evaluated before the capacity with regard to web shear tension failure is allowed to be utilised.

$$V_{Rd,cw} = \frac{I \cdot b_w}{S} \sqrt{\left(f_{ctd}\right)^2 + \alpha_l \, \sigma_{cp} f_{ctd}} \tag{4-5}$$

Furthermore it is important to consider the risk for tensile stresses caused by restraints. Due to this it is questionable to rely on that the concrete will remain uncracked in the case of frame bridges, which are statically indeterminate.

Also the capacity with regard to web shear compression failure is influenced by an axial compressive stress according to Equation (4-6). In case of moderate prestressing the compressive strength of the struts will be increased due to the biaxial stress state, compare with Section 2.6.2.

$$V_{Rd,max} = \alpha_{cw} b_w z \nu_1 f_{cd} \frac{1}{\cot\theta + \tan\theta} \tag{4-6}$$

4.2.3 Discussion

Mechanically this is a rather simple method. An axial compressive force increases the shear capacity in a straight forward way and the result should be reliable. The behaviour of the strengthened structure should to a large extent correspond to a regular post-tensioned structure.

One critical issue with this method is that an additional load is applied on the structure due to the eccentricity of the tendon force in the regions near the supports. This effect is reduced by the inclination of the tendon near the ends; however, there will still be regions where the moment caused by the eccentricity of the tendon force will give unfavourable effects with regard to the moment capacity. For this method to be applicable it is necessary that this additional load effect can be resisted and this has to be evaluated for each case individually.

Another potential risk with regard to serviceability is that there are stress concentrations in the concrete at the bend where a hole meets a groove. In this region there is a risk of large tensile stresses in the concrete surrounding the tendon which could cause cracks and consequently corrosion of the existing reinforcement.

In the region where the tendons are anchored there is a risk of local concrete compression failure. The force needs to be distributed over a sufficiently large area in order to avoid this failure. In addition, this force causes a risk of splitting of the concrete due to the tensile stresses which develop when the stress field spreads.

4.3 Method 2 – Vertical post-tensioned steel wires with external anchors

This method is inspired by Öberg's method described in Section 3.2. The method has been tested and has shown good strengthening properties and it can directly be applied to slabs. However, the calculations in Öberg (1990) were not performed according to the truss model adopted in EC2 and due to this the design procedure is here modified in order to relate the method to the truss model. In addition, it is chosen here to only regard vertically installed wires, since it was shown that the inclination, as mentioned in Section 3.2, had a small effect on the capacity in the ultimate limit state (Öberg, 1990).

4.3.1 Implementation in practice

In this case the active anchor will be mounted on the bottom side of the slab in order to not interfere too much with the road topping and to give the active anchor more space. The holes for the steel wires will be drilled vertically through the whole depth of the slab.

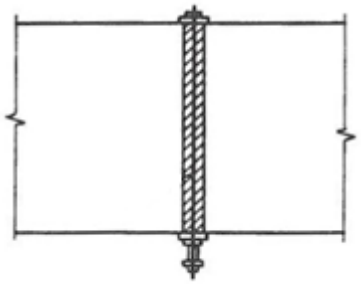

Figure 4.5 Drilled hole with inserted wire and injected with grout. (Öberg, 1990)

4.3.2 Mechanical behaviour

Favourable effects with regard to shear capacity can be obtained by applying prestressing in the vertical direction. However, since this is a rather unusual procedure these effects are not considered in the design methods in EC2. Consequently, what is being presented in this section might not be directly according to EC2.

The steel wires themselves will by their strength increase the shear capacity with regard to shear sliding failure. At a load level for which interlocking effects and friction in the crack interface is insufficient to transfer the shear force a new equilibrium can be obtained by means of the steel wires. They act as fully anchored ties in a truss model and the failure is governed by yielding of the steel, which according to EC2 is calculated as:

$$V_{Rd,s} = \frac{z \cot \theta}{s} f_{ywd} A_{sw} \quad (4\text{-}7)$$

In case of prestressing, the steel wires can be utilised to a higher degree than what would be possible without prestressing. When a strengthening method is applied on a reinforced concrete structure, it is already subjected to the load from its self-weight. If non-tensioned shear reinforcement is inserted, it will not start to deform until a load in addition to the self-weight is applied on the structure and this may lead to problems with regard to serviceability. At the point where yielding occurs in the shear reinforcement, large deformations will have taken place in the concrete and shear cracks might be wide. If the shear reinforcement is post-tensioned on the other hand, an initial strain will be induced and as a result the deformations in the concrete when the steel starts to yield are smaller and the crack widths will be limited. For this reason it might also be possible to make use of high strength steel, which may be questionable in case of non-tensioned shear reinforcement.

Furthermore, Öberg (1984) evaluated the results from a number of tests on the basis of the 'addition principle' for shear resistance, which was adopted by the Swedish code at the time, BBK 79. Here it was shown that the degree of utilisation of high strength shear reinforcement at shear failure of a reinforced concrete member depends on the magnitude of the post-tensioning, i.e. it is not only favourable with regard to serviceability to post-tension the shear reinforcement but also in the ultimate limit state. Since the steel stress at shear failure is not necessarily as high as the yield stress, a value of the maximum stress in the ultimate limit state needs to be calculated. The magnitude of the additional stress which was obtained in the shear reinforcement at failure was determined from the test results. The steel stress at failure was according to Öberg (1984) calculated as:

$$\sigma_{sv,max} = \sigma_{sv,0} + \Delta\sigma_{sv} = \sigma_{sv,0} + 700 \leq f_{0.2} \text{ [MPa]} \quad (4\text{-}8)$$

where

$\sigma_{sv,0}$ is the effective prestress in the steel

$\Delta\sigma_{sv}$ is the additional stress obtained at failure

By replacing f_{ywd} in Equation (4-7) this gives a capacity of:

$$V_{Rd,s} = \frac{z \cot \theta}{s} \sigma_{sv,max} A_{sw} \quad (4\text{-}9)$$

This value of $\Delta\sigma_{sv}$ was determined on the basis of the 'addition principle' with a 45° truss model and in the Swedish Road Administration's publication Bro 2004 the method presented by Öberg (1984) was allowed for retrofit design. However, the newest publication TK Bro relates to EC2 and due to this the method is no longer applicable. In order to arrive at a procedure which corresponds to the model in EC2

the method in Öberg (1984) should be recalibrated against the test results on the basis of a variable inclination truss model without a concrete contribution term. However, this is not treated in this report.

The effect on the capacity with regard to web shear compression failure from a vertical prestress is not discussed in EC2. However, some similarities to the effects from longitudinal prestressing should reasonably exist. In EC2 moderate longitudinal prestressing has a favourable effect on the capacity with regard to web shear compression failure due to the fact that it creates a biaxial compression state in the inclined struts which increases the compressive strength of the concrete. Since vertical prestressing also contributes to biaxial compression, the effect from this should be similar. A suggestion for how this can be handled is to combine the longitudinal and the vertical prestress to a resultant which is obtained according to Figure 4.6 as:

$$\sigma_{cp,r} = \sqrt{\sigma_{cp}^2 + \sigma_{cp,v}^2} \tag{4-10}$$

where

σ_{cp} is the longitudinal prestress

$\sigma_{cp,v}$ is the vertical prestress

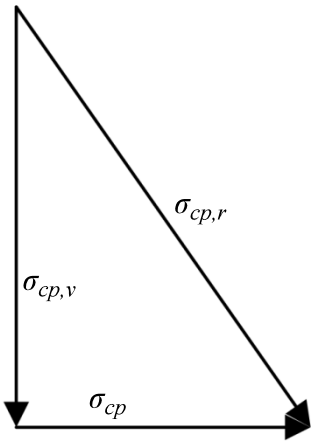

Figure 4.6 Resultant of vertical and longitudinal prestress

The expression for how to calculate the capacity with regard to web shear compression failure is:

$$V_{Rd,max} = \alpha_{cw} b_w z v_1 f_{cd} \frac{1}{\cot\theta + \tan\theta} \tag{4-11}$$

The factor α_{cw} in the case of longitudinal and vertical prestressing acting simultaneously is here proposed to be calculated in a similar manner as in Section 2.6.2:

α_{cw} = 1.0 for non-prestressed members (national parameter)

$= 1 + \sigma_{cp,r} / f_{cd}$ for $0 < \sigma_{cp,r} \leq 0.25 f_{cd}$

$= 1.25$ for $0.25 f_{cd} < \sigma_{cp,r} \leq 0.5 f_{cd}$

$= 2.5(1 - \sigma_{cp,r} / f_{cd})$ for $0.5 f_{cd} < \sigma_{cp,r} \leq 1.0 f_{cd}$

In the areas where the wires are anchored it is necessary to check the local concrete strength. If the load is too large there is a risk for crushing of the concrete. This can be checked according to Equation (4-12). In addition, it is necessary to consider the risk of splitting of the concrete. The stress field will spread from the area where the wires are anchored and cause tensile stresses in the concrete which must be resisted. However, calculation methods for this effect are not treated in this report.

$$\sigma_c = \frac{P_{max}}{A_{washer}} \leq f_{cd} \tag{4-12}$$

where

P_{max} is the maximum force in the wire

A_{washer} is the area of the washer at the anchor

The vertical prestressing forces are assumed to be uniformly distributed over the top and bottom sides of the slab according to Figure 4.7. This assumption does not entirely represent practice, although, the calculation procedure is significantly simplified.

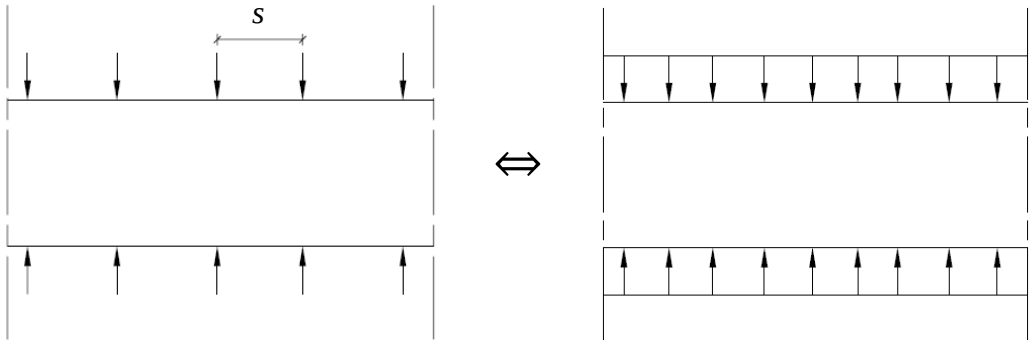

Figure 4.7 Simplified distribution of prestressing forces.

4.3.3 Discussion

The approach for considering the effect from the biaxial compression on the capacity with regard to web shear compression failure is rather rough since the strut inclination is not regarded. It is the component of the prestress perpendicular to the strut that gives a favourable effect and the magnitude of this depends on the strut inclination. However, since the inclination is not regarded in EC2 for the case of longitudinal prestressing, it is considered sufficient to use the procedure proposed above.

An alternative unverified way to take advantage of the vertical prestressing force is to utilise the capacity with regard to web shear tension failure for an uncracked biaxially loaded concrete section. In order to study the state of stresses in the slab element at the centroidal axis Mohr´s circle, see Figures 4.8 and 4.9, is used and Equation (4-13) was derived in Appendix A.

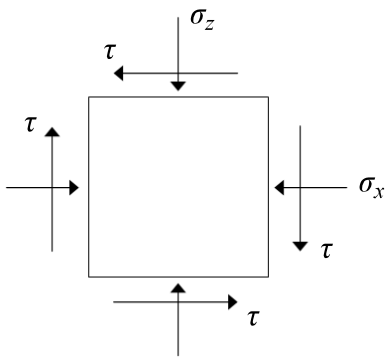

Figure 4.8 Element stresses

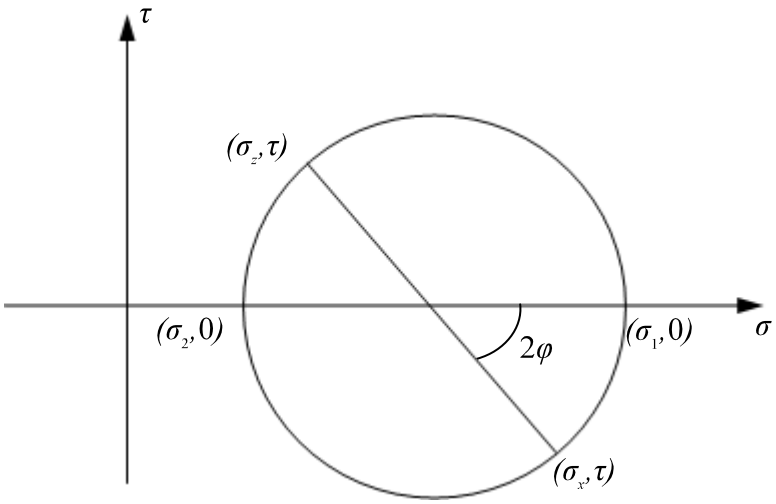

Figure 4.9 The state of stresses in a biaxially loaded slab presented by means of Mohr´s circle. σ_z is the vertical stress, σ_x is the axial stress

A web shear crack appears when the principal tensile stress σ_2 reaches the concrete tensile strength f_{ct}. The shear force that causes a web shear crack in a biaxially loaded member is then:

$$V_{cw} = \frac{I \cdot b_w}{S} \sqrt{(\sigma_z \sigma_x) - f_{ct}(\sigma_z + \sigma_x) + f_{ct}^2} \tag{4-13}$$

According to EC2 the capacity with regard to web shear tension failure can only be utilised if the member is uncracked in bending since it will then be no risk that inclined cracks develop from bending cracks. Hence, the only shear crack which can occur is when the principal tensile stress in the web reaches the tensile strength of the concrete. As opposed to longitudinal prestressing, vertical prestressing cannot prevent bending cracks. Nevertheless, it should be possible to control the stress state by means of vertical prestressing such that bending cracks do not develop into inclined cracks in the web. To be able to make use of this theory it is necessary to define a condition for how far the bending cracks should be allowed to propagate. As a help to determine this point the principal stress directions can be studied according to Equations (4-14) and (4-15). The direction of the smallest (tensile) principal stress in this point should be parallel to the longitudinal axis of the member or close to this, i.e. the angle should be $\varphi = 90°$ or close to this.

$$\tan 2\varphi = \frac{2\tau}{\sigma_x - \sigma_z} \quad \text{if} \quad \sigma_x \geq \sigma_z \tag{4-14}$$

$$\tan(180° - 2\varphi) = \frac{2\tau}{\sigma_z - \sigma_x} \quad \text{if} \quad \sigma_x < \sigma_z \tag{4-15}$$

With this point defined, an analysis of the stress state in this point can be performed by means of Mohr's circle. If the smallest principal stress according to Equation (4-16) is larger than the tensile strength of the concrete (with tension defined negative) the concrete here will be uncracked.

$$\sigma_2 = \frac{\sigma_z + \sigma_x}{2} - \sqrt{\left(\frac{\sigma_x - \sigma_z}{2}\right)^2 + \tau^2} \tag{4-16}$$

It can be seen in Equation (4-16) and Figure 4.9 that if $\sigma_z > \sigma_x$, the vertical stress σ_z needs to be large in relation to the shear stress τ in order to influence the principal stress σ_2 noticeably. This will be more evident if the difference between σ_x and σ_z is large which will be the case if a large bending moment is present in the actual section.

4.4 Method 3 – Vertical post-tensioned steel bars with internal anchor

Another alternative method which makes use of the beneficial effects of vertical post-tensioning is presented in this section.

4.4.1 Implementation in practice

In order to avoid the traffic disturbance, which the previous method causes, the anchor in the top of the slab is in this method embedded in the concrete slab and consists of an internal anchor shown in Figure 4.10. After installation the bar is post-tensioned in order to achieve the same beneficial effects as described for Method 2. Holes are drilled vertically from the bottom side of the slab as deep as possible in order to acquire maximum effect out of the anchors. Careful measurement of the drilling depth is necessary in order to avoid full penetration of the slab and damage of the sealing layer that protects the concrete from water. As in the previous method it is important to know where the existing reinforcement bars are placed in the slab. Since the road topping is not removed in this method it will be harder to localise the upper reinforcement.

The type of anchor is a forward undercut anchor and this is chosen in order to obtain a large effective height of the bar relative to the drilling depth, see Figure 4.11. The anchor has an internal thread which allows both bolts and threaded rods with various lengths. Figure 4.10 shows the installation procedure where firstly a hole is drilled and cleaned. Secondly, the undercut is obtained by using the expansion elements of the anchor as a drill. After anchorage a post-tensioning force is applied.

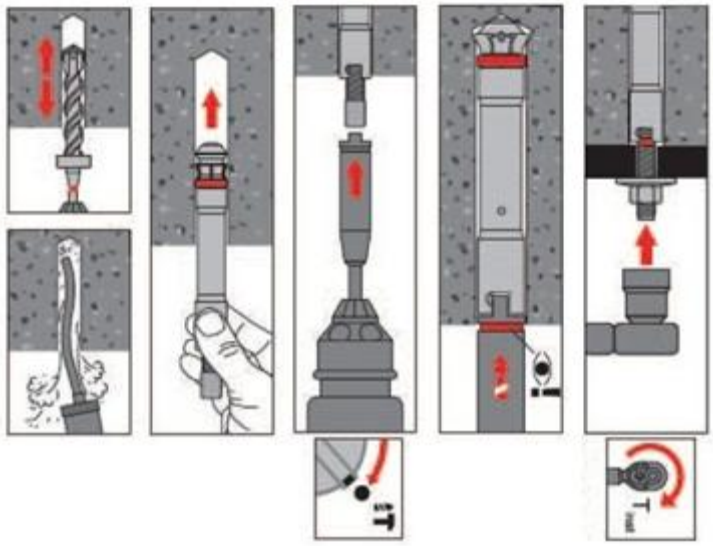

Figure 4.10 Installation of an undercut anchor. (HILTI, 2009)

4.4.2 Mechanical behaviour

The fundamentals for this mechanical model are the same as for Method 2, which means that shear failure modes are prevented in the same way. In addition the following requirements need to be fulfilled.

Since the anchor is embedded in the concrete slab, the effective embedment length of the bar h_{ef}, see Figure 4.11, will be smaller than in Method 2. For this method to function, in the case of a simply supported slab, the anchor needs to be anchored in the node in the compression zone in the truss model, see Figure 4.11. The anchorage in the node at the tensile zone is not a problem, since the anchor is placed on the concrete face. The compression zone for slabs is often relatively small; this could therefore be a critical issue.

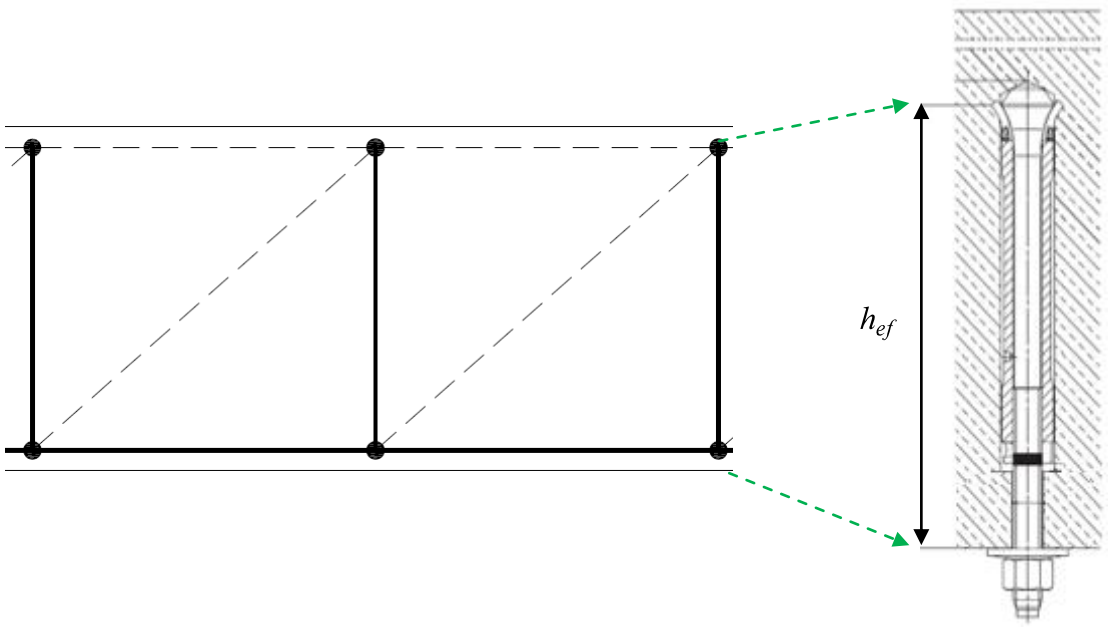

Figure 4.11 Truss model for a strengthened simply supported concrete slab to the left. Dashed line shows struts and bold line shows ties. The effective height h_{ef} is illustrated to the right in the figure.

The undercut anchor is not developed with the purpose to act as shear reinforcement but rather to anchor fastenings in concrete members. Nevertheless, it is reasonable to assume that the load acting on the anchor just as well could be a shear force. However the mechanical behaviour for the two different fields of application differs and this is discussed later in this section.

In this method only failures regarding tension loading of the anchor is considered. The resistance of the undercut anchor can be determined by four different failure modes: failure of the anchor itself (i.e. yielding of the steel), pull-out failure, concrete cone failure and concrete splitting failure, see Figure 4.12.

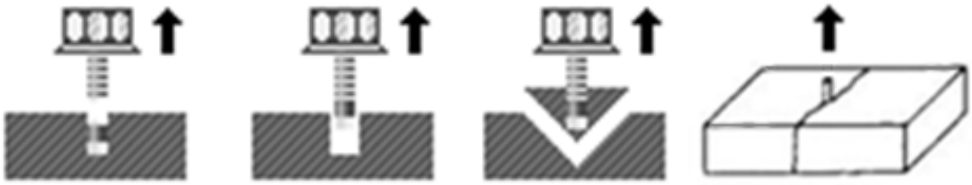

a) b) c) d)

Figure 4.12 Failure modes associated with tension loading. a) Steel failure. b) Pull-out failure. c) Concrete cone failure d) Splitting failure. (HILTI, 2009)

To calculate the shear capacity according to EC2 with regard to shear sliding failure Equation (4-17) should be used in this case with the design value of the tensile capacity of the anchor. The design checks that need to be done are according to the Concrete Capacity-Method and presented in Table 4.1, (Eligehausen et al., 2006).

$$V_{Ed} = \frac{z \cot \theta}{s} N_{Ed} \cdot n_{trans} \tag{4-17}$$

where

n_{trans} total number of units in the actual section

Table 4.1 Design checks required for tension loads.

Steel failure	$N_{Ed} \leq N_{Rd,s} = N_{Rk,s}/\gamma_{Ms}$
Pull-out failure	$N_{Ed} \leq N_{RD,p} = N_{Rk,p}/\gamma_{Mp}$
Concrete cone failure	$N_{Ed} \leq N_{Rd,c} = N_{Rk,c}/\gamma_{Mc}$
Splitting failure	$N_{Ed} \leq N_{Rd,sp} = N_{Rk,sp}/\gamma_{Msp}$

The characteristic load for steel failure of the anchor is presented in Equation (4-18).

$$N_{Rk,s} = A_s \cdot f_{uk} \tag{4-18}$$

For undercut anchors pull-out failure occurs, if the mechanical interlock is inadequate. Increasing load on the anchor increases the pressure from the undercut on the concrete and at failure the concrete is being crushed locally in the bearing area. The characteristic resistance $N_{Rk,p}$ is derived from results of approval tests and specified in the European Technical Approval, which, as for example Hilti's recommendations are based on, see Equation (4-19). $N_{Rd,p}$ is the design pull-out resistance where $N^0_{Rd,p}$ is an empirical value and f_B is the influence of the concrete strength, see Equation (4-20).

$$N_{Rd,p} = N^{0}_{Rd,p} \cdot f_B \tag{4-19}$$

$$f_B = \sqrt{\frac{f_{ck,cube}}{25\ \text{MPa}}} \tag{4-20}$$

The failure load for each anchor, with regard to concrete cone failure, will be reduced if the number of anchors included in a group is increased since the individual failure cones overlap each other, see Figure 4.13. The concrete cone failure for a group will then result in a common failure cone. However, since the anchors will be mounted over the whole width and over the length required for strengthening of the slab, a concrete cone failure would imply that this whole volume would break out. This is not at all likely, and especially not when the anchors have this relatively high effective length and are anchored in the compressive zone. Instead it should be reasonable to assume that the shear force is transferred by the truss model.

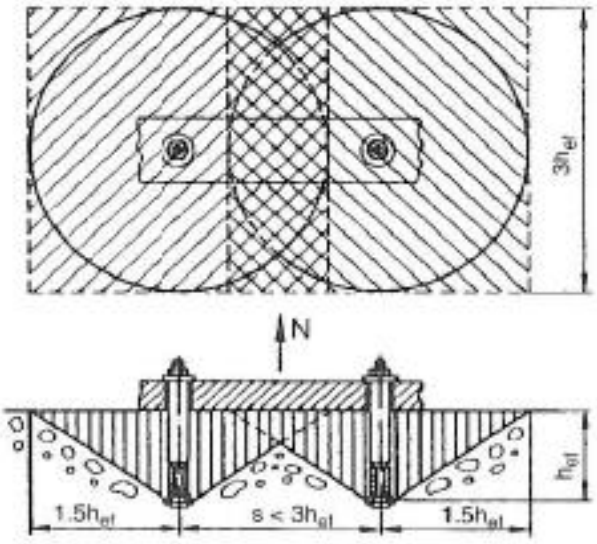

Figure 4.13 Influence of anchor spacing on shape of concrete cone failure surface of a group with two anchors loaded in tension. (Eligehausen et al., 2006)

The type of anchor was chosen partly with regard to the prestressing effect on the adjacent concrete. Due to creep in the highly stressed concrete at the tip of the anchor and relaxation the prestressing force decreases over time. According to Figure 4.14 an undercut anchor has least decrease of prestressing force over time, thus an undercut anchor seems to be most suitable in this case.

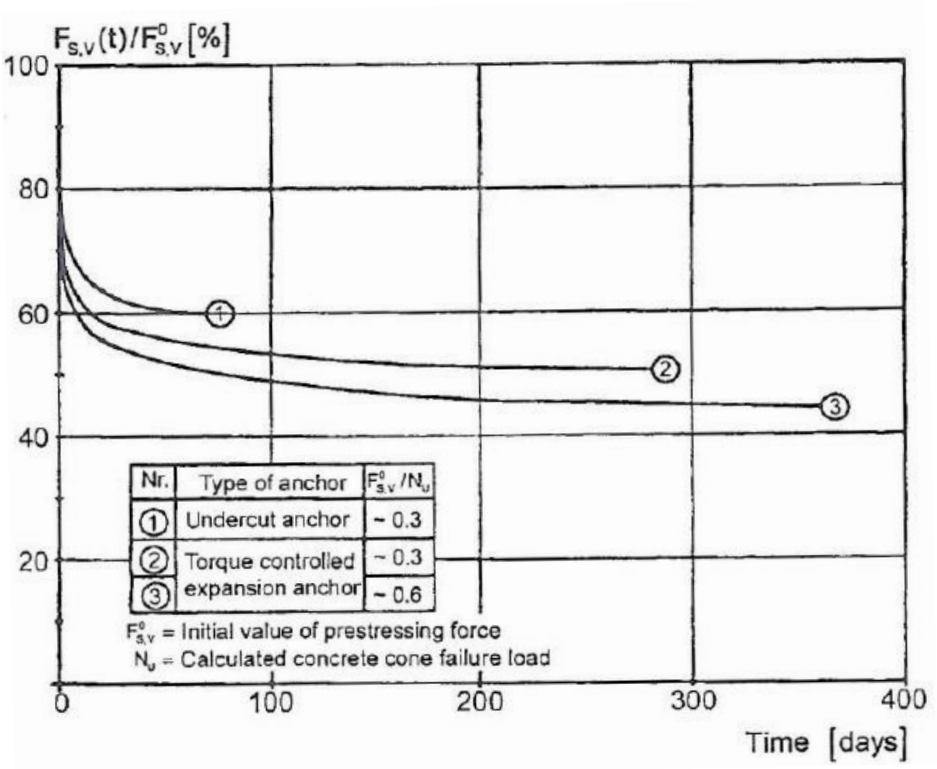

Figure 4.14 Decrease of prestressing force in anchors plotted against time.(Eligehausen et al., 2006)

The vertical prestressing force is applied in the same way as in Method 2. According to Figure 4.14 the prestressing force in undercut anchors goes down to 60 % of the initial value of the prestressing force after 50 days. Either this needs to be regarded when installing the anchors or re-torqing needs to be performed.

4.4.3 Discussion

It could be difficult to anchor the bar beyond the node in the truss model since the top reinforcement can be hard to locate and avoid and the slab is also not allowed to be fully penetrated.

Usually, threaded bars have a more brittle behaviour than what normal reinforcement steel has. It is therefore important to consider this in the choice of bar and ensure that it has sufficient possibility for plastic redistribution in order for it to work with a variable inclination truss model. Alternatively, a steeper strut inclination can be chosen in the truss model.

4.5 Method 4 – Vertical FRP bars with anchorage by bond

This method is inspired by the method presented in Section 3.1.3 by De Lorenzis & Nanni (2001). However, since their method was intended for beams it has been modified.

4.5.1 Implementation in practice

For this method the carbon FRP bars are instead mounted internally in drilled holes in the slab. In order to avoid interference with the road topping it is preferable to drill the holes from below the slab. The epoxy could be placed in the drilled holes by means of for example a capsule and then the carbon FRP bar can be inserted.

4.5.2 Mechanical behaviour

The mechanical model is here proposed to be based on the preliminary approach presented by De Lorenzis & Nanni (2001) since their theoretical approach showed good correspondence to their experimental results. The failure mode observed was de-bonding of one or more bars and splitting of the epoxy cover. When they succeded to prevent splitting of the epoxy cover, another failure mode appeared as shown in Figure 4.15. The picture shows that the crack has propagated along the bending reinforcement which according to De Lorenzis & Nanni (2001) was the failure mode in this case. This could imply that the FRP bars may not have had sufficient bond and were not sufficiently anchored in the node in the tension zone. However, this is not discussed in their theoretical approach. In our case the failure mode concerning splitting of the epoxy cover will be prevented by the way the bars are installed in the slab.

Figure 4.15 Observed failure mode from tests. (De Lorenzis & Nanni, 2001)

The assumptions made are that there is a uniform distribution of bond stresses along the effective length of the FRP bars in the ultimate limit state and that the ultimate bond stress is reached in all the bars intersected by a crack simultaneously in the ultimate limit state. According to De Lorenzis & Nanni (2001) the contribution of the FRP bars can be calculated according to the 'addition principle' and with a fixed crack inclination of 45°, as in Equation (4-21), provided that the existing steel is yielding.

$$V_{Rd,FRP} = V_c + V_s + V_{FRP} \tag{4-21}$$

The contribution to the shear resistance by the FRP bars is here denoted V_{FRP}. It is determined either by bond failure V_{1F} or by tensile failure of the bar itself, V_{2F}.

The idea is that the bond capacity of the FRP, V_{1F}, may be computed as the sum of the forces resisted by the FRP bars intersected by a shear crack. The total contribution is estimated as the product of the average bond strength and the surface area of the shortest part of a bar intersected by a crack, see Equation (4-22) and see Figure 4.16. L_{tot} is the sum of all the effective lengths of the bars crossed by a crack, but calculated in the most unfavourable way.

$$V_{1F} = n_{trans}\, \pi\, \phi\, f_b\, L_{tot} \tag{4-22}$$

where

$$L_{tot} = \sum L_i \tag{4-23}$$

n_{trans} the number of bars in the transversal direction

ϕ the nominal bar diameter

f_b the average bond strength

L_i the effective length of the bar crossed by a crack

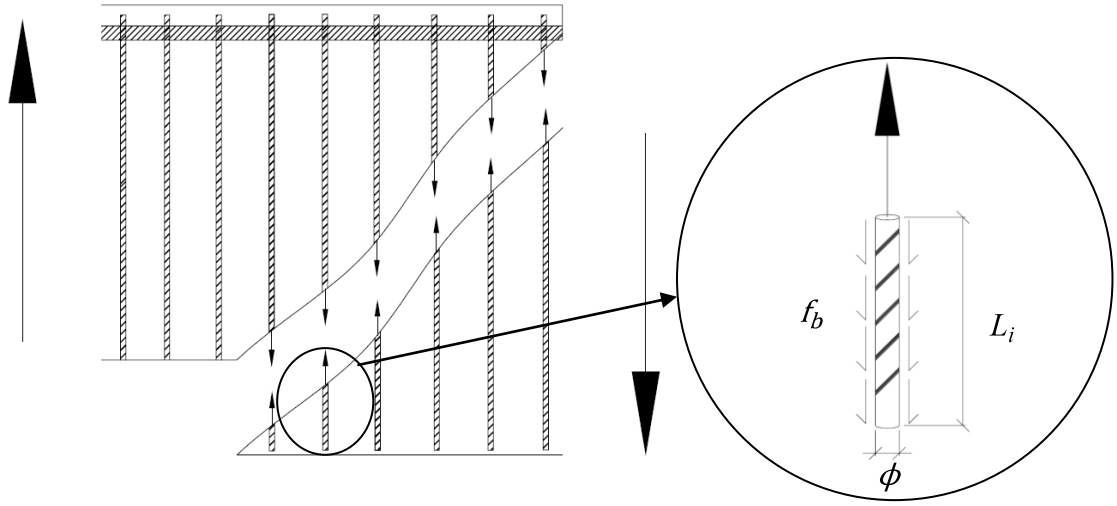

Figure 4.16 Free body diagram for the cracked slab to the left and for the shortest part of a bar that is intersected by a crack to the right.

The maximum strain allowed in the FRP bars is 4‰. FRP bars have a much higher ultimate strain but this limit is suggested in order to maintain the shear resistance contribution from the concrete, such as friction and interlocking effects. This is necessary since the method is based on the 'addition principle'. The effective length $\overline{L_i}$ of a bar crossed by a crack corresponding to the tensile strain 4‰ is presented in Equation (4-24) which leads to Equation (4-25) and shown in Figure 4.17. The maximum strain 4‰ is reached at the failure load V_{2F}. To explain how V_{2F} is computed the case shown in Figure 4.17 where three bars are crossing a crack is taken as an example. For cases with other spacing ranges see Appendix G. As presented in Equation (4-26) V_{2F} is based on the same assumptions as V_{1F}. If one or more effective lengths are longer than $\overline{L_i}$, at ultimate limit state, these will carry a tensile load corresponding to the tensile strain 4‰, as for the two bars in the middle in Figure 4.17. For the bars shorter than $\overline{L_i}$, the tensile load will be the product of f_b and their surface area.

$$\overline{L_i} \; f_b \; \pi \; \phi = \frac{\pi \; \phi^2}{4} E_{FRP} \cdot 0.004 \tag{4-24}$$

from where $\overline{L}_i$ can be expressed as:

$$\overline{L}_i = 0.001 \frac{\phi E_{FRP}}{f_b} \tag{4-25}$$

where

E_{FRP} the modulus of elasticity of FRP bars

$$V_{2F} = n_{trans} \pi \phi f_b (2\overline{L}_i + d_{net} - 3s_{long}) \tag{4-26}$$

where

$d_{net} = d_r - 2c$ the reduced length of the FRP bar (4-27)

d_r is the length of the FRP bars

c the concrete cover of longitudinal steel reinforcement

s_{long} the longitudinal spacing between the bars

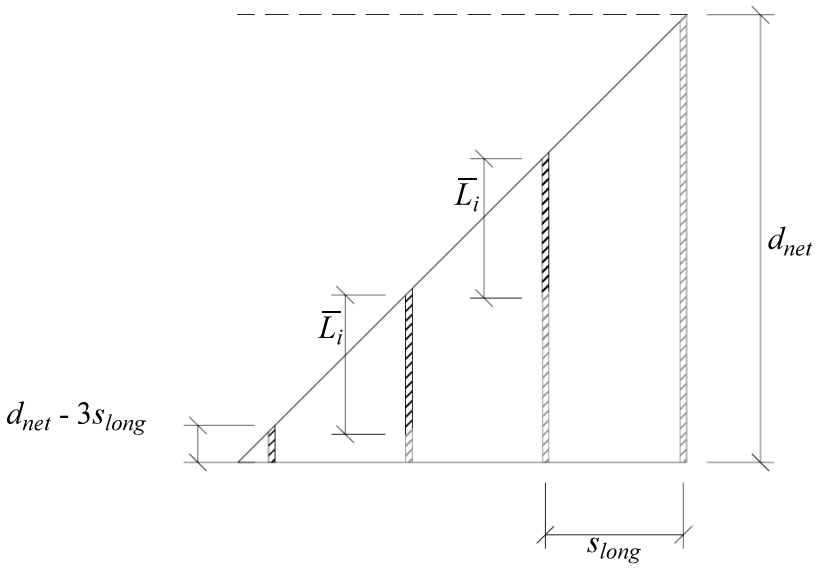

Figure 4.17 Illustration of a case where three bars are crossing a crack of 45˚.

According to De Lorenzis & Nanni (2001) the V_c term is computed according to the ACI 318 Code as in Equation (4-28) but here converted to SI units.

$$V_c = 3.5 \cdot 4.448 \cdot \mathrm{N} \sqrt{\frac{f'_c}{6896.1 \cdot \mathrm{Pa}}} \left(\frac{39.37}{\mathrm{m}}\right)^2 b_w \, d \tag{4-28}$$

where

f'_c concrete compression strength

To be consistent it is chosen to calculate the concrete contribution according to EC2, as presented in Section 2.6.1 and in Equation (4-29). This is also partly because it is not clear if f'_c, used above, is established according to international standards.

$$V_{Rd,c} = \left[C_{Rd,c} k \left(100 \rho_l f_{ck}\right)^{1/3} + k_1 \sigma_{cp} \right] b_w d \tag{4-29}$$

The steel contribution is computed as:

$$V_s = \frac{A_{sw} f_{ywd} \, 0.9d}{s} \tag{4-30}$$

where

A_{sw} the nominal cross-sectional area of a shear reinforcement unit

4.5.3 Discussion

What is presented above does not correspond to EC2 where the concrete term V_c is not permitted to use. Though, one important difference between FRP and steel shear reinforcement should be noticed. The choice of crack inclination which is allowed in case of steel stirrups in EC2 will not be appropriate when it comes to FRP. As can be seen in Figure 4.18, this material does not exhibit the same yielding properties as steel; hence there is no possibility for plastic redistribution of stresses. The consequence of this is that the crack inclination at ultimate limit state will be close to the inclination when cracking starts and the choice should not deviate much from 45°.

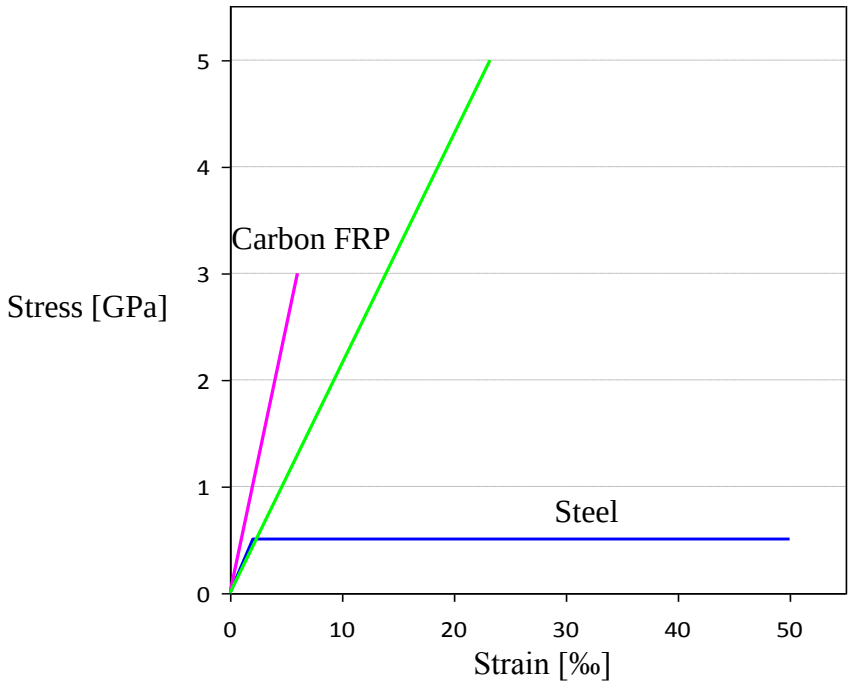

Figure 4.18 Stress-strain diagrams for CFRP (carbon FRP) and steel. (fib , 2001)

Excluding the V_c-term and using the strut inclination of 45° would imply that the theory no longer corresponds to the results from the experiments. At this steep inclination friction and interlocking effects in the concrete in fact do influence the shear capacity. Consequently, the variable strut inclination method in EC2 might not be suitable for materials which do not exhibit possibility for plastic deformation.

An alternative approach could be used. If the V_c-term is not adopted, but the strut inclination of 45° is kept, the restriction of the maximum tensile strain in the FRP bar should no longer be limited to 4‰, but rather to the actual maximum tensile strain. This strain could be for example for the types of FRP bars used by De Lorenzis & Nanni (2001), according to Equation (4-31), equal to 17.9‰. Crack widths in serviceability limit state still needs to be considered and the bond-controlled failure could still be the limiting factor.

$$\varepsilon_u = \frac{f_{FRP,tu}}{E_{FRP}} = \frac{1875}{104.8 \cdot 10^3} = 17.9‰ \qquad (4\text{-}31)$$

Another alternative method could be to use steel and take advantage of the choice of a low strut inclination.

What could be questioned in De Lorenzis' & Nanni's model is if the failure mode observed in Figure 4.15 is being considered. This failure mode indicates that the bars are not being anchored in the nodes in the truss model. The required anchorage length for the bars to become fully anchored in the nodes should reasonably be longer than the distance c. Still, the theoretical model gives results that correspond well to experiments and is therefore interesting.

It is important to be aware of that these experiments were performed on beams and the expression for the V_{FRP} term was adapted thereafter. It is therefore not sure that the same correspondence will appear when it comes to slabs and further experiments and investigations are required.

De Lorenzis' & Nanni's model is doubtful in many ways, especially their reasoning about that the bars are only crossed by one crack, when in fact shear cracks can occur parallel to each other at the same time. A bar will then be crossed by several cracks and consequently this calculation method cannot be trusted.

4.6 Method 5 – Closed carbon FRP links

The method for strengthening with regard to punching shear presented in Section 3.1.2 can also be used for shear strengthening of a whole slab. With this procedure the mechanical behaviour of the strengthened structure can rather easily be explained.

4.6.1 Implementation in practice

Before this method can be applied on a slab bridge it is necessary that the road topping is removed and the concrete surface on both the top and bottom side of the slab is accessible. As described in Section 3.1.2 holes are drilled through the depth of the slab in which FRP strips pass through. In difference to the case in Section 3.1.2 where the strips are applied locally at a column support, it is in the case of strengthening a whole slab necessary to drill holes along the whole width of the slab. Each FRP strip is inserted into two holes as seen in Figure 4.19 and this is repeated for each pair of holes in the transversal as well as the longitudinal direction. The edges of the holes are chamfered in order to avoid damage to the FRP strips and premature failure.

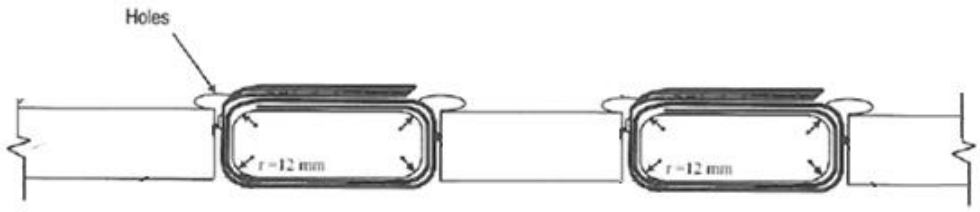

Figure 4.19 Installation of closed carbon FRP links.

Before the FRP strips are mounted into the holes they are saturated with epoxy. The strips then become very flexible and the epoxy bonds the strips to the concrete and ties them together in the overlapping region.

4.6.2 Mechanical behaviour

Since the FRP strips are bonded to the concrete surface with epoxy and form closed links around the concrete section, they can be regarded as fully anchored in both the compression and the tension zone. Due to this all the strips which cross a shear crack will transfer shear force in a similar manner as for internal steel stirrups. According to Bayrak & Binici (2006) the capacity with regard to punching shear failure in the strengthened zone can be calculated according to the 'adition principle' with a 45° strut inclination as:

$$V_{Rd,FRP} = V_c + V_{FRP} = \frac{1}{4}\sqrt{f_{cd}}\, b\, d + \varepsilon_{eff}\, E_{FRP}\, A_{FRP}\, \frac{0.9d}{s} \tag{4-32}$$

However, the V_c term in Equation (4-32) should be used in case of punching shear failure and it is not applicable when a whole slab is strengthened. In order to modify this expression to fit the case in question it is here chosen to replace the V_c term in Equation (4-32) with the term $V_{Rd,c}$ term from EC2, which expresses the shear capacity of the concrete without reinforcement. The capacity can then be expressed according to Equation (4-33). The reason why the variable strut inclination method is not adopted here is because the carbon FRP does not exhibit plastic deformation properties as mentioned in Section 4.5.3.

$$V_{Rd,FRP} = V_{Rd,c} + V_{FRP} \tag{4-33}$$

where

$$V_{Rd,c} = \left[C_{Rd,c} k \left(100 \rho_1 f_{ck}\right)^{1/3} + k_1 \sigma_{cp}\right] b_w d$$

$$V_{FRP} = \varepsilon_{eff}\, E_{FRP}\, A_{FRP}\, \frac{0.9d}{s}$$

In one of the tests conducted by Bayrak & Binici (2006) failure occurred by rupture of the FRP strips at one of the chamfered corners. The strain gauges were placed on the vertical part of the FRP strips and here the maximum strain was about 80% of the ultimate strain. This indicates that there are strain concentrations at the corners. As a safe approximation Bayrak & Binici (2006) proposes, on the basis of their test, a limitation of the maximum allowed strain in the FRP to ε_{eff} = 4‰.

In the tests performed by Bayrak & Binici (2006) the specimens did not contain any existing steel stirrups. In a structure which contains steel stirrups it should be possible to add the capacities from the two materials as shown in Equation (4-34) under the condition that the steel stirrups yields before failure occurs in the FRP.

$$V_{Rd,FRP} = V_{Rd,c} + V_{FRP} + V_s \quad (4\text{-}34)$$

where

$$V_s = \frac{f_{ywd} A_{sw} 0.9d}{s}$$

It should be reasonable to assume that the capacity with regard to web shear compression failure can be calculated according to EC2 as seen in Equation (4-35).

$$V_{Rd,max} = \alpha_{cw} b_w z \, v_1 f_{cd} \frac{1}{\cot\theta + \tan\theta} \quad (4\text{-}35)$$

4.6.3 Discussion

It cannot be sure that the modification of the expression gives a result which corresponds to practice before tests have been performed.

The fact that the FRP strips ruptured at the corners indicates that they are not sufficiently bonded to the concrete in the drilled holes. If the bond would have been sufficient the rupture would have taken place where the FRP strip crosses a crack. This is due to the strain localisation which arises here when the crack opens. A consequence of the lack of bond is that the shear cracks will become wider than in the case of good bond between the FRP strips and the concrete. The explanation to this is that the deformation in the FRP caused by the opening of a shear crack is evenly distributed over the whole vertical part of the FRP strip in the case of poor bond. If the bond is good on the other hand the deformation in the FRP will be distributed over a much smaller length and causes a larger strain. To sum up it can be said that if the FRP strips are not bonded to the concrete in the holes the shear crack widths will be larger than if they are bonded, however, the capacity in the ultimate limit state is not influenced.

The fact that $\varepsilon_{eff} = 4‰$ is larger than ε_{sy} for normal strength steel implies that if the existing structure contains steel stirrups the steel should yield before failure occurs in the FRP. However, the steel stirrups have localised strain at the cracks and as mentioned above the FRP strips do not seem to have this. Due to this it might not be safe to assume that the capacities of the different materials can be added.

In addition, problems with regard to serviceability could arise since the structure is already deformed by the load from the self-weight when the links are inserted. Cracks widths might be large already for a rather low strain in the FRP.

An alternative for how to achieve an initial strain in the FRP could be to apply counteracting loads from the bottom of the slab before the links are inserted. This should correspond to a more or less unloaded structure at the point of insertion.

5 Case study and evaluation

In order to exemplify the different strengthening methods presented in Chapter 4, a real life case has been chosen on which the methods are theoretically applied. Here, the case is described and results from calculations are presented. This chapter also contains an evaluation, where the adapted methods are compared to each other with regard to predefined evaluation parameters based on own estimations. The evaluation is performed according to a methodology suitable for conceptual design.

5.1 Case study

The case is a slab frame bridge in two spans. The bridge is located in Stockholm where the railroad "Skarpnäcksbanan" crosses the road "Sparrmansvägen", see Figure 5.1.

Figure 5.1 Photo of the north side of the bridge over "Sparrmansvägen".(Google Maps, 2010)

The bridge was designed in 1957 and the task is to enhance the shear capacity in a certain section with 30%. To achieve this, the shear capacity of a one meter wide strip of the bridge slab in the region near one of the end supports is evaluated. This is shown in Appendix B. The geometry and other conditions for the bridge are presented in forms of drawings in Appendix C. The evaluation was based on the following assumptions:

- The skewness of the bridge is neglected, that is, sectional forces are presumed to act in the same direction as the existing reinforcement steel.
- The influence of load near support is also neglected.
- The influence of the inclined resultant in the compressive zone caused by the varying height of the slab near the supports, see Figure 5.2, is neglected.
- The earth pressure is assumed to act on the slab as a normal force. The filling material is blast stone.
- In a complete strengthening design using a method which inserts vertical reinforcement the strut inclination would have been chosen according to Equation (4-1) and (4-2) in Section 4.1. In our simplified case we do not have adequate information and therefore it is estimated that the longitudinal reinforcement bars have sufficient anchorage length and that it is possible to

choose the angle to be $\theta = 21.8^{\circ}$. This corresponds to $\cot\theta = 2.5$ and is the lowest inclination allowed to choose according to EC2, see Section 2.6.

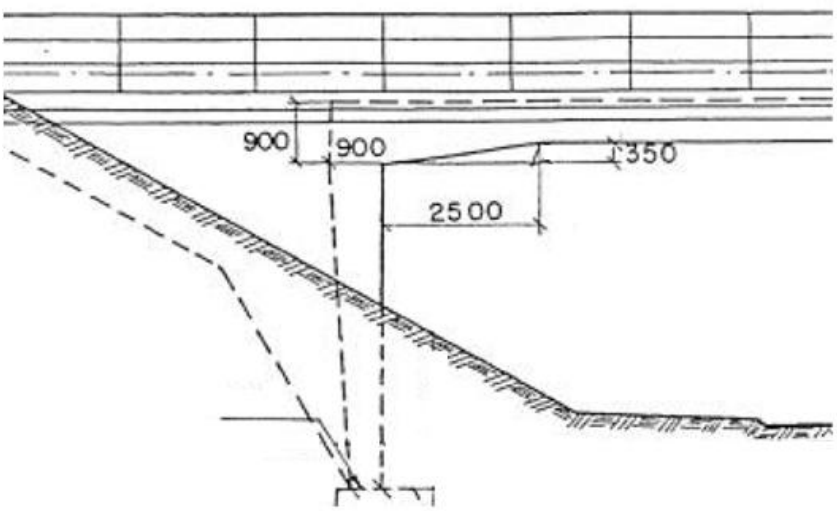

Figure 5.2 End support of the slab frame bridge and the slab with varying height.

The shear capacity of the section at a distance $z\cot\theta$ from the support for the non-strengthened structure is, see Figure 5.3:

$$V_{Rd,c} = 386.6 \text{ kN} \tag{5-1}$$

The increased load effect which the strengthened structure should be able to resist at the same section is 30% higher:

$$V_{Ed} = 1.3 \cdot V_{Rd,c} = 502.6 \text{ kN} \tag{5-2}$$

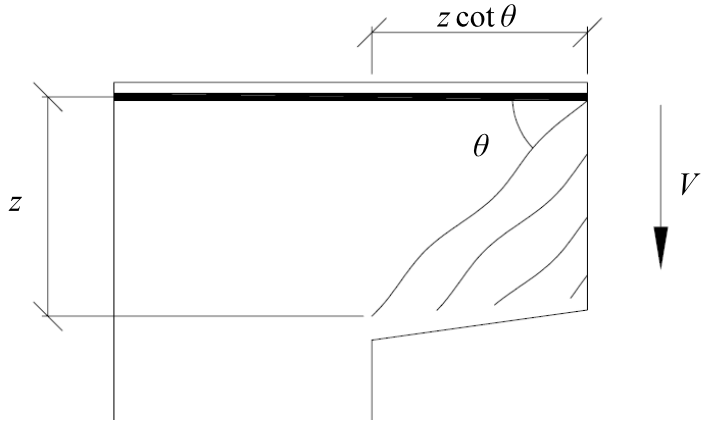

Figure 5.3 Section in the slab for calculation of shear capacity.

When post-installed reinforcing members are inserted it is important to consider the exact location of the existing reinforcement. In order not to cause unnecessary damage to the structure the reinforcement bars can be located by means of a Ground Penetration Radar. In this way the information obtained from the drawings can be verified.

As shown in Figure 5.4 the longitudinal reinforcement has a spacing of 100 mm in the top and 80 mm in the bottom in the most heavily reinforced section in the actual region. Unfortunately the difference in spacing between the top and bottom reinforcement might result in problems if vertical post-installed reinforcement are to be inserted. The existing transversal reinforcement has a spacing of 300 mm in both the top and bottom and this provides better possibility to place a desired amount of vertical reinforcement. Not until the exact arrangement of existing reinforcement has been measured on site can the final location of new units be determined. The ratio between transversal and longitudinal spacings can be adjusted if it proves to be necessary after measurements.

The longitudinal top reinforcement bars are bent at the frame corner and they continue vertically in the frame wall with the same spacing of 100 mm as seen in Appendix C.

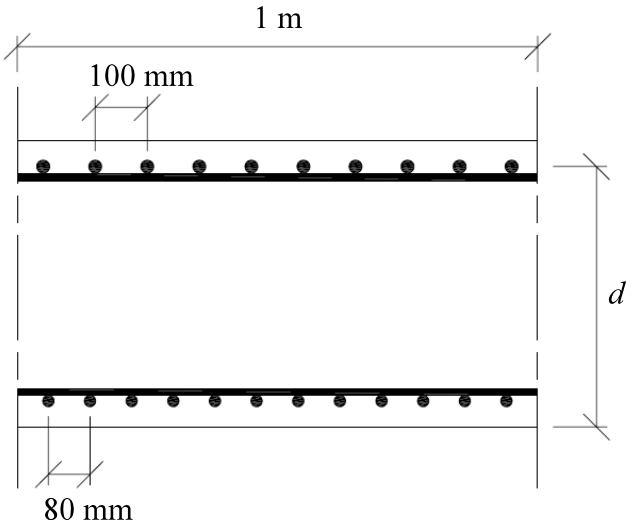

Figure 5.4 Existing reinforcement arrangement in the most heavily reinforced section in the actual region.

5.2 Evaluation parameters

Evaluation parameters are used in order to compare the methods to each other. Unlike the requirements in Section 4.1 the parameters do not need to be fulfilled; they are rather desirable qualities.

5.2.1 Selection of parameters for the actual case

The parameters described below are chosen after discussion with Westerdahl[1] and they are weighted against each other with regard to their importance in the case in question. The choice of parameters and the weighting of them is just an example and they will differ from case to case. Each method is graded with regard to these parameters on a scale from 1 to 5, where 5 is the best performance.

- ***Traffic disturbance***

  It is important to disturb the traffic as little as possible when a strengthening method is applied to a bridge. If the road above or under the bridge needs to be closed it would result in rerouting of the traffic. This causes inconvenience for the road users and national economical costs. A high grade with regard to this parameter represents little traffic disturbance.

- ***Experience from practice***

  It is preferable to make use of strengthening methods which have been used and tested in practice. In this way, unexpected events, which have not been foreseen during planning, can be avoided during construction. A high grade represents good experience from practice.

- ***Durability***

  To choose a durable solution is important from an economical point of view. It is advantageous if the choice of strengthening method can minimise the risk of problems during the remaining service life. Another durability aspect is that it is important to be able to easily inspect critical details. A high grade represents a durable solution.

- ***Aesthetic interference***

  When a strengthening procedure is applied to an existing bridge it might change its appearance. It is desirable to not interfere too much with the aesthetics or to restore the original look after strengthening. A high grade represents little deviance from the original appearance.

- ***Costs***

  The cost of a strengthening project is of course an important parameter. Both the choice of material and technique for strengthening affects the cost for a certain method. A high grade represents low costs.

- ***Risks***

  Making use of a method could involve certain risks. Unexpected difficulties could for example emerge during strengthening. Furthermore, uncertainties regarding the mechanical behaviour can exist. A high grade represents low risks.

[1] Jonas Westerdahl Structural Engineer Sweco Infrastructure AB, discussion 21st May 2010.

5.2.2 Weighting of parameters

In order to use the parameters in the evaluation they need to be weighted against each other. In a real life situation this needs to be discussed with the client in order to end up with the most desirable solution. In our case we discussed the weighting with Westerdahl[2]. The parameters' importance in our evaluation is shown in Table 5.1. The parameter "Traffic disturbance" is heavily weighted since it is costly to disturb the traffic. "Costs" is also a heavy economical post and is therefore also highly ranked. "Risks" and "Durability" is almost equally weighted on the third respectively fourth place. "Aesthetic interference" and "Experience from practice" are considered as less important parameters.

Table 5.1 Evaluation parameters with weighting factors.

Ranking	Weighting factor	Parameter
1	37%	*Traffic disturbance*
2	19%	*Costs*
3	18%	*Risks*
4	13%	*Durability*
5	8%	*Aesthetic interference*
6	5%	*Experience from practice*

5.3 Results

The calculation results from when the strengthening methods were theoretically applied to the case are presented in this section.

5.3.1 Method 1 – Near surface mounted longitudinal post-tensioned carbon FRP

Since this method is not suitable for continuous slabs, it is assumed that the case consists of a one span frame in order to be able to evaluate this method.

The carbon FRP is chosen to be StoFRP Bar M according to the product property sheet Sto Scandinavia AB (2006). The material properties are as shown below.

[2] Jonas Westerdahl Structural Engineer Sweco Infrastructure AB, discussion 21st May 2010.

Ultimate tensile strength: $f_{FRP,tu} = 2$ GPa

Modulus of elasticity: $E_{FRP} = 245$ GPa

Cross-sectional area: $A_{FRP} = 200$ mm^2

These properties are used to calculate the capacity of the strengthened structure according to the procedure described in Section 4.2. The calculations are presented in Appendix D and the results are shown below.

In order to achieve the required capacity increase the average axial stress in the concrete due to post-tensioning should be:

$$\sigma_{cp} = 1.049 \text{ MPa}$$

A suitable spacing with regard to the existing reinforcement in the frame wall is chosen:

$$s = 200 \text{ mm}$$

With this spacing the required force in each carbon FRP bar is as shown below. Here it is assumed that the magnitude of the cross-sectional stress is determined by the thickest part of the slab, h_0, to be on the safe side.

$$P_{FRP} = \sigma_{cp} \cdot s \cdot h_0 = 283.3 \text{ kN}$$

If it is approximated that this force is the largest developed force in the tendon the capacity of the bar can be checked.

$$\sigma_{FRP} = \frac{P_{FRP}}{A_{FRP}} = 1.42 \text{ GPa} < f_{FRP,tu} = 2 \text{ GPa}$$

Evaluation

In order to apply this strengthening method it is necessary to perform excavations outside the frame walls in order to access the area where the tendons are to be anchored. Due to this it is necessary to close the bridge for traffic during a period of time. However, if the strengthening procedure can be coordinated with replacement of the road topping, the excavations do not involve much additional work. Moreover, a large part of the strengthening procedure is performed from below the slab; therefore it might be possible to reduce the time when the bridge needs to be closed.

Near surface mounted carbon FRP reinforcement is a rather well-known technique when it comes to strengthening of existing reinforced concrete structures. However, the most common application for this method is to use it in order to increase bending capacity. Nevertheless it should be possible to take advantage of some of these experiences.

Drilling with high accuracy is required in order to connect the grooves in the bottom surface of the slab to the holes in the frame wall. Related to this, the relatively large amount of reinforcement at the frame corners might cause problems.

This method is very advantageous with regard to aesthetic interference. The FRP bars are completely embedded in the structure and since the grooves in the concrete surface are filled with grout they will not be visible.

Rather large production costs are related to this method. Due to the large post-tensioning required in the slab the tendons have to be placed with a small spacing which results in much work for drilling and sawing grooves.

Since carbon FRP is not degraded when exposed to outdoor conditions this procedure has an advantage with regard to durability. However, a disadvantage is that the anchors of the tendon will not be accessible during the service life and inspection of them and re-tensioning of the tendon will not be possible.

A potential risk with this method is that it can be difficult to avoid the existing reinforcement when the holes are to be drilled at the frame corner. The exact location of the reinforcement bars cannot be determined until the work on site is initiated and it is not sure even then that all bars can be located.

Based on the discussion above, grades are given to the method with regard to the different evaluation parameters according to Table 5.2.

Table 5.2 Grading with regard to evaluation parameters.

Parameter	**Grade (1-5)**
Traffic disturbance	2
Experience from practice	2
Durability	2
Aesthetic interference	5
Costs	2
Risks	4

5.3.2 Method 2 – Vertical post-tensioned steel wires with external anchors

When this method is theoretically applied on the case described in Section 5.1 the following steel properties are chosen:

Steel quality: B500B

Yield strength: $f_{yk} = 500$ MPa

Wire diameter: $\phi = 6$ mm

With these values as input data the capacity of the strengthened structure is evaluated and the calculations are presented in Appendix E. The results from the calculations are presented below.

The transversal spacing is chosen in order to fit with the existing reinforcement arrangement, see Section 5.1, as good as possible. An initial value of the transversal spacing is chosen as:

$$s_{trans} = 240 \text{ mm}$$

The required spacing in the longitudinal direction can be calculated. A suitable longitudinal spacing for the post-installed wires with regard to the existing reinforcement is:

$$s_{long} = 150 \text{ mm}$$

This results in the following number of units if it is assumed that the regions within $\Delta l = 3$ m from the end supports is strengthened with the spacing above:

$$n_{units} = \frac{b_{slab} \cdot \Delta l}{s_{trans} \cdot s_{long}} = \frac{8.648 \cdot 3}{0.24 \cdot 0.15} \approx 720$$

This results in the following shear capacity with regard to shear sliding failure with a strut inclination of $\theta = 21.8°$:

$$V_{Rd,s} = 646.6 \text{ kN}$$

$$V_{Rd,s} > V_{Ed} = 502.6 \text{ kN}$$

Unfortunately the existing reinforcement arrangement limits the choice of spacing in such a way that this large over-capacity is obtained. The capacity with regard to web shear compression failure is:

$$V_{Rd,max} = 2413 \text{ kN}$$

$$V_{Rd,max} > V_{Ed} = 502.6 \text{ kN}$$

In order to decide to what degree the vertical wires should be prestressed a condition which corresponds to that of pre-installed bars was sought. This has been obtained by calculating the steel stress which would appear in pre-installed bars when the structure is loaded by its self-weight only. It is also important to consider long term effects. This could be done by increasing the post-tension which is applied in the wires at mounting, however, this is not treated in this report. The calculations for the required steel stress are presented in Appendix E and the tendon force in the wires after long time should be:

$$\sigma_{pw} = 62.1 \text{ MPa}$$

$$P = \sigma_{pw} A_{swi} = 1.8 \text{ kN}$$

Evaluation

In order to anchor the wires on the top side it is necessary to close the bridge for traffic and remove the road topping. The large amount of holes implies that the time when the bridge needs to be closed might be long. If Öberg's method could be modified by increasing the diameter of the wires the amount of holes could be reduced.

Research has been made by Öberg on the subject and many tests have been performed. Although to the authors' knowledge it is not known if any full scale strengthenings have been performed, the experience from practice can be considered to be rather good.

The possibility to post-tension the wires is favourable with regard to serviceability, since shear crack widths can be minimised. In addition it is possible to re-tension the wires if for example creep effects have caused problems. Another advantage with regard to durability is that the holes are grouted which protects the steel wires from corrosion. The fact that the anchors are exposed could cause durability problems, however the galvanised steel has rather good resistance to degradation.

The active anchors on the bottom side of the slab will be visible and from an aesthetic point of view this might be unfavourable.

As mentioned above, many holes need to be drilled in the slab which will be time consuming and result in a high production cost. The steel wires are of standard steel and will on the other hand not cause a high cost.

The main risk with this method is the difficulty to avoid the existing reinforcement. A small spacing is required between the drilled holes but there is a rather large amount of longitudinal reinforcement in the structure. Since the road topping needs to be removed it should be possible to locate the bars approximately from both the top and bottom sides which is positive.

Based on the discussion above, grades are put on the method with regard to the different evaluation parameters according to Table 5.3.

Table 5.3 Grading with regard to evaluation parameters.

Parameter	**Grade (1-5)**
Traffic disturbance	1
Experience from practice	3
Durability	3
Aesthetic interference	2
Costs	2
Risks	3

5.3.3 Method 3 – Vertical post-tensioned steel bars with internal anchor

The calculations for when this method has been theoretically applied to the case are presented in Appendix F. Since the case is a slab frame bridge the strengthened zone in question will have a tensioned upper edge and a compressed lower edge as shown by the truss model in Figure 5.5. The undercut anchors therefore need to be anchored above the tensile reinforcement.

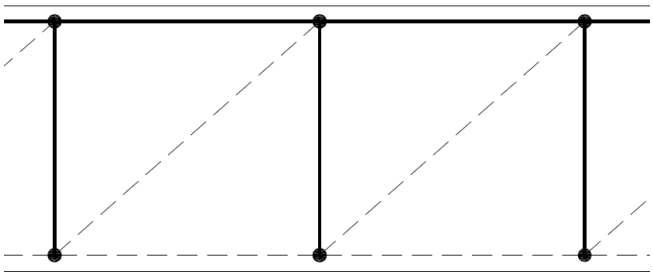

Figure 5.5 Truss model for the strengthened concrete slab frame. Dashed lines show struts and bold lines show ties.

In order to exemplify the method on the case a product, heavy duty anchor (HDA), from HILTI Anchor selection scheme was chosen. A heavy duty anchor has high load capacity and is applicable both in cracked and uncracked concrete. The anchor is equipped with automatic undercutting. The galvanized steel version is chosen as material (HILTI, 2009). The calculations where optimized in order to choose the smallest suitable undercut anchor available at Hilti.

Mechanical properties of HDA:

Steel strength: $f_{uk} = 800$ MPa

Anchor diameter: $\phi = 10$ mm

Stressed cross-section: $A_s = 58$ mm^2

Design steel resistance per anchor: $N_{Rd,s} = 30.7$ kN

Design pull-out resistance per anchor: $N_{Rd,p} = 16.7$ kN

With these values as input data the capacity of the strengthened structure is evaluated and the calculations are presented in Appendix F. The results from the calculations are presented below.

The transversal spacing is chosen in order to fit with the existing reinforcement arrangement, see Section 5.1, as good as possible. A possible transversal spacing is chosen as:

$$s_{trans} = 240 \text{ mm}$$

The required spacing in the longitudinal direction can be calculated. A suitable longitudinal spacing for the undercut anchors with regard to the existing reinforcement is:

$$s_{long} = 300 \text{ mm}$$

The total number of units used in the strengthened region under the same assumptions as in Method 2 is:

$$n_{units} = \frac{b_{slab} \cdot \Delta l}{s_{trans} \cdot s_{long}} = \frac{8.648 \cdot 3}{0.24 \cdot 0.3} \approx 360$$

This results in the following shear capacity with regard to shear sliding failure with a strut inclination of $\theta = 21.8°$:

$$V_{Rd,s} = 524.9 \text{ kN}$$

$$V_{Rd,s} > V_{Ed} = 502.6 \text{ kN}$$

The prestressing force is chosen according to similar assumptions as in Method 2 but also with regard to creep according to Figure 4.14 where the prestressing force is reduced with 60% after 50 days:

$$\sigma_{pw} = 22.38 \text{ MPa}$$

$$P = \sigma_{pw} A_{swi} = 3.5 \text{ kN}$$

$$k_{creep} = \frac{1}{60\%} = 1.667$$

$$P_{eff} = k_{creep} \cdot P = 5.9 \text{ kN}$$

The capacity with regard to web shear compression failure is:

$V_{Rd,max} = 2415$ kN

$V_{Rd,max} > V_{Ed} = 502.6$ kN

Evaluation

As mentioned in Section 4.4, this strengthening method causes little disturbance of the traffic over the bridge since all strengthening work is done from the bottom side of the slab. The strengthening procedure still interferes with the traffic activities under the bridge and a diversion of the traffic is required.

The experience from practice is low since the undercut anchors have not been used in the purpose to act as shear reinforcement before.

When it comes to durability similar effects are obtained as in Method 2. However, loss due to creep will be larger but, as written earlier, it is possible to re-tension the bars. The fact that the anchors are exposed could cause durability problems, however the galvanised steel has rather good resistance to degradation.

When it comes to aesthetics the active anchors will interfere in the same way as in Method 2 with the exception that this method only has half the amount of strengthening units.

A lot of money is saved as it is not necessary to remove the road topping. The cost for the anchors will also be relatively low since the smallest anchor dimension available was chosen and relatively few holes need to be drilled. However, each hole needs to be accurately measured since the whole slab is not allowed to be penetrated. Also, each hole needs to be drilled twice due to the undercut drilling procedure. Both of these procedures are time-consuming and therefore costly.

The risk for not being able to anchor the bar beyond the node in the truss model is relatively high, since the top reinforcement can be hard to locate and avoid and as mentioned above, the slab is not allowed to be fully penetrated. The consequence of this is that the mechanical model will not work.

Based on the discussion above, grades are given to the method with regard to the different evaluation parameters according to Table 5.4.

Table 5.4 Grading with regard to evaluation parameters.

Evaluation parameters	**Grade (1-5)**
Traffic disturbance	4
Experience from practice	1
Durability	3
Aesthetic interference	2
Costs	4
Risks	1

5.3.4 Method 4 – Vertical FRP bars with anchorage by bond

The calculations for when this method is theoretically applied on the case are presented in Appendix G. Similar carbon FRP bars as the ones used by De Lorenzis & Nanni (2001) are used here:

Modulus of elasticity of bars: E_{FRP} = 104.8 GPa

Nominal bar diameter: ϕ = 9.5 mm

Bond strength based on results obtained from bond tests:

$$f_B = 6.9 \text{ MPa}$$

The transversal and longitudinal spacing is chosen in order to have a first preliminary estimation as:

s_{trans} = 200 mm

s_{long} = 200 mm

This results in the following contribution to the shear capacity of the FRP bars with regard to bond failure:

V_{1F} = 599.5 kN

The shear capacity with regard to fracture of the FRP bars is:

V_{2F} = 391.0 kN

The contribution from the FRP bars will therefore be the smaller of these two:

V_{FRP} = 391.0 kN

The contribution from the concrete would be:

$$V_{Rd,c} = 356.4 \text{ kN}$$

The total shear capacity is calculated as:

$$V_{Rd,FRP} = V_{Rd,c} + V_{FRP} = 777.6 \text{ kN}$$

Evaluation

The result that the FRP bars fail before bond failure is unrealistic, since in the experiments all the specimens failed by bond failure.

It is also questionable if it is possible to fill the holes in the slab with epoxy as efficiently as the grooves in the experimental study, since the holes are not as accessible as the grooves.

To sum up, it is concluded together with the discussion in Section 4.5.3 that this strengthening method does not fulfil the requirement of appropriate behaviour of the truss model. Therefore it will not be further discussed in the evaluation.

5.3.5 Method 5 – Closed carbon FRP links

The material properties are chosen according to Bayrak & Binici (2006).

Ultimate tensile strength: $f_{FRP,tu} = 4$ GPa

Modulus of elasticity: $E_{FRP} = 225$ GPa

Maximum strain: $\varepsilon_{eff} = 4‰$

Cross-sectional area: $A_{FRP} = 25$ mm^2

The cross-sectional area refers to one strip. One link can consist of a long strip which has been stitched in a number of layers through the holes. In this case the following choice has been made:

Number of layers: $n_{lay} = 3$

Total FRP area: $A_{FRP,tot} = n_{lay} A_{FRP} = 75$ mm^2

With these values as input data the capacity of the strengthened structure is evaluated and the calculations are presented in Appendix H. The results from the calculations are presented below.

The transversal spacing of the vertical parts of the links is chosen in order to fit with the existing reinforcement arrangement, see Section 5.1, as good as possible. An initial value of the transversal spacing is chosen as:

$s_{trans} = 320$ mm

The required spacing in the longitudinal direction can be calculated. A suitable longitudinal spacing for the links with regard to the existing reinforcement is:

$s_{long} = 300$ mm

The total amount of holes required in the strengthened region under the same assumptions as in Method 2 is:

$$n_{units} = \frac{b_{slab} \cdot \Delta l}{s_{trans} \cdot s_{long}} = \frac{8.648 \cdot 3}{0.32 \cdot 0.3} \approx 270$$

As a result, the following capacity with regard to shear sliding failure is obtained:

$V_{Rd,FRP} = 537.9$ kN

$V_{Rd,FRP} > V_{Ed} = 502.6$ kN

Capacity with regard to web shear compression failure:

$V_{Rd,max} = 2025$ kN

$V_{Rd,max} > V_{Ed} = 502.6$ kN

Evaluation

Also this method requires closing the bridge from traffic when the work is performed. The number of holes which needs to be drilled is significantly less compared to the other similar methods; hence the time when the bridge needs to be closed is decreased.

Rather many research experiments have been performed using this strengthening procedure, mostly with regard to punching shear. However, to the authors' knowledge no applications of the method have been performed on slab bridges which are in use.

Since there is no possibility to post-tension the strips, there might be a risk for large shear crack widths. The use of carbon FRP as a material on the other hand is advantageous with regard to durability.

The strips will be visible from below the slab but since they are bonded tightly to the concrete surface it will not interfere much with the aesthetics of the structure.

The small amount of drilling holes is also advantageous with regard to production cost. Nevertheless, the fact that it is necessary to remove the road topping results in a high cost.

As for most of the methods there is a risk when it comes to avoiding the existing longitudinal reinforcement. It is estimated that the risk is the same as for Method 2.

Based on the discussion above, grades are given to the method with regard to the different evaluation parameters according to Table 5.5.

Table 5.5 Grading with regard to evaluation parameters.

Parameter	**Grade (1-5)**
Traffic disturbance	2
Experience from practice	3
Durability	3
Aesthetic interference	4
Costs	3
Risks	3

5.4 Comparison of the methods

The grades for each method are weighted with the weighting factors from Section 5.2.2 and put together in the evaluation matrix shown in Table 5.6.

Table 5.6 Evaluation matrix.

		Method 1	**Method 2**	**Method 3**	**Method 5**
Parameters	*Weighting factor*	*Weighted grade*			
Traffic disturbance	*37%*	0,74	0,37	1,48	0,74
Experience from practice	*5%*	0,1	0,15	0,05	0,15
Durability	*13%*	0,26	0,39	0,39	0,39
Aesthetic interference	*8%*	0,4	0,16	0,16	0,32
Costs	*19%*	0,38	0,38	0,76	0,57
Risks	*18%*	0,72	0,54	0,18	0,54
Total:	*100%*	2,6	1,99	3,02	2,71

As can be seen in Table 5.6 Method 3 obtains the highest grade in the evaluation matrix. The most crucial grade is the one for "Traffic disturbance" since Method 3 is the only method which does not involve removing of the road topping and since this factor was weighted heavily. Also the grade for "Costs" contributes relatively much to the total. The fact that Method 3 was given a low grade in the case of "Experience from practice" did not influence the total result to a great extent, since that factor was weighted lightly.

6 Conclusions

The main conclusion from this project is that the methods 1, 2, 3 and 5 described in Chapter 4 all are suitable for strengthening of concrete slab bridges with regard to shear capacity.

Furthermore, it can be concluded from the evaluation in the previous chapter that Method 3, involving vertically mounted post-tensioned steel rods with internal anchor, is the most suitable method for the bridge selected for the case study. The condition for this method to be applicable is that it fulfils the requirements stated in Section 4.1. In order to be able to proceed with the evaluation it has been assumed that these requirements are fulfilled.

Since the result from the evaluation depends on the case in question it should also be noted that from a more general point of view all the methods in the evaluation are of interest. For example, in a case where the road topping needs to be replaced regardless of the strengthening procedure, the traffic disturbance parameter will not be as heavily weighted. This will in turn give a completely different result from the evaluation.

Some issues discussed in the report are in need of further investigation. For example, it would be interesting to see more studies regarding the possibility to utilise the capacity with regard to web shear tension failure for a vertically prestressed member. This topic is discussed in Section 4.3.3, but no conclusions could be drawn regarding its potential.

There is also a need for further investigations regarding the use of carbon FRP as shear reinforcement. Some interesting questions which need to be answered are mentioned below:

- Can the variable inclination truss model be utilised, even if the reinforcing material does not exhibit yielding properties?
- If so, is it necessary to restrict the choice of angle further?
- If a 45° angle is required, can the contribution from friction and interlocking effects be regarded?

7 Bibliography

Banverket, 2005. *Bärighetsberäkning av järnvägsbroar*. Borlänge, Sweden: Banverket.

Banverket & Vägverket, 2009. *TK Bro*. Borlänge, Sweden: Vägverket.

Bayrak, B. & Binici, O., 2006. *FRP retrofitting of reinforced concrete two-way slabs - fib Bulletin 35 - Retrofitting of concrete structures by externally bonded FRPs*. Lausanne, Switzerland: Fédération internationale du béton.

Boverket, 1998. *Boverkets handbok om betongkonstruktioner, band 1, konstruktion, BBK 94*. Karlskrona, Sweden: Boverket, Byggavdelning.

Boverket, 2004. *Boverkets handbok om betongkonstruktioner, band 1, konstruktion, BBK 04*. Karlskrona, Sweden: Boverket, Byggavdelningen.

Broo, H., 2006. *Design and assesment for shear and torsion in prestressed concrete bridges - A state-of-the-art investigation*. Göteborg, Sweden: Chalmers University og Technology Report no. 2006:2, Division of Structural Engineering, Concrete Structures.

CEN/TC250/SC2, 2004. *Eurocode 2: Design of concrete structures - Part 1: General rules and rules for buildings*. Brussels, Belgium: European Committee for Standardization.

Collins, M.P. & Mitchell, D., 1991. *Prestressed concrete structures*. Englewood cliffs, USA: Prentice Hall.

De Lorenzis, L. & Nanni, A., 2001. Shear strengthening of reinforced concrete beams with near-surface mounted fiber-reinforced polymer rods. *ACI Structural Journal*, Vol. 98, No. 1, January-February, pp.pp.60-68.

Eligehausen, R., Mallée, R. & Silva, J.F., 2006. *Anchorage in Concrete Construction*. Berlin: Ernst & Sohn.

Engström, B., 2007. *Beräkning av betongkonstruktioner*. Göteborg, Sweden: Chalmers tekniska högskola Rapport nr. 2007:13, Institutionen för bygg-och miljöteknik.

Engström, B., 2009. *Design and analysis of prestresses concrete structures*. Göteborg, Sweden: Chalmers University of Technology Report 2009:2, Department of Civil and Environmental Engineering.

Esfahani, M.R., Kianoush, M.R. & Moradi, A.R., 2009. Punching shear strength of interior slab-column connections strengthened with carbon fiber reinforced polymer sheets. *Engineering Structures*, Vol. 31(7), pp.1535-42.

fib , 2001. *Bulletin 14 - Externally bonded FRP reinforcement for RC structures*. Lousanne, Switzerland: Fédération internationale du béton.

FIP, 1991. *Repair and stregthening of concrete structures*. London, England: Thomas Telford Service Ltd.

Google Maps, 2010. *http://maps.google.se/*. [Online] Available at: http://maps.google.se/maps?hl=sv&tab=wl [Accessed 13 April 2010].

HILTI, 2009. *Anchor Fastening Technology Manual*. 62009th ed. Schaan, Lichtenstein: Hilti Corporation.

Matta, F. et al., 2007. Externally post-tensioned carbon FRP bar sustem for deflection control. *Construction and Building Materials*, Vol. 23 (2009)(4), pp.1628-39.

Monti, G., 2006. *Modelling aspects and design issues for anchorages, shear strengthening and confinement - fib Bulletin 35 - Retrofitting of concrete structures by externally bonded FRPs*. Lausanne, Switzerland: Fédération internationale du béton.

Mukherjee, A. & Rai, G.L., 2008. Performance of reinforced concrete beams externally prestressed with fiber composites. *Construction and Building Materials*, Vol. 23 (2009)(2), pp.822-28.

Muttoni, A., 2008. Punching shear strength of reinforced concrete slabs without transverse reinforcement. *ACI Structural Journal*, Vol. 105(4), pp.440-50.

Nordin, H. & Täljsten, B., 2006. Concrete Beams Strengthened with Prestressed Near Surface Mounted CFRP. *Journal of Composites for Construction*, Vol. 10(1), pp.60-68.

Seracino, R. & Oehlers, D.J., 2004. *Design of FRP and Steel Plated RC Structures*. 1st ed. Oxford: Elsevier Ltd.

Sissakis, K. & Sheikh, S.A., 2007. Strengthening Concrete Slabs for Punching Shear with Carbon Fiber-Reinforced Polymer Laminates. *ACI Structural Journal*, Vol. 104(1), pp.49-59.

Sto Scandinavia AB, 2006. *Förstärkning av bärande konstruktioner med StoFRP System*. [Online] PDF format. Available: [http://www.sto.se] /Broschyrer/Kolfiberförstärkning/Visa broschyr. [Accessed 15 May 2009].

Triantafillou, T.C., 2006. *General concept and design aspects - Materials and techniques - fib Bulletin 35: Retrofitting of concrete structures by externally bonded FRPs*. Lousanne, Switzerland: Fédération internationale du béton.

Triantafillou, T.C. & Papanicolaou, G.C., 2006. Shear strengthening of reinforced concrete members with textile reinforced mortar (TRM) jackets. *Materials and Structures*, Vol. 39(1), pp.93-103.

Täljsten, B., 2002. *CFRP-strengthening - Concrete structures strengthened with near surface mounted CFRP laminates*. (Electronic) PDF format. Available: "http://www.quakewrap.com/technical-papers-on-Fiber-Reinforced-Polymer.php" /CFRP-Strengthening - Concrete Structures Strengthened With Near Surface Mounted CFRP Laminates (2010-03-10).

Wang, H.-l., Jin, W.-l., Cleland, D.J. & Zhang, A.-h., 2009. Strengthening an in-service reinforcement concrete bridge with prestressed CFRP bars. *Journal of Zhejiang University Science A*, Vol. 10(5), pp.635-44.

Vägverket, 2009. *Metodbeskrivning 802 Bärighetsutredning av byggnadsverk*. Borlänge, Sweden: Vägverket.

Öberg, S., 1984. Efterspänd skjuvarmering för förstärkning av betongkonstruktioner. *Bygg & Teknik*, (8), pp.24-30.

Öberg, S., 1990. Publication 90:1 *Post tensioned shear reinforcement in rectangular RC beams*. Diss. Chalmers University of Technology. Göteborg, Sweden: Chalmers University of Technology.

Appendix A

Shear force at web shear tension failure for a biaxially stressed section

In order to study the state of stresses in the slab element at the centroidal axis Mohr´s circle is used.

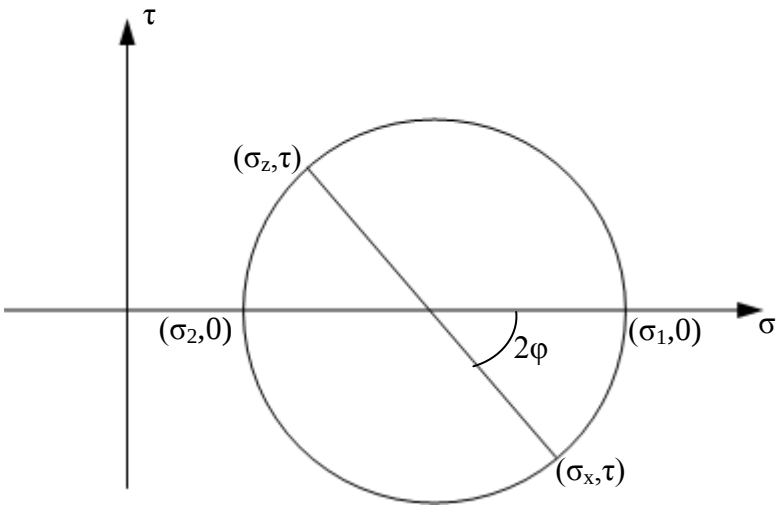

The largest principal stress for a biaxial loaded section can be calculated as

$$\sigma_2 = \frac{1}{2}(\sigma_z + \sigma_x) - \sqrt{\left(\frac{\sigma_z - \sigma_x}{2}\right)^2 + {\tau_2}^2} \qquad \Rightarrow$$

$$\left(\frac{\sigma_z - \sigma_x}{2}\right)^2 + {\tau_2}^2 = \left(\frac{1}{2}(\sigma_z + \sigma_x) - \sigma_2\right)^2$$

From this expression the shear stress can be solved as

$$\tau_2 = \sqrt{\left(\frac{1}{2}(\sigma_z + \sigma_x) - \sigma_2\right)^2 - \left(\frac{\sigma_z - \sigma_x}{2}\right)^2} \qquad \Rightarrow$$

$$\tau_2 = \sqrt{\frac{1}{4}(\sigma_z + \sigma_x)^2 - \sigma_2(\sigma_z + \sigma_x) + {\sigma_2}^2 - \frac{1}{4}({\sigma_z}^2 - 2\sigma_z\sigma_x + {\sigma_x}^2)} \qquad \Rightarrow$$

$$\tau_2 = \sqrt{\frac{1}{4}({\sigma_z}^2 + 2\sigma_z\sigma_x + {\sigma_x}^2) - \sigma_2\sigma_z - \sigma_2\sigma_x + {\sigma_2}^2 - \frac{1}{4}({\sigma_z}^2 - 2\sigma_z\sigma_x + {\sigma_x}^2)} \quad \Rightarrow$$

$$\tau_2 = \sqrt{(\sigma_z\sigma_x) - \sigma_2(\sigma_z + \sigma_x) + {\sigma_2}^2}$$

A web shear crack appears when the principal tensile stress σ_2 reaches the concrete tensile strength f_{ct}. The shear force that causes a web shear crack in a biaxial loaded member is then

$$V_{cw} = \frac{I \cdot b_w}{S}\sqrt{(\sigma_z\sigma_x) - f_{ct}(\sigma_z + \sigma_x) + {f_{ct}}^2}$$

Appendix B

Case study – Evaluation of shear capacity for the un-strengthened structure

Properties of existing materials

Concrete class: Btg I K350

$f_{ck} := 25MPa$

$f_{ck.cube} := \frac{f_{ck}}{0.7} = 35.714MPa$

$f_{ctk} := 1.8MPa$

$\gamma_c := 1.5$

$f_{cd} := \frac{f_{ck}}{\gamma_c} = 16.667MPa$

$f_{ctd} := \frac{f_{ctk}}{\gamma_c} = 1.2 \cdot MPa$

Steel class: Ks40

$d_s := 25mm$

$f_{yk} := 390MPa$

$\gamma_s := 1.15$

$f_{yd} := \frac{f_{yk}}{\gamma_s} = 339.13MPa$

$A_{si} := \frac{\pi \cdot d_s^{\,2}}{4} = 490.874mm^2$

Geometry

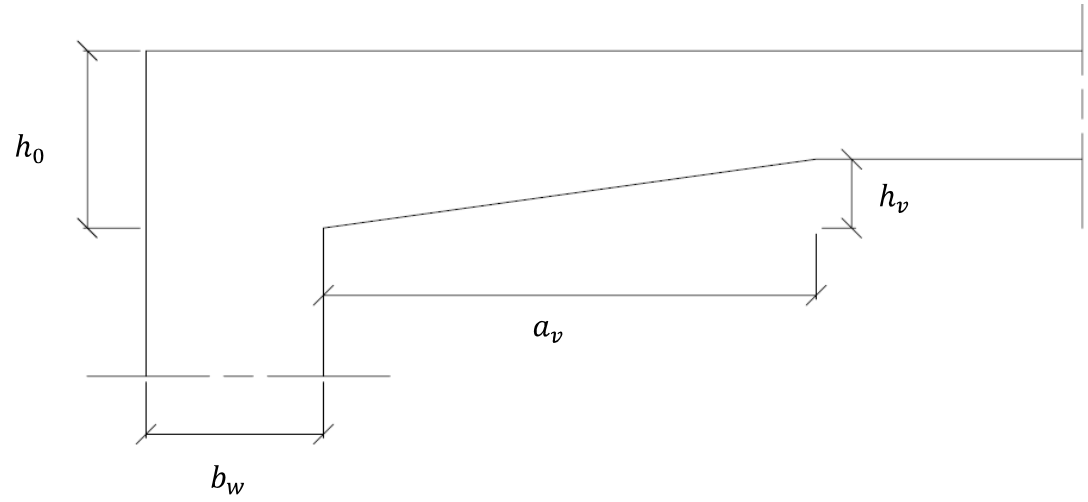

$h_0 := 900mm$ $a_v := 2.5m$

$b_w := 900mm$ $h_v := 350mm$

$h_{slab} := h_0 - h_v = 550mm$

$b := 1m$

$c := \max(1.5 \cdot d_s, 30mm) = 0.038m$

$c_c := c + \frac{d_s}{2} = 0.05m$

$d_0 := h_0 - c_c = 0.85m$

Influence of earth pressure

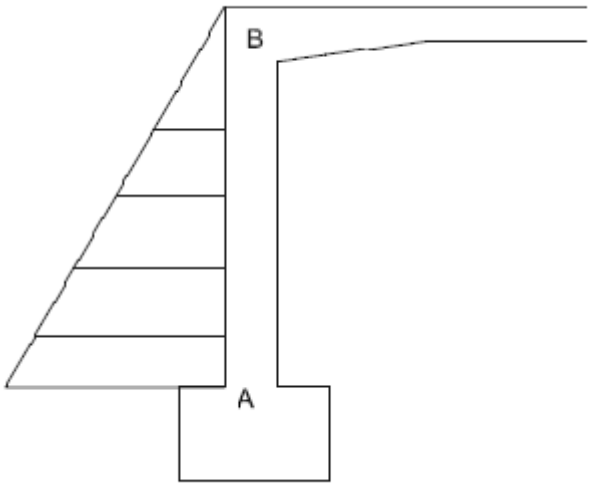

Figure B-1: Earth pressure on frame wall

The following assumptions are made in order to estimate the influence of the earth pressure:

- The frame wall is assumed to be simply supported on the top and bottom side, respectively.
- The normal force in the slab caused by the earth pressure is assumed to correspond to the reaction force in point B of Figure B-1.
- It is assumed that the normal force is acting in neutral plane of the slab.
- The density of the blast stone is assumed to be 18 kN/m ^{3}.

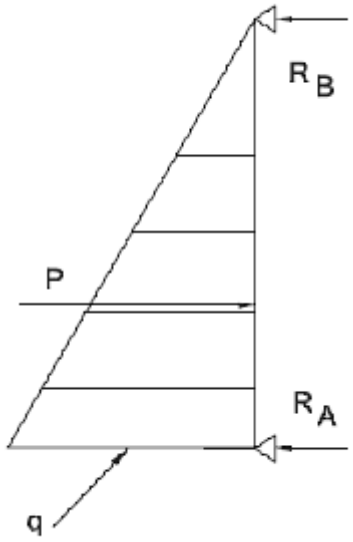

Figure B-2: Simplified static model of frame wall

$\gamma_r := 18\frac{kN}{m^3}$

$L := 44.48m - 38.19m = 6.29m$

$q := \gamma_r \cdot L = 113.22\frac{kN}{m^2}$

$P := q \cdot \frac{L}{2} = 356.077\frac{kN}{m}$

Moment equilibrium around A gives:

$R_b := \frac{P}{3} = 118.692\frac{kN}{m}$

Approximation of shear force due to self-weight

In order to estimate the required initial strain in the post-tensioned vertical reinforcement the shear force corresponding to the self-weight needs to be calculated. This is performed by regarding the supports of the bridge as fixed and the slab is assumed to have a uniform depth.

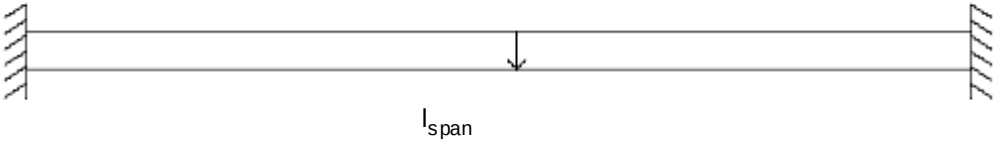

Figure B-3: Approximation of first span of bridge slab.

Concrete density: $\rho_c := 24\frac{kN}{m^3}$

Span length: $l_{span} := 14m$

Bridge width: $b_{slab} := 8.648m$

Approximate uniform depth: $h_{slab} = 550\cdot mm$

Cross-sectional area (approximated from Appendix C):

$A_c := b_{slab}\cdot h_{slab} = 4.756m^2$

Distributed load from self-weight:

$g_k := \rho_c\cdot A_c = 114.154\frac{kN}{m}$

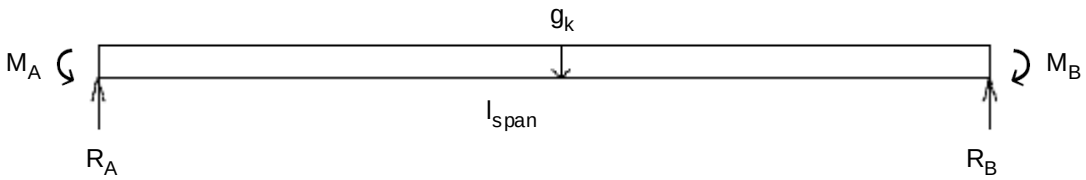

Figure B-4: Forces acting on the slab part.

Approximated shear force at end support A, total width:

$R_A := \frac{g_k\cdot l_{span}}{2} = 799.075kN$

Shear force on a 1m strip:

$V_g := \frac{R_A}{b_{slab}}\cdot b = 92.4\cdot kN$

Evaluation of shear force capacity

The capacity with regard to shear sliding failure will be evaluated at x = 0.9d (Section 1) from the support and the capacity with regard to web shear compression failure will be evaluated at x = 2.5 m where the depth of the slab is lowest.

$$x := \begin{pmatrix} 0 \\ 0.9 d_0 \\ 0.9 \cdot 2.5 d_0 \\ 2.5 m \end{pmatrix} = \begin{pmatrix} 0 \\ 0.765 \\ 1.912 \\ 2.5 \end{pmatrix} m$$

$$d := d_0 - \frac{h_v}{a_v} \cdot x = \begin{pmatrix} 0.85 \\ 0.743 \\ 0.582 \\ 0.5 \end{pmatrix} m$$

$$z := 0.9 \cdot d = \begin{pmatrix} 0.765 \\ 0.669 \\ 0.524 \\ 0.45 \end{pmatrix} m$$

Capacity with regard to shear sliding failure at Section 1

$$V_{Rd.c} = \left[C_{Rd.c} \cdot k \cdot \left(100 \rho_l \cdot \frac{f_{ck}}{MPa} \right)^{\frac{1}{3}} MPa + k_1 \cdot \sigma_{cp} \right] \cdot b \cdot d_0$$

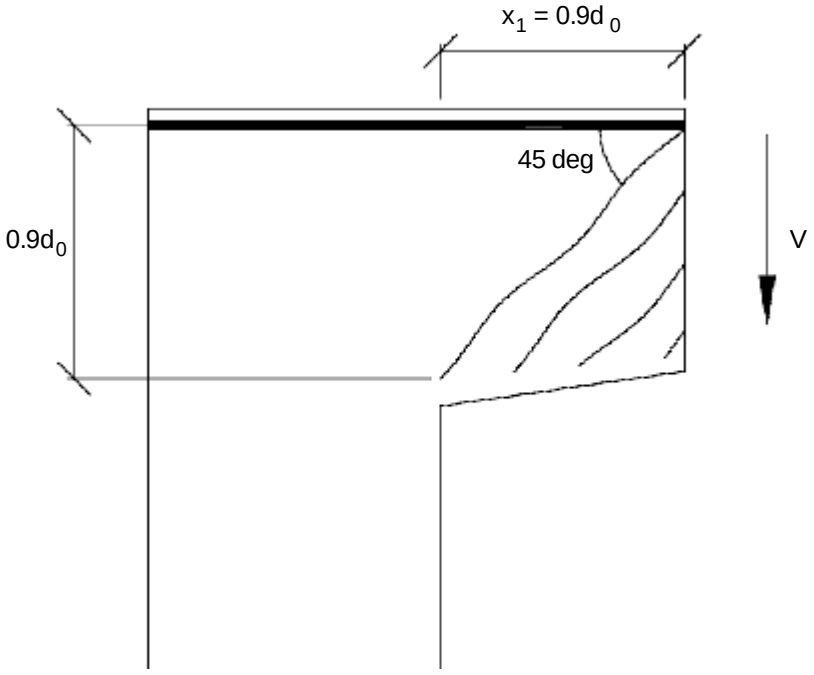

Figure B-5 Section for check of capacity with regard to shear sliding failure.

$x_1 = 0.765\text{m}$ $d_0 = 0.85\text{m}$

Spacing of each bar type: $s_e := 300\text{mm}$

Number of bar types in section: $n_1 := 3$

Total reinforcement area in section: $A_{s.1} := A_{si} \cdot n_1 \cdot \frac{b}{s_e} = 4.909 \times 10^3 \cdot \text{mm}^2$

$$C_{Rd.c} := \frac{0.18}{\gamma_c} = 0.12$$

$$k := 1 + \sqrt{\frac{200\text{mm}}{d_0}} = 1.485 \qquad < 2 \quad \text{OK}$$

$$\rho_{l.1} := \frac{A_{s.1}}{b \cdot d_0} = 5.775 \times 10^{-3} \qquad < 0.02 \quad \text{OK}$$

$$k_1 := 0.15$$

$$\sigma_{cp} := \frac{R_b}{d_0} = 0.14\,\text{MPa}$$

$$\nu_{min} := 0.035(k)^{\frac{3}{2}} \cdot \sqrt{\frac{f_{ck}}{\text{MPa}}}\,\text{MPa} = 0.317\,\text{MPa}$$

$$\left| \nu_{min} + k_1 \cdot \sigma_{cp} \right| \cdot b \cdot d_0 = 287.006\,\text{kN}$$

$$V_{Rd.c} := \left[C_{Rd.c} \cdot k \cdot \left(100 \rho_{l.1} \cdot \frac{f_{ck}}{\text{MPa}} \right)^{\frac{1}{3}} \text{MPa} + k_1 \cdot \sigma_{cp} \right] \cdot b \cdot d_0 = 386.649\,\text{kN}$$

$$\text{Check}_1 := \begin{cases} \text{"OK"} & \text{if } V_{Rd.c} \geq \left| \nu_{min} + k_1 \cdot \sigma_{cp} \right| \cdot b \cdot d_0 \\ \text{"Not OK"} & \text{otherwise} \end{cases} = \text{"OK"}$$

Appendix C

Drawings

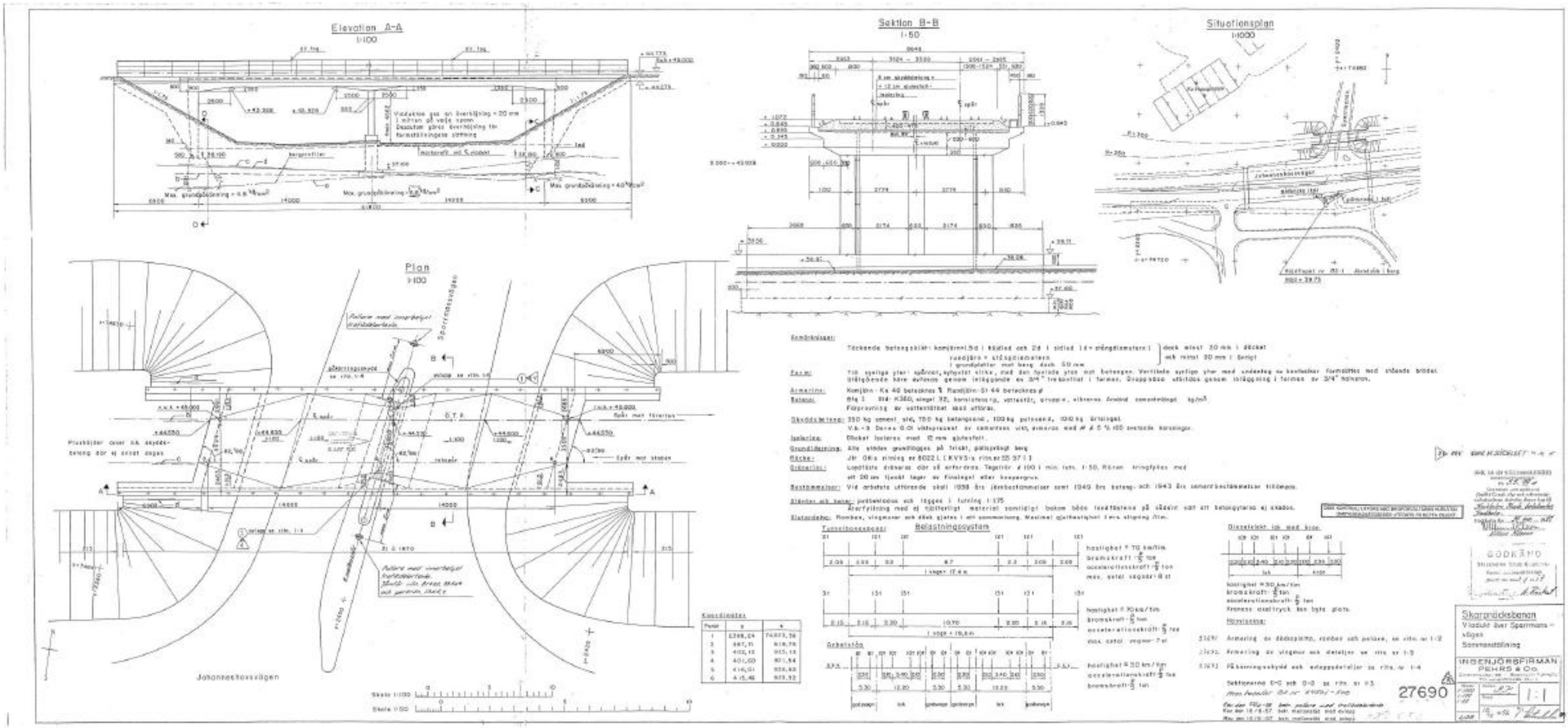

Elevation A-A
1:100
Sektion B-B
1:50
Situationsplan
1:1000
Plan
1:100
Sparrmansvägen
Johanneshovsvägen
Koordinater
Belastningssystem
Tunnelbanevagnar
Arbetståg
Dieselelekt. lok med vagn
Hänvisning:
Armering av däckplatta, ramben och pelare, se ritn. nr 1-2
Armering av vingmur och detaljer se ritn. nr 1-3
Påkörningsskydd och avloppsdetaljer se ritn. nr 1-4
Sektionerna C-C och D-D se ritn. nr 1-5
Skarpnäcksbanan
Viadukt över Sparrmans-vägen
Sammanställning
INGENJÖRSFIRMAN
PEHRS & Co.
27690
1:1

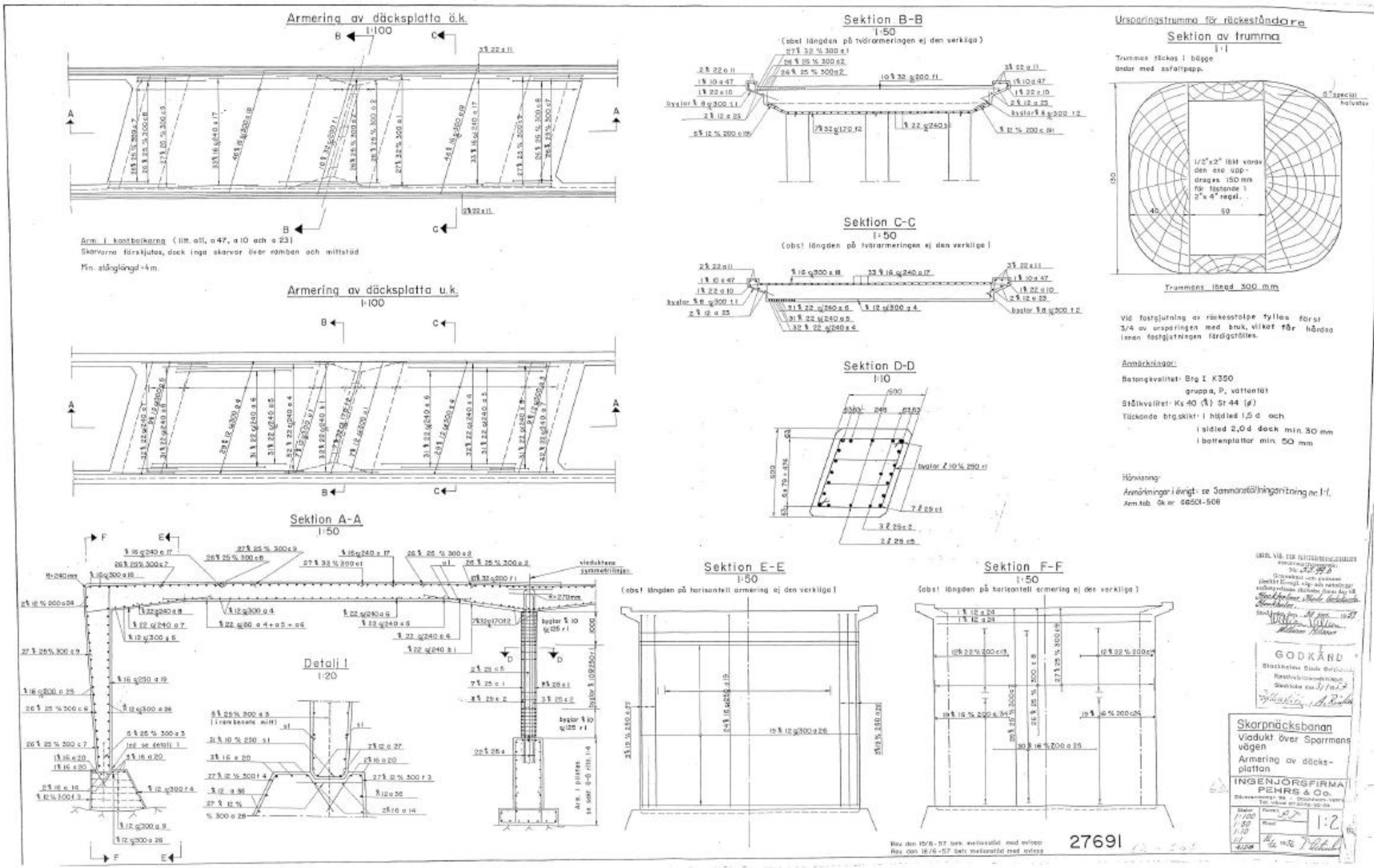

Armering av däcksplatta ö.k.
1:100
Arm. i kantbalkarna (litt. a11, a47, a10 och a23)
Skarvarna förskjutas, dock inga skarvar över ramben och mittstöd
Min. stånglängd = 4 m.
Armering av däcksplatta u.k.
1:100
Sektion A-A
1:50
Detalj I
1:20
Sektion B-B
1:50
(obs! längden på tvärarmeringen ej den verkliga)
Sektion C-C
1:50
(obs! längden på tvärarmeringen ej den verkliga)
Sektion D-D
1:10
Sektion E-E
1:50
(obs! längden på horisontell armering ej den verkliga)
Sektion F-F
1:50
(obs! längden på horisontell armering ej den verkliga)
Urspargingstrumma för räckeståndare
Sektion av trumma
1:1
Trumman täckas i bägge ändar med asfaltpapp.
Trummans längd 300 mm
Vid fastgjutning av räckesstolpe fylles först 3/4 av urspäringen med bruk, vilket får hårdna innan fastgjutningen färdigställes.
Anmärkningar:
Betongkvalitet: Btg I K350
grupp a, P, vattentät
Stålkvalitet: Ks 40 och St 44
Täckande btg.skikt: i höjdled 1,5 d och
i sidled 2,0 d dock min. 30 mm
i bottenplattor min. 50 mm
Hänvisning:
Anmärkningar i övrigt: se Sammanställningsritning nr 1:1.
GODKÄND
Skarpnäcksbanan
Viadukt över Sparrmans vägen
Armering av däcksplattan
INGENJÖRSFIRMA PEHRS & Co.
1:2
Rev. den 15/6-57 betr. mellanstöd med avlopp
Rev. den 18/6-57 betr. mellanstöd med avlopp
27691

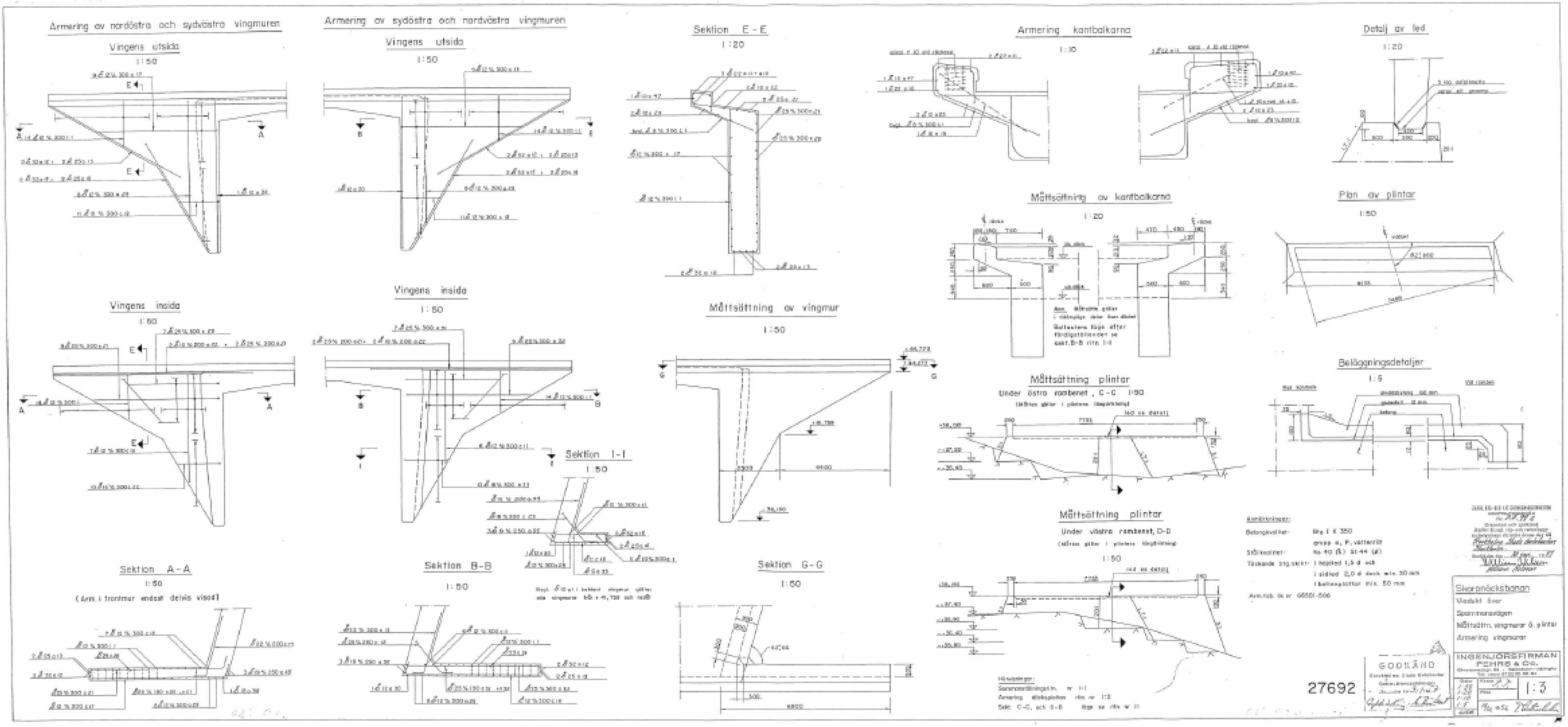

Armering av nordöstra och sydvästra vingmuren
Vingens utsida
1:50
Armering av sydöstra och nordvästra vingmuren
Vingens utsida
1:50
Sektion E-E
1:20
Armering kantbalkarna
1:10
Detalj av led
1:20
Måttsättning av kantbalkarna
1:20
Plan av plintar
1:50
Vingens insida
1:50
Vingens insida
1:50
Måttsättning av vingmur
1:50
Måttsättning plintar
Under östra rambenet, C-C 1:50
Beläggningsdetaljer
1:5
Sektion I-I
1:50
Måttsättning plintar
Under västra rambenet, D-D
1:50
Sektion A-A
1:50
Sektion B-B
1:50
Sektion G-G
1:50
Anmärkningar:
Betongkvalitet: Btg. I K 350
grupp a, P, vattentät
Stålkvalitet: Ks 40 (Ä) St 44 (Ø)
Täckande btg.skikt: i hejdled 1,5 d och
i sidled 2,0 d dock min. 30 mm
i bottenplattor min. 50 mm
Skarpnäcksbanan
Viadukt över
Spannmarsvägen
Måttsättn. vingmurar ö. plintar
Armering vingmurar
INGENJÖRSFIRMAN
FEHRS & Co.
GODKÄND
27692
1:3

Appendix D

Calculations for Method 1

Input data

StoFRP Bar M:

$f_{tu} := 2GPa$

$E_{FRP} := 245GPa$

$\varepsilon_{tu} := \frac{f_{tu}}{E_{FRP}} = 8.163 \times 10^{-3}$

$A_{FRP} := 20mm \cdot 10mm = 200mm^2$

Capacity with regard to shear sliding failure of strengthened section

$$V_{Rd.c} = \left[C_{Rd.c} \cdot k \cdot \left(100 \rho_l \cdot \frac{f_{ck}}{MPa} \right)^{\frac{1}{3}} MPa + k_1 \cdot \sigma_{cp} \right] \cdot b \cdot d_0$$

This capacity should be increased to:

$V_{Ed} = 502.644kN$

To achieve this, the following concrete stress due to post-tensioning is required:

$$\sigma_{cp.str} := \frac{\frac{V_{Ed}}{b \cdot d_0} - C_{Rd.c} \cdot k \cdot \left(100 \rho_{l.1} \cdot \frac{f_{ck}}{MPa} \right)^{\frac{1}{3}} MPa}{k_1} = 1.049MPa \quad < \quad 0.2 \cdot f_{cd} = 3.333MPa$$

Capacity with regard to web shear compression failure of strengthene section

$V_{Rd.max} = 0.5 b_w d_3 \cdot \nu \cdot f_{cd}$

$$\nu := 0.6 \cdot \left(1 - \frac{f_{ck}}{250MPa} \right)$$

$V_{Rd.max} := 0.5 b_w \cdot d_3 \cdot \nu \cdot f_{cd} = 2.025 \times 10^3 \cdot kN$

Required force in FRP bar

Choose tendon spacing: $s_{tendon} := 0.3m$

Assume a uniform cross-sectional stress along the crack with the magnitude determined by the thickest part of the slab to be on the safe side.

$P_{FRP} := \sigma_{cp.str} \cdot s_{tendon} \cdot h_0 = 283.338kN$

$\sigma_{FRP} := \frac{P_{FRP}}{A_{FRP}} = 1.417GPa \quad < \quad f_{tu} = 2 \cdot GPa$

Required force distribution area

To avoid local compressive failure of the concrete at anchorage of the tendon the following force distribution area is required:

$A_{distr} := \frac{P_{FRP}}{f_{cd}} = 0.017m^2$

For example, a square steel plate would need the width: $b_{plate} := \sqrt{A_{distr}} = 0.13m$

Appendix E

Calculations for Method 2

Input data

Steel quality B500B:

$f_{ywk} := 500MPa$

$f_{ywd} := \frac{f_{ywk}}{\gamma_s} = 434.783MPa$

Choice of crack inclination:

$\theta := 22deg$

$d_w := 6mm$

$A_{swi} := \frac{\pi \cdot d_w^2}{4} = 2.827 \times 10^{-5} m^2$

Choice of transversal spacing between bars:

$s_{trans} := 240mm$

$n_{trans} := \frac{b}{s_{trans}} = 4.167$

Shear reinforcement area in 1m strip:

$A_{sw} := n_{trans} \cdot A_{swi} = 1.178 \times 10^{-4} m^2$

Shear sliding failure

$$V_{Ed} = \frac{z_0 \cdot \cot(\theta)}{s_{long}} \cdot f_{ywd} \cdot A_{sw}$$

$V_{Ed} = 502.644kN$

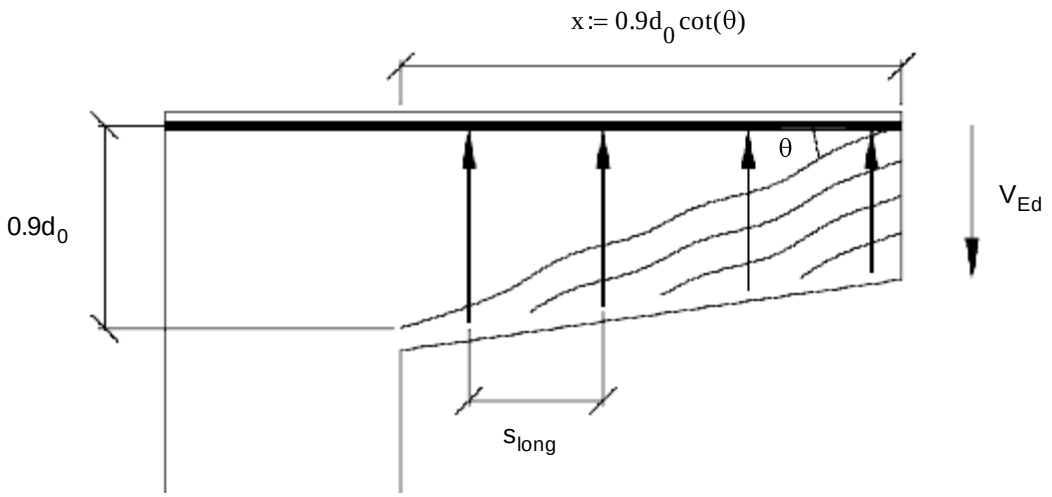

Figure E-1: Section for check of capacity with regard to shear sliding failure for strengthened structure.

$$s_{long} := \frac{z_0 \cdot \cot(\theta)}{V_{Ed}} \cdot f_{ywd} \cdot A_{sw} = 0.193\,m$$

Choose a value suitable with the existing reinforcement arrangement:

$s_{long} := 0.15\,m$

Maximum allowed spacing:

$s_{max} := 0.75 \cdot d_0 = 0.638\,m$

$$Check\_spacing := \begin{cases} "OK" & \text{if } s_{long} \le s_{max} \\ "not\ OK" & otherwise \end{cases} = "OK"$$

$$V_{Rd.s} := \frac{z_0 \cdot \cot(\theta)}{s_{long}} \cdot f_{ywd} \cdot A_{sw} = 646.568\,kN$$

Choice of prestressing

Prestressing should correspond to the steel stress under the load from the self-weight if regular internal stirrups with the same properties as the post-installed bars would have been used.

$$\sigma_{pw} := \frac{V_g \cdot s_{long}}{z_0 \cdot \cot(\theta) \cdot A_{sw}} = 62.134\,MPa$$

$$P := \sigma_{pw} \cdot A_{swi} = 1.757\,kN$$

$$k := \frac{\sigma_{pw}}{f_{ywd}} = 0.143$$

Web shear compression failure

$$V_{Rd.max.str} = \alpha_{cw} \cdot b \cdot z \cdot \nu \cdot f_{cd} \cdot \frac{1}{\cot(\theta) + \tan(\theta)}$$

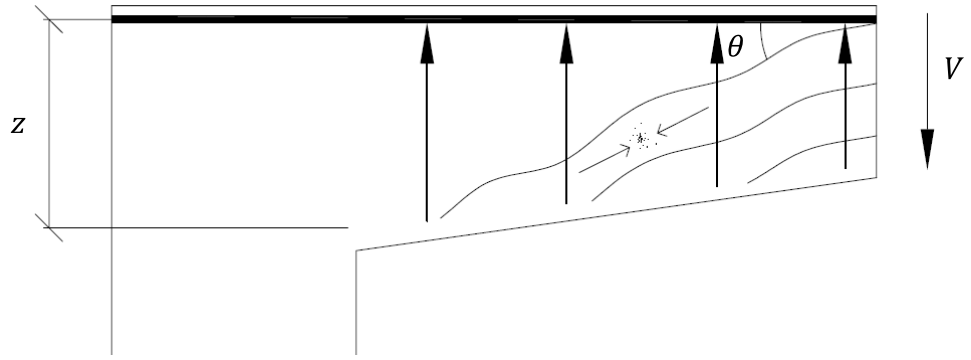

Figure E-2: Section for check of capacity with regard to web shear compression failure for strengthened structure.

Concrete stress due to vertical prestressing:

$$\sigma_{cp.v} := \frac{P}{s_{long} \cdot s_{trans}} = 0.049\,MPa$$

Stress resultant on inclined strut due to prestressing:

$$\sigma_{cp.r} := \sqrt{|\sigma_{cp}|^2 + \sigma_{cp.v}^2} = 0.148\,MPa$$

$$\alpha_{cw} := \begin{cases} 1 + \frac{\sigma_{cp.r}}{f_{cd}} & \text{if } 0 < \sigma_{cp.r} \le 0.25 \cdot f_{cd} \\ 1.25 & \text{if } 0.25 \cdot f_{cd} < \sigma_{cp.r} \le 0.5 \cdot f_{cd} \\ 2.5 \cdot \left(1 - \frac{\sigma_{cp.r}}{f_{cd}}\right) & \text{if } 0.5 \cdot f_{cd} < \sigma_{cp.r} \le 1.0 \cdot f_{cd} \end{cases} = 1.009$$

$$V_{Rd.max.str} := \alpha_{cw} \cdot b \cdot z_0 \cdot \nu \cdot f_{cd} \cdot \frac{1}{\cot(\theta) + \tan(\theta)} = 2.413 \times 10^3 \cdot kN$$

Appendix F

Calculations for Method 3

Input data

A heavy duty anchor HDA-P M16 from HILTI is chosen.

$f_{ywk} := 640MPa$

$f_{ywd} := \frac{f_{ywk}}{\gamma_s} = 556.522MPa$

$\theta := 22deg$

$d = \begin{pmatrix} 0.85 \\ 0.743 \\ 0.582 \\ 0.5 \end{pmatrix} m$

$h_{ef} := \frac{d_0 + d_2}{2} + \frac{d_s}{2} = 0.729m$

Stressed cross-section

$A_{swi} := 58mm^2$

Maximum allowed spacing:

$s_{max} := 0.75 d_0 = 0.638m$

Choice of transversal spacing between bars:

$s_{trans} := 240mm$

$n_{trans} := \frac{b}{s_{trans}} = 4.167$

$A_{sw} := n_{trans} \cdot A_{swi} = 2.417 \times 10^{-4} m^2$

Steel resistance

From HILTI table:

$N_{Rd.s.i} := 30.7 \cdot kN$

$N_{Rd.s} := N_{Rd.s.i} \cdot n_{trans} = 127.917 kN$

Concrete pull-out resistance

$N_{Rd.p.0} := 16.7 kN$

$f_B := \left(\frac{f_{ck.cube}}{25 MPa} \right)^{\frac{1}{2}} = 1.195$

$N_{Rd.p.i} := N_{Rd.p.0} \cdot f_B = 19.96 kN$

$N_{Rd.p} := N_{Rd.p.i} \cdot n_{trans} = 83.168 kN$

Shear sliding failure

$$V_{Ed} = \frac{z_0 \cdot \cot(\theta)}{s_{long}} \cdot N_{Rd}$$

Where N_{Rd} is the total capacity of the anchors of a 1 m wide a cross-section.

$V_{Ed} = 502.644 kN$

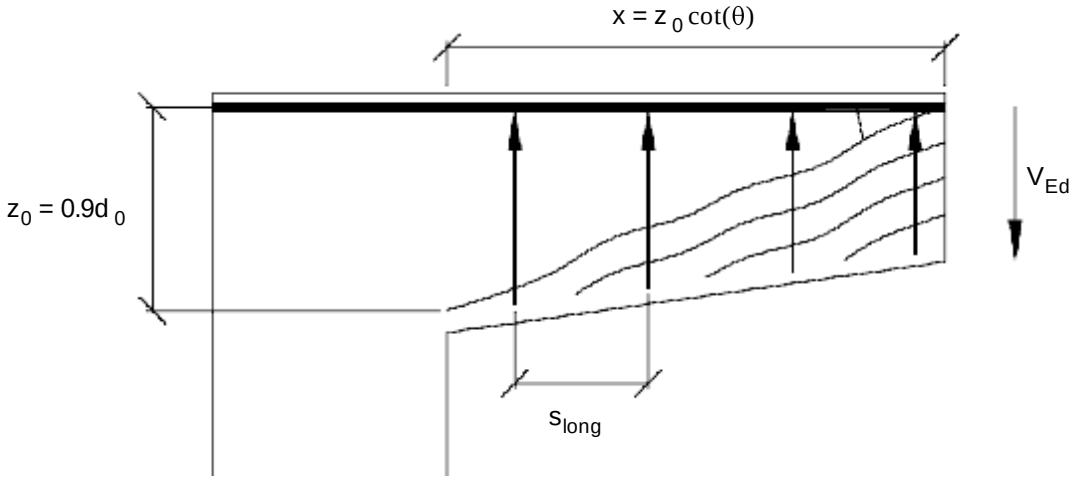

Figure F-1: Section for check of capacity with regard to shear sliding failure for strengthened structure.

$N_{Rd} := \min\left(N_{Rd.s}, N_{Rd.p}\right) = 83.168\,kN$

$s_{long} := \frac{z_0 \cdot \cot(\theta)}{V_{Ed}} \cdot N_{Rd} = 0.313\,m$

Choose a value suitable with the existing reinforcement arrangement:

$s_{long} := 300\,mm$

Maximum allowed spacing:

$s_{max} := 0.75 d_0 = 0.638\,m$

$Check\_spacing := \begin{cases} \text{"OK"} & \text{if } s_{long} \le s_{max} \\ \text{"not OK"} & \text{otherwise} \end{cases} = \text{"OK"}$

$V_{Rd} := \frac{z_0 \cdot \cot(\theta)}{s_{long}} \cdot N_{Rd} = 524.912\,kN$

Choice of prestressing

Prestressing should correspond to the steel stress under the load from the self-weight if regular internal stirrups with the same properties as the post-installed bars would have been used.

$\sigma_{pw} := \frac{V_g \cdot s_{long}}{z_0 \cdot \cot(\theta) \cdot A_{sw}} = 60.579\,MPa$

$P := \sigma_{pw} \cdot A_{swi} = 3.514\,kN$

The prestressing force should be increased with regard to the creep effect in the concrete.

$k_{creep} := \frac{1}{0.6} = 1.667$ From Figure 4.14

$P_{ef} := k_{creep} \cdot P = 5.856 \times 10^3\,N$

Web shear compression failure

$$V_{Rd.max.str} = \alpha_{cw} \cdot b \cdot z \cdot \nu \cdot f_{cd} \cdot \frac{1}{\cot(\theta) + \tan(\theta)}$$

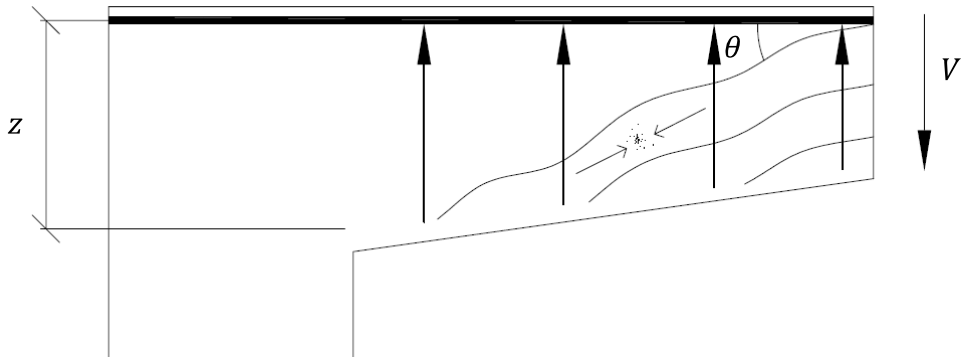

Figure F-2: Section for check of capacity with regard to web shear compression failure for strengthened structure.

Concrete stress due to vertical prestressing:

$$\sigma_{cp.v} := \frac{P_{ef}}{s_{long} \cdot s_{trans}} = 0.081\,MPa$$

Stress resultant on inclined strut due to prestressing:

$$\sigma_{cp.r} := \sqrt{|\sigma_{cp}|^2 + \sigma_{cp.v}^2} = 0.162\,MPa$$

$$\alpha_{cw} := \begin{cases} 1 + \frac{\sigma_{cp.r}}{f_{cd}} & \text{if } 0 < \sigma_{cp.r} \le 0.25 f_{cd} \\ 1.25 & \text{if } 0.25 f_{cd} < \sigma_{cp.r} \le 0.5 f_{cd} \\ 2.5 \cdot \left(1 - \frac{\sigma_{cp.r}}{f_{cd}}\right) & \text{if } 0.5 f_{cd} < \sigma_{cp.r} \le 1.0 f_{cd} \end{cases} = 1.01$$

$$V_{Rd.max.str} := \alpha_{cw} \cdot b \cdot z_0 \cdot \nu \cdot f_{cd} \cdot \frac{1}{\cot(\theta) + \tan(\theta)} = 2.415 \times 10^3 \cdot kN$$

Total amount of anchors:

$$\frac{8.648m \cdot 3m}{s_{long} \cdot s_{trans}} = 360.333$$

Appendix G

Calculations for Method 4

Input data

Elastic modulus of FRP rods:

$E_{FRP} := 104.8GPa$

Nominal rod diameter:

$\phi := 9.5mm$

Average bond strength based on results obtained from bond tests:

$f_b := 6.9MPa$

Maximum allowed spacing:

$s_{max} := 0.75 d_0 = 0.638m$

Choice of transversal spacing between bars:

$s_{trans} := 200mm$

$n_{trans} := \frac{b}{s_{trans}} = 5$

Choice of longitudinal spacing between bars:

$s_{long} := 200mm$

$n_{long} := \frac{0.9 d_0}{s_{long}} = 3.825$

$\gamma_{Ms} := 1.25$

$\gamma_M := 1.5$

Shear capacity

$V_{Rd.FRP} = V_{Rd.c} + V_{FRP}$

$V_{FRP} = \min\left(V_{1F}, V_{2F}\right)$

Bond-controlled failure

$V_{1F} = n_{trans} \cdot \pi \cdot \phi \cdot f_b \cdot L_{tot}$

Length of rod:

$$d_r := \frac{d_2 + d_0}{2} + c_c = 0.766\text{m}$$

$d_{net} := d_r - 2 \cdot c = 0.691\text{m}$

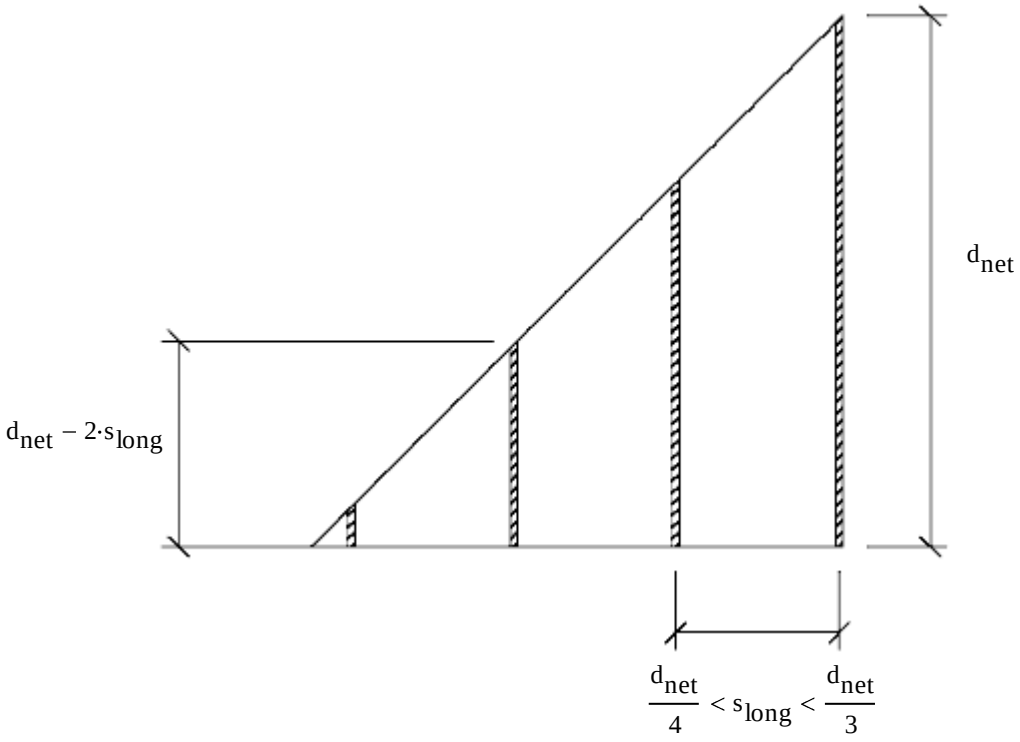

Figure G-1 Illustration of notations.

$$L_{tot.min} := \begin{cases} d_{net} - s_{long} & \text{if } \frac{d_{net}}{3} < s_{long} < d_{net} \\ 2 \cdot d_{net} - 4 \cdot s_{long} & \text{if } \frac{d_{net}}{4} < s_{long} < \frac{d_{net}}{3} \end{cases} = 0.582\text{m}$$

$L_{tot.min} = 0.582\text{m}$

$V_{1F} := n_{trans} \cdot \pi \cdot \phi \cdot f_b \cdot L_{tot.min} = 599.518\text{kN}$

Shear resisted by FRP rods

$$L_{\_i} := 0.001 \cdot \frac{\phi \cdot E_{FRP}}{f_b} = 0.144\,m$$

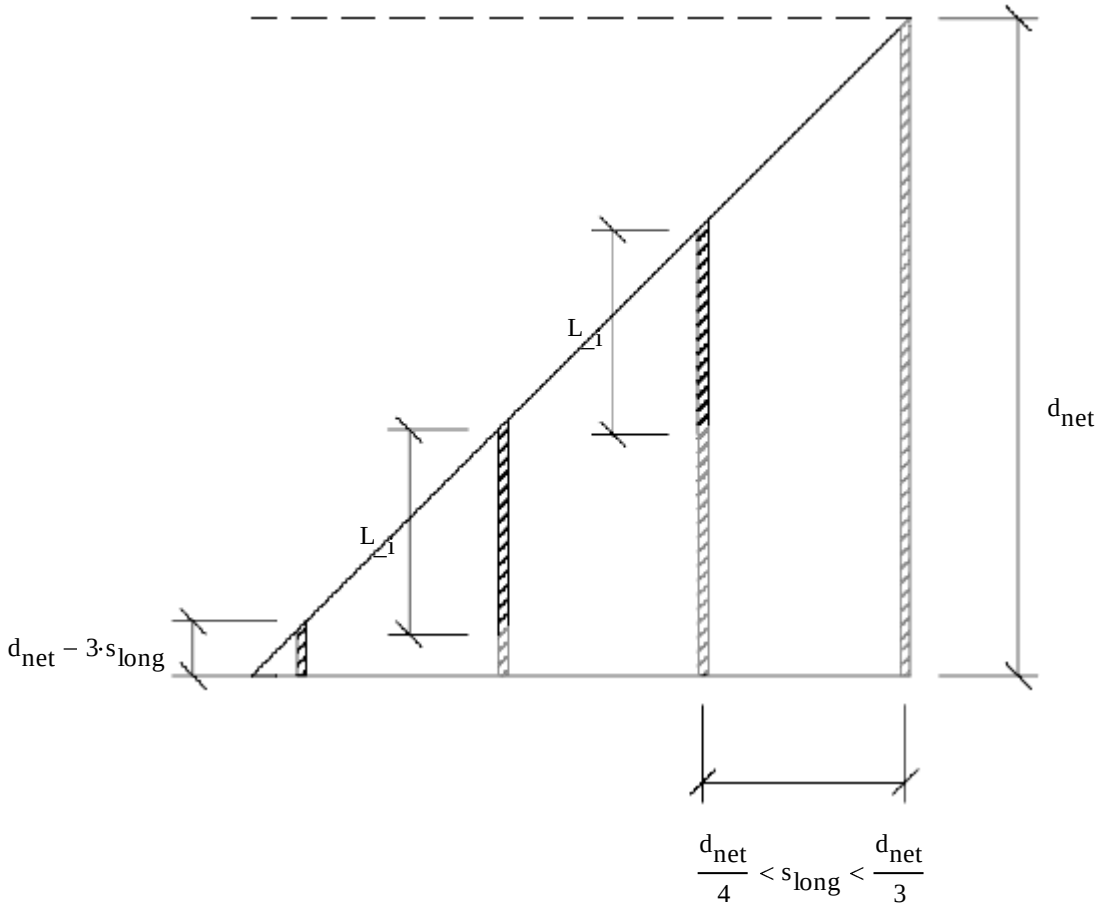

Figure G-2 Illustration of notations.

$$V_{2F} := \begin{cases} n_{trans}\cdot\pi\cdot\phi\cdot f_b\cdot L_{\_i} & \text{if } L_{\_i} < d_{net} - s_{long} \wedge \left(\frac{d_{net}}{2} < s_{long} < d_{net}\right) \\ \left\lceil n_{trans}\cdot\pi\cdot\phi\cdot f_b\cdot\left(L_{\_i} + d_{net} - 2\cdot s_{long}\right)\right\rceil & \text{if } d_{net} - 2\cdot s_{long} < L_{\_i} < s_{long} \wedge \frac{d_{net}}{3} < s_{long} < \frac{d_{net}}{2} \\ n_{trans}\cdot\pi\cdot\phi\cdot f_b\cdot 2\cdot L_{\_i} & \text{if } L_{\_i} < d_{net} - 2s_{long} \wedge \frac{d_{net}}{3} < s_{long} < \frac{d_{net}}{2} \\ \left\lceil n_{trans}\cdot\pi\cdot\phi\cdot f_b\cdot\left(L_{\_i} + d_{net} - 2\cdot s_{long}\right)\right\rceil & \text{if } s_{long} < L_{\_i} < d_{net} - 2s_{long} \wedge \frac{d_{net}}{4} < s_{long} < \frac{d_{net}}{3} \\ \left\lceil n_{trans}\cdot\pi\cdot\phi\cdot f_b\cdot\left(2\cdot L_{\_i} + d_{net} - 3\cdot s_{long}\right)\right\rceil & \text{if } d_{net} - 3s_{long} < L_{\_i} < s_{long} \wedge \frac{d_{net}}{4} < s_{long} < \frac{d_{net}}{3} \\ V_{1F} & \text{otherwise} \end{cases}$$

$$V_{2F} = 390.966\,kN$$

Concrete Capacity with regard to shear sliding failure

$$V_{Rd.c} = \left[C_{Rd.c} \cdot k \cdot \left(100 \rho_l \cdot \frac{f_{ck}}{MPa} \right)^{\frac{1}{3}} MPa + k_1 \cdot \sigma_{cp} \right] \cdot b \cdot d_0$$

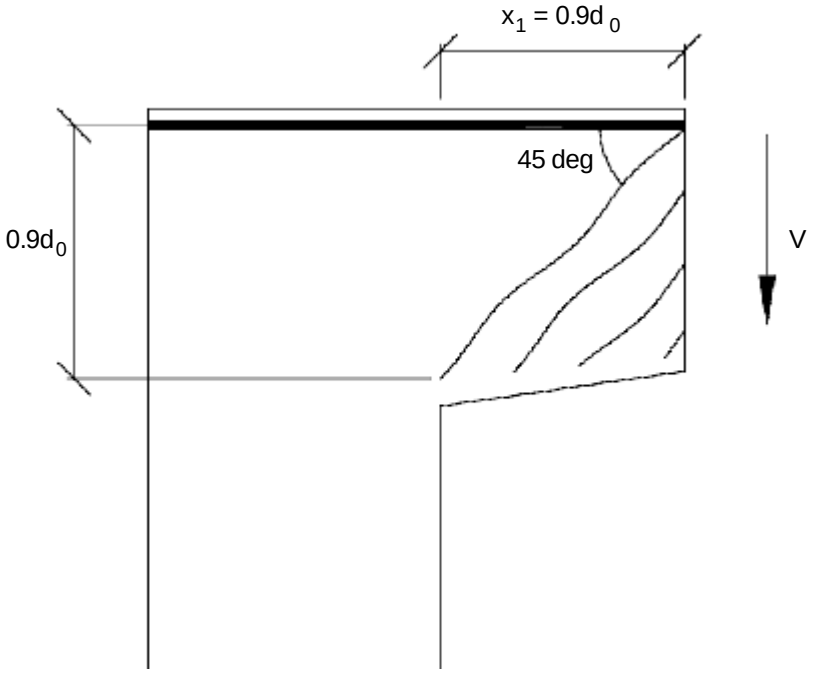

Figure G-3 Section for check of capacity with regard to shear sliding failure.

$x_1 = 0.765m$ $d_0 = 0.85m$

Spacing of each bar type: $s_e := 300mm$

Number of bar types in section: $n_1 := 3$

Total reinforcement area in section: $A_{s.1} := A_{si} \cdot n_1 \cdot \frac{b}{s_e} = 4.909 \times 10^3 \cdot mm^2$

$C_{Rd.c} := \frac{0.18}{\gamma_c} = 0.12$

$k := 1 + \sqrt{\frac{200mm}{d_0}} = 1.485 \qquad < 2 \qquad OK$

$\rho_{l.1} := \frac{A_{s.1}}{b \cdot d_0} = 5.775 \times 10^{-3} \qquad < 0.02 \qquad OK$

$k_1 := 0.15$

$\sigma_{cp} := \frac{R_b}{d_0} = 0.14\,MPa$

$\nu_{min} := 0.035 (k)^{\frac{3}{2}} \cdot \sqrt{\frac{f_{ck}}{MPa}}\,MPa = 0.317\,MPa$

$\left| \nu_{min} + k_1 \cdot \sigma_{cp} \right| \cdot b \cdot d_0 = 287.006\,kN$

$V_{Rd.c} := \left[C_{Rd.c} \cdot k \cdot \left(100 \rho_{l.1} \cdot \frac{f_{ck}}{MPa} \right)^{\frac{1}{3}} MPa + k_1 \cdot \sigma_{cp} \right] \cdot b \cdot d_0 = 386.649\,kN$

$Check_1 := \begin{cases} \text{"OK"} & \text{if } V_{Rd.c} \geq \left| \nu_{min} + k_1 \cdot \sigma_{cp} \right| \cdot b \cdot d_0 \\ \text{"Not OK"} & \text{otherwise} \end{cases} = \text{"OK"}$

Total shear capacity

$V_{FRP} := \min \left| V_{1F}, V_{2F} \right| = 390.966\,kN$

$V_{Rd} := V_{Rd.c} + V_{FRP} = 777.615\,kN$

Appendix H

Calculations for Method 5

Material properties

$f_{FRP.tu} := 4GPa$

$\varepsilon_{eff} := 4 \cdot 10^{-3}$

$E_{FRP} := 225GPa$

$t_{FRP} := 1mm$

$b_{FRP} := 25mm$

$A_{FRP} := t_{FRP} \cdot b_{FRP} = 25 \cdot mm^2$

$n_{lay} := 3$

$A_{FRP.tot} := n_{lay} \cdot A_{FRP} = 75 \cdot mm^2$

Capacity with regard to shear sliding failure of strengthened sectio

Choose transversal spacing: $s_{trans} := 320mm$

Number of strips per meter width: $n_{trans} := \frac{b}{s_{trans}} = 3.125$

Strengthening requirement:

$$V_{Rd.FRP} = V_{Rd.c} + n_{trans} \cdot \varepsilon_{eff} \cdot E_{FRP} \cdot A_{FRP.tot} \cdot \frac{z_0}{s_{long}} \quad > \quad V_{Ed} = 502.644kN$$

Calculate required spacing:

$$s_{long} := \frac{z_0}{V_{Ed}} n_{trans} \cdot \varepsilon_{eff} \cdot E_{FRP} \cdot A_{FRP.tot} = 0.321m$$

Choose: $s_{long} := 300mm$

Capacity with regard to shear sliding failure:

$$V_{Rd.FRP} := \frac{z_0}{s_{long}} n_{trans} \cdot \varepsilon_{eff} \cdot E_{FRP} \cdot A_{FRP.tot} = 537.891kN$$

Capacity with regard to web shear compression failure at x = 2.5 m:

$\theta := 45deg$

$$V_{Rd.max.FRP} = \alpha_{cw} \cdot b \cdot z_3 \cdot \nu \cdot f_{cd} \cdot \frac{1}{\cot(\theta) + \tan(\theta)}$$

$\alpha_{cw} := 1.0$ (non-prestressed)

$$V_{Rd.max.FRP} := \alpha_{cw} \cdot b \cdot z_3 \cdot \nu \cdot f_{cd} \cdot \frac{1}{\cot(\theta) + \tan(\theta)} = 2.025 \times 10^3 \cdot kN$$